

1968

# Field emission and flash filament studies of hydrogenation and dehydrogenation of cyclohexene and benzene on a tungsten surface

James Benton Condon  
*Iowa State University*

Follow this and additional works at: <https://lib.dr.iastate.edu/rtd>

 Part of the [Physical Chemistry Commons](#)

## Recommended Citation

Condon, James Benton, "Field emission and flash filament studies of hydrogenation and dehydrogenation of cyclohexene and benzene on a tungsten surface " (1968). *Retrospective Theses and Dissertations*. 3656.  
<https://lib.dr.iastate.edu/rtd/3656>

This Dissertation is brought to you for free and open access by the Iowa State University Capstones, Theses and Dissertations at Iowa State University Digital Repository. It has been accepted for inclusion in Retrospective Theses and Dissertations by an authorized administrator of Iowa State University Digital Repository. For more information, please contact [digirep@iastate.edu](mailto:digirep@iastate.edu).

This dissertation has been  
microfilmed exactly as received 68-14,781

CONDON, James Benton, 1940-  
FIELD EMISSION AND FLASH FILAMENT  
STUDIES OF HYDROGENATION AND DEHYDRO-  
GENATION OF CYCLOHEXENE AND BENZENE  
ON A TUNGSTEN SURFACE.

Iowa State University, Ph.D., 1968  
Chemistry, physical

University Microfilms, Inc., Ann Arbor, Michigan

FIELD EMISSION AND FLASH FILAMENT STUDIES  
OF HYDROGENATION AND DEHYDROGENATION OF CYCLOHEXENE  
AND BENZENE ON A TUNGSTEN SURFACE

by

James Benton Condon

A Dissertation Submitted to the  
Graduate Faculty in Partial Fulfillment of  
The Requirements for the Degree of  
DOCTOR OF PHILOSOPHY

Major Subject: Physical Chemistry

Approved

Signature was redacted for privacy.

In Charge of Major Work

Signature was redacted for privacy.

Head of Major Department

Signature was redacted for privacy.

Dean of Graduate College

Iowa State University  
Of Science and Technology  
Ames, Iowa

1968

## TABLE OF CONTENTS

	Page
INTRODUCTION	1
The Reasons for Using Tungsten as the Active Surface	2
The Investigative Tools	2
The Need for Ultra High Vacuum Conditions	4
THEORETICAL BACKGROUND FOR FIELD EMISSION MICROSCOPY	6
THEORY AND OPERATION OF FLASH FILAMENT	13
Kinetics and Low Pumped Systems	13
High Pumped Systems	17
Isothermal Operation	18
FLASH FILAMENT EXPERIMENTAL	19
Vacuum System	19
Mass Spectrometer	23
FIELD EMISSION MICROSCOPY-EXPERIMENTAL	39
The Field Emission Microscope	39
Gas Loading of the Field Emission Tube	43
The Cryostat	46
Electronics for Field Emission	49
GAS PREPARATION	55
FIELD EMISSION RESULTS	58
Migration Studies	58
Dependence of Field Emission on Reaction Temperature	62
FLASH FILAMENT RESULTS	90
Hydrogenation of Surface Residue	90

	Page
High Pumped Flash Filament Experiments	90
Room Temperature Hydrogenation and Disproportionation	105
Decomposition of Benzene and Cyclohexene	108
DISCUSSION	125
SUMMARY	128
LIST OF SYMBOLS	131
LITERATURE CITED	133
ACKNOWLEDGEMENTS	136

## INTRODUCTION

The catalytic hydrogenation reactions and dehydrogenation reactions of the series benzene, cyclohexadiene, cyclohexene, and cyclohexane have been studied rather extensively. Bond (6) and Smith (30) have presented reviews of the problem. There is still rather little known, however, about the catalytic steps that are taken in the interconversion of this series.

The thermodynamics of this series has been discussed by Janz (21). The following table gives the details of his discussion. It will be

Table 1. Change in free energy per molecule of hydrogen added in the hydrogenation of benzene (reference benzene at 0.0)

Moles H <sub>2</sub> added	Product	Change in free energy (kcal./mole) at:				
		298°K	400°K	550°K	700°K	1000°K
1	Cyclohexadiene	13.2	15.7	19.6	23.5	31.3
2	Cyclohexene	-4.5	0.9	9.4	18.0	35.5
3	Cyclohexane	-23.4	-14.8	0.0	13.6	42.0

noted that the hydrogenation is favored, that is the standard free energy change in the reaction is negative, below 550°K and that dehydrogenation is favored above 550°K. At no time, however, are the products cyclohexene, 1,3-cyclohexadiene, or 1,4-cyclohexadiene favored; these compounds would tend to disproportionate to cyclohexane and benzene at 550°K.

It is often assumed in the catalytic studies of these compounds that the only reactions occurring are interconversions in the series. Thus deuterium exchange reactions are often used in an effort to illuminate the individual steps. There is danger in this assumption (3) and the present work could indeed indicate that exchange might proceed as an independent process.

#### The Reasons for Using Tungsten as the Active Surface

Although tungsten is a very poor catalyst for at least hydrogenation of benzene it should exhibit some of the basic characteristics of all the transition metals in catalytic activity.

The purposes for using tungsten are threefold. Firstly, tungsten is an easy metal to work with in the field emission microscope. It is an easy metal from which to make field emission tips which are durable. Secondly, tungsten is easily cleaned thermally. This second point is verifiable with the use of a field emission microscope. The only treatment needed to eliminate surface carbon or tungsten carbides is a momentary heating to 2800°K. Cleaning of other metals such as nickel is not quite so easily accomplished. Thirdly, a considerable amount of work has been done and is still being done by my coworkers with tungsten and other hydrocarbons. This makes it possible to gain some insight into possible mechanisms for interconversion and decomposition by analogy to these similar systems.

#### The Investigative Tools

The investigative methods used in this study are the field emission microscopy which can follow the characteristics of adsorbed species and

flash filament mass spectroscopy which can monitor gas phase products.

There are serious limitations to the field emission microscope. As a microscope the resolution is at best only  $20\text{\AA}$  and because of this it is most useful for migration studies and detection of preferential adsorption on various crystal planes of the metal. The relation between field emission current and applied voltage in the microscope yields as additional information the surface dipole and the surface polarizability. From these pieces of information one must infer what the chemisorbed species is on the surface. Thus, in studies such as the present one, more than one model can be proposed to explain the experimental results. It is very possible, as the present work will illustrate, to eliminate a great number of other models that are inconsistent with the field emission results.

Surface reaction mechanisms can only be inferred from flash filament data even with mass spectrometric gas phase monitoring. The inference is again ambiguous; results obtained over widely varying experimental conditions permit rejection of many but not all conceivable reaction paths. "Proof" of a reaction mechanism consists of eliminating reasonable alternatives, and the quotation marks are used because the process may well depend as much on exhaustion of imagination as on diligence in elimination. This comment is not limited to surface reaction mechanisms but applies to reaction mechanisms in general.

Within these limitations the models proposed in this work are the most tenable in light of experimental evidence of this work and works of other investigators. It is hoped that the conclusions can be used



to help explain and possibly predict metallic catalytic activity with respect to aromatic compounds and related hydrogenated derivatives.

#### The Need for Ultra High Vacuum Conditions

The need for ultra high vacuum conditions with background pressures in the  $10^{-10}$  torr (mm Hg) range or better for both field emission and flash filament experiments is readily understandable in light of the kinetic equation

$$J = \frac{P}{\sqrt{2\pi m k T}} \quad 1.$$

where  $J$  is the flux of particles striking a surface,  $P$  is the pressure,  $m$  is the mass of the particle,  $k$  is Boltzmann's constant, and  $T$  is the absolute temperature. This means that for hydrogen at a pressure of  $10^{-6}$  torr, if every molecule of hydrogen striking the surface stuck, a monolayer would form in one second. In order to carry out an experiment of a minute duration where less than 1% of a monolayer of undesirable background gas is formed, a vacuum of  $10^{-10}$  torr is needed. A typical flash filament experiment takes about 5 minutes to complete. In order to control conditions it is therefore imperative to use an ultra high vacuum system (which is defined as a system that will obtain pressures of  $10^{-9}$  torr or lower).

In field emission experiments the situation is much worse. It takes four hours to do a typical field emission experiment. In this case a vacuum of  $10^{-13}$  torr is needed. These vacuums are obtained by using sealed field emission tubes cooled to 4°K. If these tubes had been previously

pumped on an ultra high vacuum system and care is taken that little hydrogen accumulates during the course of the experiment then a vacuum of  $10^{-14}$  torr is maintained.

## THEORETICAL BACKGROUND FOR FIELD EMISSION MICROSCOPY

The field emission microscope has two main uses. Firstly, it is a microscope of magnification of  $10^6$  but resolution of only  $20\text{\AA}$ . Secondly, it can measure the change in the metal's work function which in turn is related to a changed surface dipole. Changes in the surface polarizability can also be obtained by field emission, but only with poor precision and ambiguous meaning.

Field emission is the emission of electrons from a cold metal under the influence of a high electric field. The field required for measurable emission is about  $10^8$  volts per cm. Such fields are most easily obtained by applying about 2000 volts between a very small metallic needle or tip of around  $1000\text{\AA}$  radius and ground. If the tip end is nearly spherical, the field  $F$  is given by<sup>1</sup>

$$F = \frac{V}{r} \quad 2.$$

where  $V$  is the applied voltage and  $r$  the tip radius; the field for the values of  $V$  and  $r$  given is about  $2 \times 10^8$  volts per cm. The tip is other than spherical; therefore  $r$  should be replaced by a parameter  $\beta$  that is referred to as the geometry factor. This gives

$$F = \frac{V}{\beta} . \quad 3.$$

The necessary resort to metal tips of radius of around  $1000\text{\AA}$  produces a magnification of the metal emission areas. By using a phosphorescent

---

<sup>1</sup>For derivation of equations of this nature see Corson, Dale and Paul Lorrain, Introduction to Electromagnetic Fields and Waves, San Francisco, Cal., W. H. Freeman and Company, 1962, or similar text books.

screen at the position of the applied high voltage one can observe the final point in the electron's trajectory. To first approximation, electron trajectories are straight lines perpendicular to the tip surface. The screen therefore gives a magnified mapping of emission areas; in this work the tip-to-screen distance was about 5 cm, the tip radius about  $1000\text{\AA}$ , and the magnification factor  $5 \times 10^5$ . A tangential velocity component on emission is chiefly responsible for loss of resolution. With a screen size of around 5 cm. this will give a magnification of  $5 \times 10^5$ . Figure 1 shows a clean tungsten field emission pattern with some of the crystal faces indexed. Since usually adsorbed chemical species change the emission characteristics, it is quite easy to observe such things as the migration of adsorbed layers over distances as small as  $100\text{\AA}$ .

Field emission is a quantum mechanical tunnel effect and was first explained by Fowler and Nordheim in 1928 (13). The derivation of the equation was exact for the model presented. An approximate treatment was given by Good and Mueller (17) and is much better suited to treatment of realistic metal surface models. In low temperature field emission, the current and field are related to good approximation by

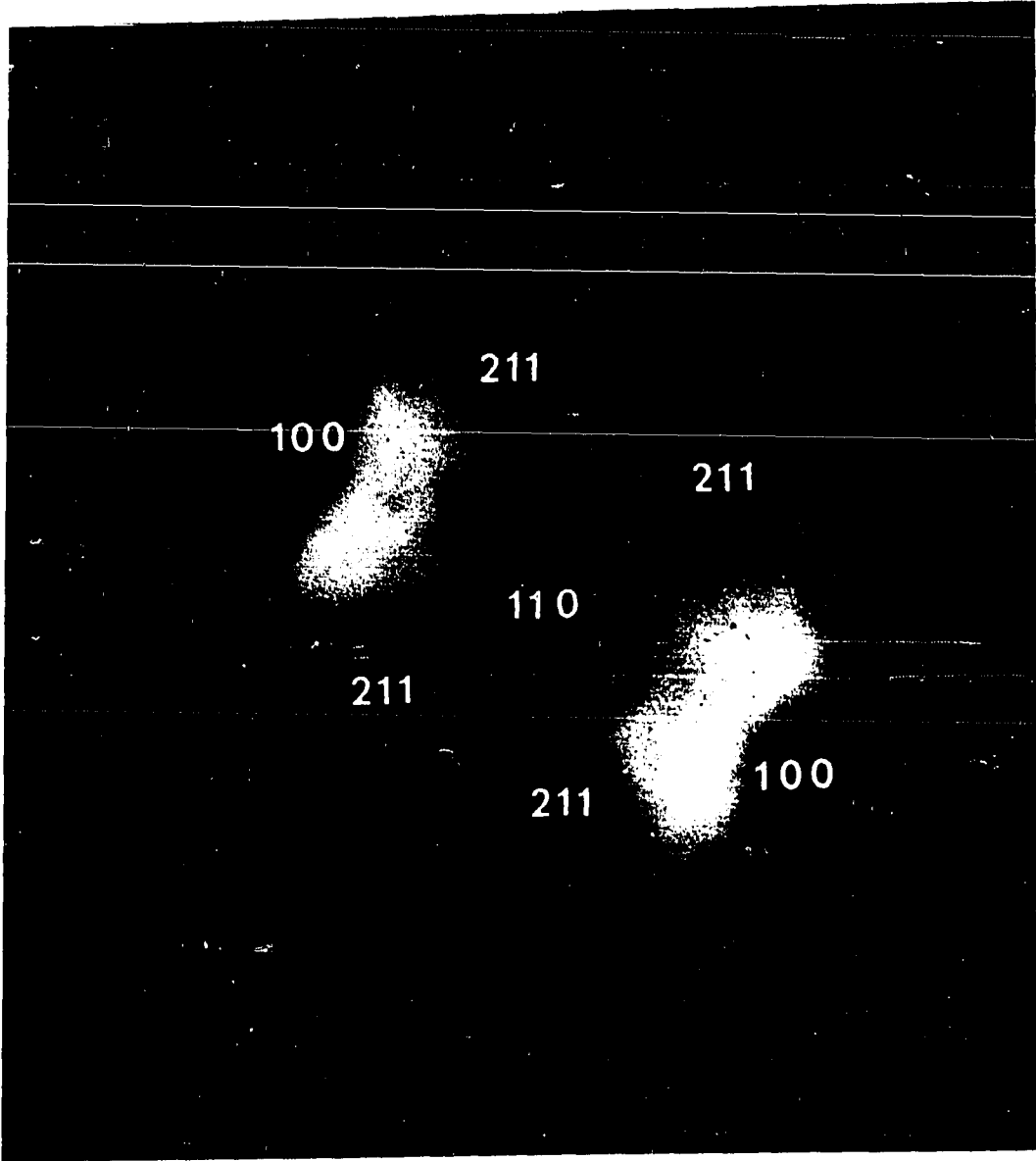
$$I = 6.2 \times 10^6 \frac{(\mu/\phi)^{\frac{1}{2}}}{(\mu + \phi)} A F^2 \exp(-6.80 \times 10^7 \phi^{3/2}/F) \quad 4.$$

where  $\phi$  is the work function,  $\mu$  is the Fermi energy, and A the emitting area. This equation in terms of applied voltage and in logarithmic form is then

$$\log I/V^2 = -\frac{b \phi^{3/2}}{V} + C \quad 5.$$

Figure 1. A clean tungsten field emission micrograph with some of the principal crystal planes indexed

This is a mapping of the work function of the field emission tip with the low work function planes indicated by the light areas and the high work function planes indicated by the dark areas.



where  $I$  is the field emission current and  $b$  and  $C$  are constants if the geometry factor does not change. The factor

$$\log \frac{(\mu / \phi)^{\frac{1}{2}}}{(\mu + \phi)}$$

does not change greatly and is included in  $C$ . Upon adsorption of material on the metal surface this equation must be modified due to the additional dipole and polarizable layer. On  $N_s$  surface sites an evenly distributed layer of adsorbate molecules (or adatoms) each with a normal dipole component  $\mu_0$  will by classical electrostatics create a surface potential of

$$\Delta\phi = -4\pi N_s \theta \mu_0 \quad 6.$$

(where  $\theta$  is the surface coverage) which will result in a work function shift. Field emission measures a work function averaged over all emitting areas (an emitting area being defined as a region of common work function) and the weighting of the average depends on the variations in the work function from area to area and the size of the areas. Where the areas are larger than  $50\text{\AA}$  in diameter the field emission work function will be nearly that of the areas of lowest work function. This "window" effect explains why the field emission work function of clean tungsten is approximately that for the 100 and 111 planes. If the areas are smaller than  $20\text{\AA}$  diameter and evenly distributed the work function will be the average weighted by area; this case has been examined by Young (35) to explain deviations found in measuring the work function on single crystal planes.

Interpretation of a work function shift during the course of a reaction depends on whether the "window" effect or the geometric averaging

model applies. If adsorbate and chemisorbed products migrate and agglomerate or bond preferentially to a particular crystal plane then the former model should be used. The latter model is preferred when the adsorbate molecules (and adatoms) are fairly evenly distributed. The decision as to which model to use is dictated by the field emission micrographs; with little change in anisotropy during the course of the reaction the geometric averaging model is used and with large variations in patterns, the "window" effect applies.

To determine  $\phi$  one can assume that the geometry of the tip does not change appreciably upon adsorption of gases and heating. This assumption is a very good one up to 800°K for a thermally annealed tungsten tip. This means that since  $b$  is a constant and if  $S$  is the slope of the plot  $\log I/V^2$  vs.  $1/V$  then

$$\phi_1 / \phi_0 = (S_1 / S_0)^{2/3} . \quad 7.$$

The subscripts 0 and 1 in this equation designate the values for the clean tungsten and the tungsten with adsorbed material. Using the value of 4.5 eV for the work function for clean tungsten this yields

$$\phi_1 = 4.5 (S_1 / S_0)^{2/3} \quad 8.$$

or

$$\Delta\phi = 4.5 (1.0 - (S_1 / S_0)^{2/3}). \quad 9.$$

The "single point method" provides another convenient work function comparison. If one adjusts the experiments such that only one field emission current is used and if it is assumed that the constant  $C$  never



changes from one determination to the next then the equation

$$\phi_1 / \phi_0 = (V_1 / V_0)^{2/3} \quad 10.$$

is true. Unfortunately the "constant" C in Equation 4 depends on the surface polarizability,  $\alpha$ , which can change greatly during surface reactions; the relation is

$$C_1 - C_0 = 2.5 \log \phi_1 - 1.633 + [4.43 \times 10^7 (\phi_1 - \phi_0)d] / \phi_1^{3/2} \\ + 1.67 \times 10^8 N_s \theta \alpha \quad 11.$$

where d is the thickness of the layer (13).

## THEORY AND OPERATION OF FLASH FILAMENT

The flash filament apparatus may be operated in an isothermal mode. In this case the filament (the sample with an active surface) is kept at constant temperature and gases are admitted to the reaction cell. The gases are monitored with a mass spectrometer to identify the type and quantity of products and reactants. This method of operation requires control experiments to make certain the reactions observed are taking place on the filament only.

Another method of operation utilizes the change in reaction rates with increased temperatures. By monitoring products with continuous heating from a low temperature one may utilize the Polanyi-Wigner equation,

$$\frac{-dn}{dt} = v n^q \exp(-\Delta H^\ddagger/RT) \quad 12.$$

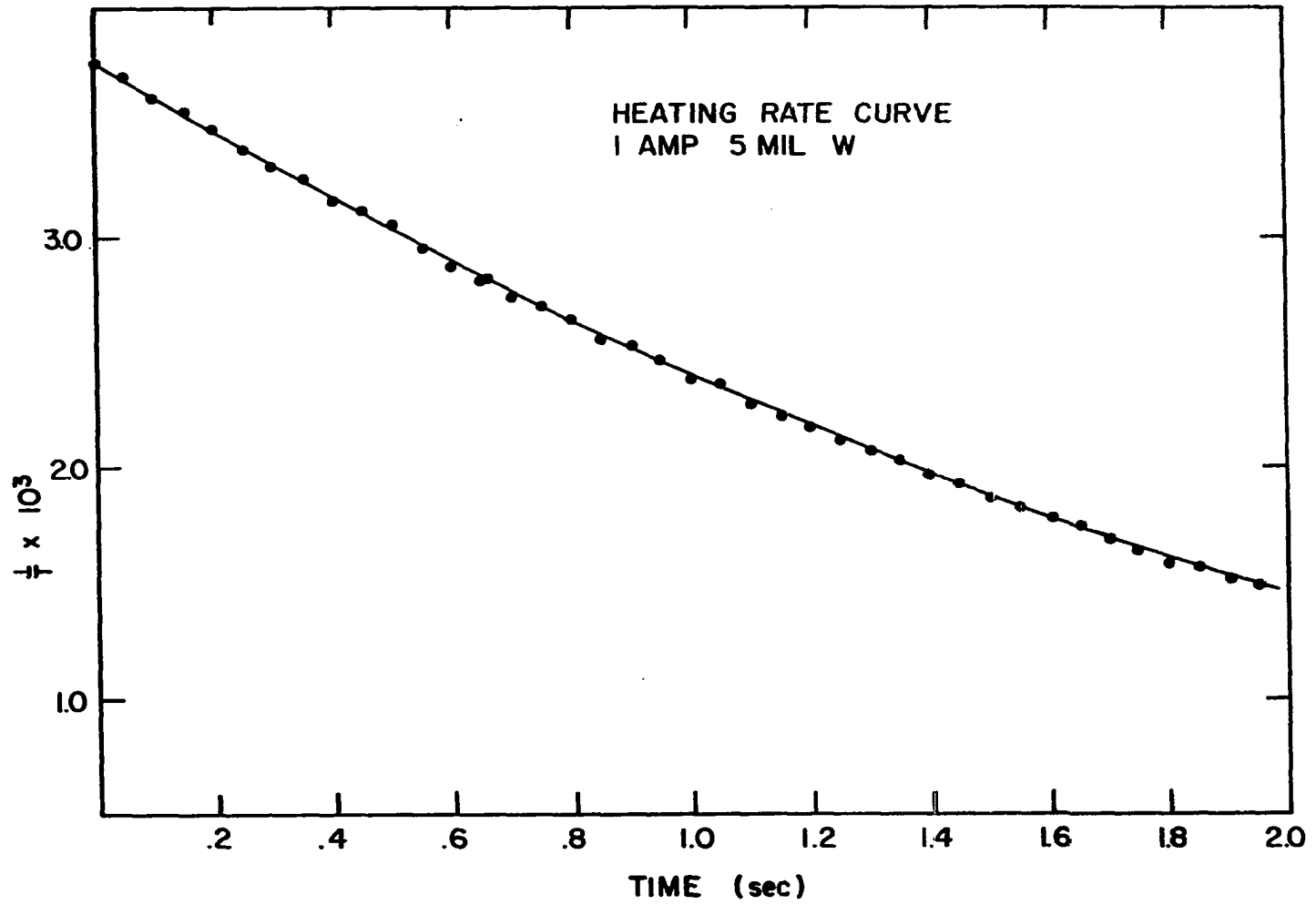
where  $q$  is the order of the reaction, to gain insight into the reaction mechanism.

## Kinetics and Low Pumped Systems

In the second method of operation gases are adsorbed on the filament at a low temperature, usually 90°K, and the filament is resistance heated. During this heating the gas phase is monitored with either the mass spectrometer or ion gauge. Very often a constant current is used to heat the filament. In this case the temperature  $T$  and time  $t$  are approximately related by  $1/T = g + ht$ , where  $g$  and  $h$  are constants, as shown in Figure 2. With the inverse relationship the kinetic analysis

Figure 2. The heating rate obtained by passing 1 amp through a 5 mil tungsten wire

This figure shows the near linear relationship between time (abscissa) and the inverse of the temperature (ordinate) when constant current heating is used.



is simplified greatly. The equations for this analysis have been discussed by Redhead (26) and Ehrlich (12).

For a system with some pumping the amount of gas evolved,  $n$ , from the surface is given by

$$n = \frac{V_s}{RT_s} (P - P_0) + \frac{S_s}{V_s} \int_{t_0}^t (P - P_0) dt \quad 13.$$

where  $V_s$  is the volume of the system,  $T_s$  is the temperature of the system,  $S_s$  is the pumping speed in liters per second,  $t$  designates time, and the subscript 0 indicates the initial values.

To obtain the frequency factor and activation energy for simple mechanisms one uses the correct values for the amount of gas evolved and the equations:

$$\log_e Q(n) = \log_e \frac{vR}{h\Delta H} - \frac{\Delta H^\ddagger}{RT} \quad 14.$$

where  $Q(n) = \log_e n/n_0$  for a first order reaction 15.

and  $Q(n) = \frac{n_0 - n}{n_0 n}$  for a second order reaction. 16.

By plotting  $\log_e Q(n)$  vs.  $1/RT$  the activation energy is obtained from the slope and the frequency factor is obtained from the intercept where  $T = \infty$ . If  $1/T$  does not vary linearly with time the above equations must be modified (23,26).

It is clear from Equation 13 that the greater the pumping speed in the system the more difficult it is to correct for pumping. A slight error in the estimation of the pumping speed can result in a very large

error in a plot of  $n$  vs.  $t$ . This difficulty is overcome by reducing the pumping speed to a minimum and decreasing the length of time required for a flash.

Reaction paths other than a one step reaction with constant activation energy require a more complex analysis. Models assuming a variation in activation energy with coverage have been suggested (19,34) and for the simplest case (23) the variation is assumed linear. The Polanyi-Wigner equation in this case becomes

$$\frac{-dn}{dt} = v n^q \exp(-(\Delta H^\ddagger - \alpha'\theta)/RT) \quad 17.$$

where  $\theta$  is the surface coverage and  $\alpha'$  is a constant. For models involving reaction sequences, intermediate equilibria or steady states more complex equations must be derived to obtain quantities for comparison with experimental data.

#### High Pumped Systems

It is often advantageous to work in systems that are highly pumped. It has been shown by Redhead (26) that for a particular species coming off the surface with an activation energy of  $\Delta H^\ddagger$  the concentration of the species in the gas phase will reach a maximum at a temperature given by

$$T (\text{°K}) = \Delta H^\ddagger (\text{kcal.}) / 0.06 \quad 18.$$

The resolution of desorption peaks depends on the pumping speed, the heating rate and the reaction path. It is also affected by any change in  $\Delta H^\ddagger$  with surface coverage. This technique is useful in identifying

with the mass spectrometer the various species and the relative  $\Delta H^\ddagger$ 's for their formation. High pumping can be accomplished with an open path to a vacuum pump.

### Isothermal Operation

For isothermal operation the filament is kept at a constant temperature either with a constant temperature bath in the reentrant dewar of the reaction cell or the temperature of the entire flask is kept constant as with room temperature operation.

To follow reactions the filament is preconditioned and gases are admitted to the system. The products are then monitored with the mass spectrometer. The preconditioning of the surface can constitute cleaning and possibly predosing with another gas.

To eliminate the possibility that the products observed may be produced in other portions of the system, control experiments must be performed. The easiest method for control is to contaminate the filament to such an extent that it becomes inactive. If no reactions occur with a contaminated filament during this control experiment then the reactions observed otherwise occur only on the filament. Luckily this was the case in all the reactions studied.

Very rapid reactions can be followed using this technique. By using the rapid scanning capabilities of the quadrupole mass spectrometer and a very high speed recorder, complete mass scans from mass 2 amu. to mass 80 amu. can be taken every 0.1 second.

## FLASH FILAMENT EXPERIMENTAL

## Vacuum System

The necessity for ultrahigh vacuum has already been discussed. In the present case these vacuums were obtained with the aid of an Ultex D. I. vacuum pump with a pumping speed of 20 liters per second. Figure 3 is a schematic of the system used.

In order to achieve ultra high vacuum the pumping must be great enough to overcome the evolution of gases from leaks, including desorption from the system's walls. Since there is a limit on the pumping speed it is best to try to reduce gas evolution to a minimum. To reduce desorption of gases, mostly water, at room temperature operation the system is operated for about 8 hours at 400°C. This was done by enclosing most of the system in a portable oven. Those portions of the system not inside the oven, with the exception of the gas bulb, were heated with heating tapes or infra red lamps. This "bake out" allows an increased rate of desorption from the system's walls for a short time. When the temperature of the system is reduced to room temperature and all filaments thoroughly outgassed the residual gas pressure is no greater than  $2 \times 10^{-10}$  torr.

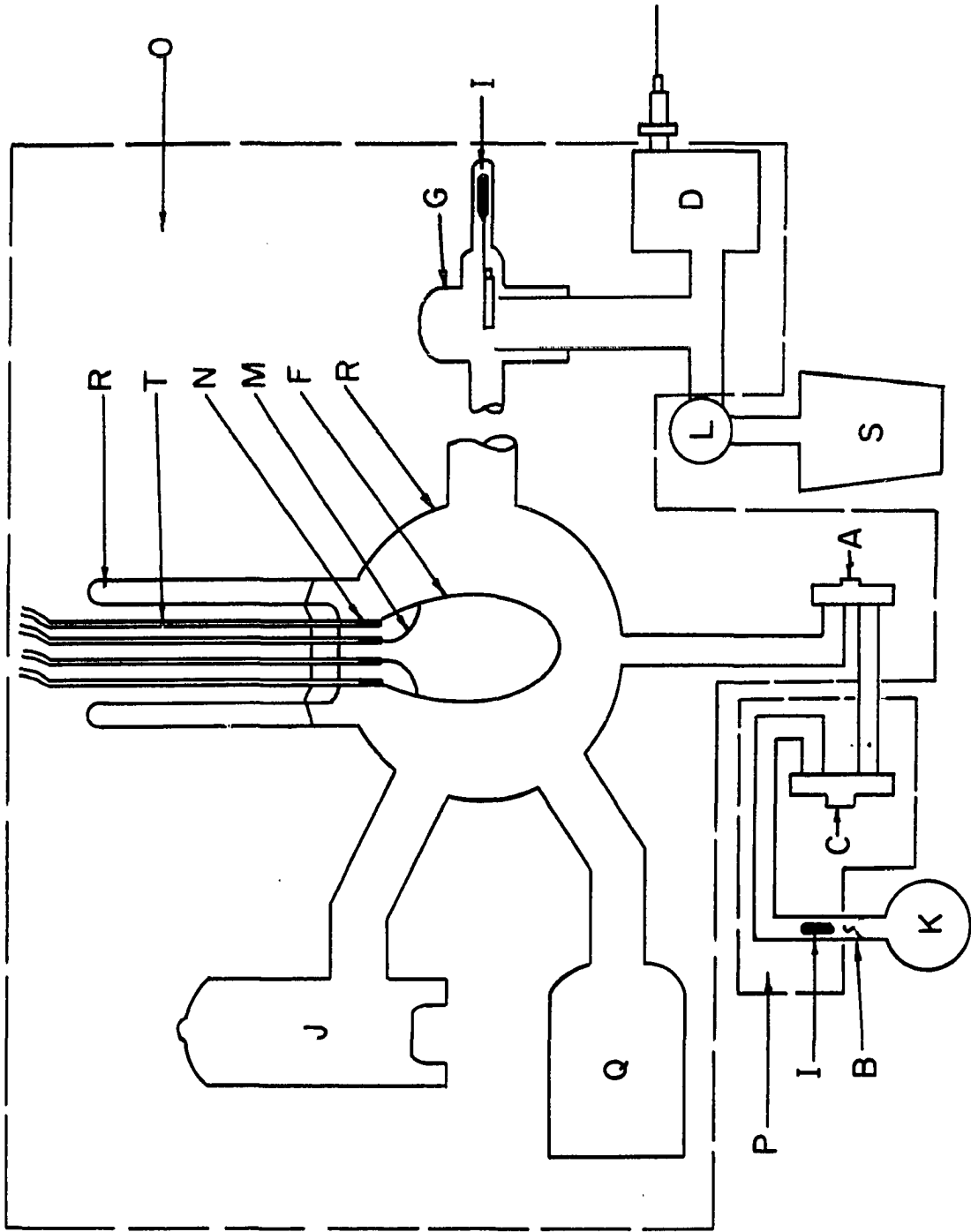
The system was made of metal and Pyrex glass. The mass spectrometer used was an Ultex quadrupole 150. The ion gauges were Westinghouse type 5966. The valves used for gas handling were either Granville-Phillip variable leak or type "C" valves. All connections made on the system were welded, brazed, glass-metal seals, or ultra high vacuum flanges.

The hydrocarbons were contained in gas bulbs with a break off seal



Figure 3. Schematic of flash filament apparatus with the components listed below

- K gas ampule
- B break off seal
- I iron slug
- P section of system bakeable before break off seal is broken
- C Granville-Phillips type "C" valve
- A Granville-Phillips type variable leak valve
- Q Ultex 150 quadrupole mass spectrometer
- J ionization gauge
- R evacuated reentrant dewar
- T tungsten lead ins
- N nickel wrappings for spot welding filament to lead ins
- M 3 mil tungsten sensing leads
- F 5 mil tungsten sample filament
- R reaction cell
- G sliding ground glass valve
- D Ultex D. I. vacuum pump
- O area baked out (D. I. pump heated with infra red lamps)



inside the system. They were introduced into the system by raising a glass encased iron slug with a magnet and dropping it on the break off seal. The hydrogen was admitted and at the same time purified by means of a palladium hydrogen diffuser. Gas flow regulation was achieved with the Granville-Phillip variable leak valves. It was convenient to use type "C" valves in series with the variable leaks. These were placed on the gas side of the variable leaks and were closed during bakeouts so that the variable leak valves could be baked out open. The leak valves could not be baked closed.

For some experiments it is convenient to lower the pumping speed from the reaction cell. A magnetically operated ground glass valve served the purpose effectively. Since ion gauges were situated on both sides of the glass valve, the pressure could be followed in the reaction cell or the pumped side independently. The D. I. pump also could be used as a pressure measuring device. This permitted estimation of the pressure drop  $\Delta P$  across the valve from Equation 19:

$$-\frac{dP}{dt} = -P \frac{S}{V_s} + L\Delta P \quad 19.$$

for if  $dP/dt$  is small then  $\Delta P$  is directly proportional to  $P$ . This can be used to advantage in hydrogen monitoring. Since hydrogen is rapidly pumped by an ion gauge with a hot filament (20) the ion gauge in the reaction cell must be off during a non-pumped flash filament experiment. The D. I. pump or the ion gauge on the pumped side can be used together with equation 19 to obtain  $P$ ; indeed, with the valve adjusted to a pumping speed of only 0.02 liter per second the pressure rise on the

pumped side was 1/3 the cell pressure, and was readily observed. It was also observed that no measurable time lag existed for a pressure rise to occur on the pumped side of the valve in response to a pressure rise in the reaction cell.

The reaction bulb was a 500 ml. bulb with a press seal on a reentrant dewar and ports leading to the ground glass valve, the mass spectrometer, the ion gauge and the variable leak valves. The filament was spot welded to the four lead press seals and sensing leads were spot welded to the filament. The temperature of the filament could thus be detected by measuring the resistance between the sensing leads. The following equations give the relationship between resistance and temperature for pure tungsten. For below 620°K

$$T = 239 \frac{\Omega}{\Omega_{295}} + 55, \quad 20.$$

and for above 620°K

$$T = 195 \frac{\Omega}{\Omega_{295}} + 159 \quad 21.$$

where  $\Omega$  is the resistance and  $\Omega_{295}$  is the measured resistance at 295°K. Figure 4 compares Equations 20 and 21 with experimental data of Robert Rye (27).

#### Mass Spectrometer

The mass spectrometer was attached directly to the reaction cell. In the ionization region of the mass spectrometer hydrocarbons are fragmented, each with a characteristic fragmentation or cracking pattern.

Figure 4. A plot of the quotient of tungsten's resistance by its resistance at 295°K vs. absolute temperature (27)

This plot can be fit by two equations, one below 620°K which is

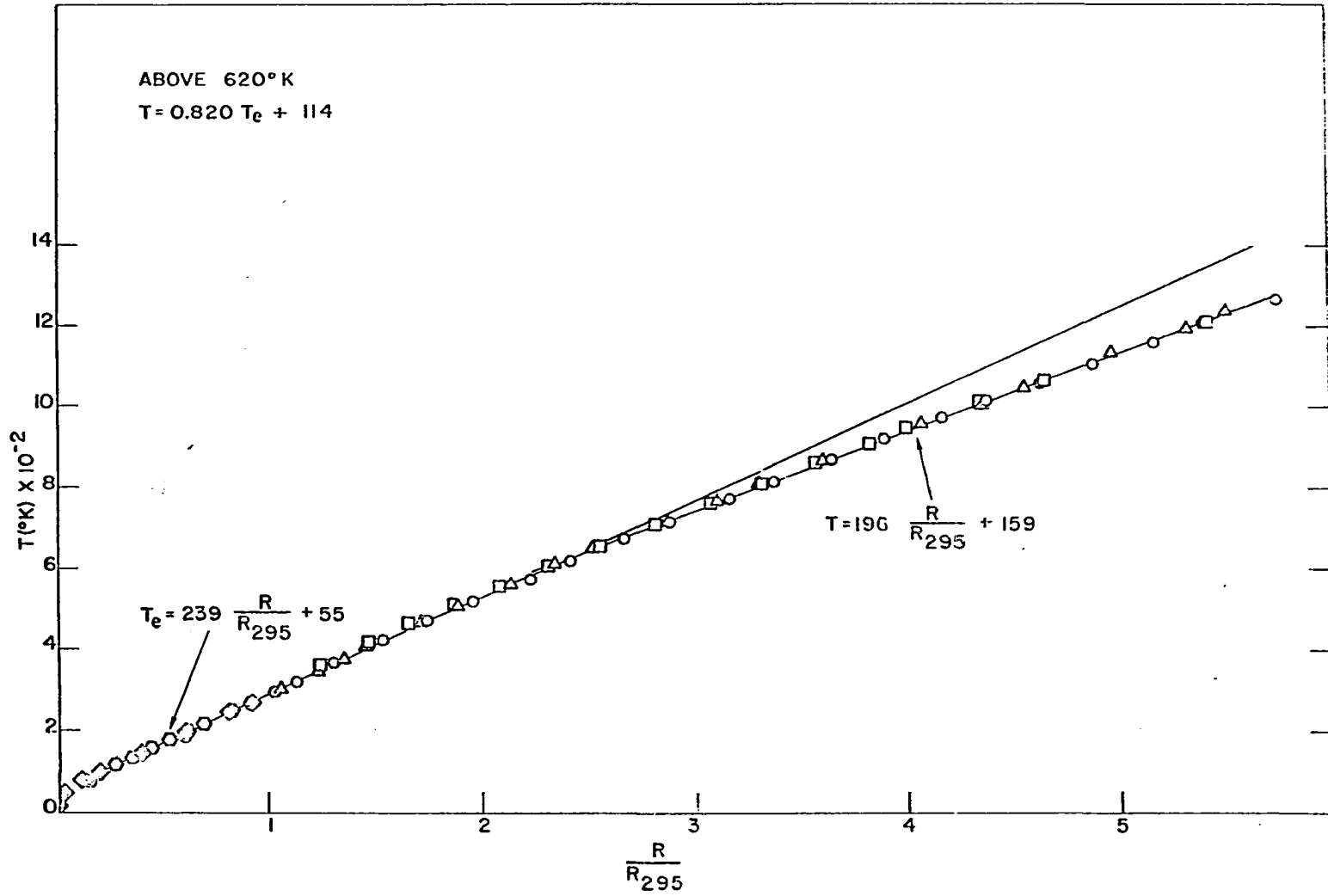
$$T(^{\circ}\text{K}) = 239 \frac{R}{R_{295}} + 55$$

and one above 620°K which is

$$T(^{\circ}\text{K}) = 196 \frac{R}{R_{295}} + 159$$

where R is the resistance,  $R_{295}$  (shown as  $R_{295}$  in figure) is the resistance at 295°K and T is the absolute temperature.

TUNGSTEN



Figures 5 through 8 show the latest certified cracking patterns for those hydrocarbons of interest taken from American Petroleum Institute (API) Tables (2). These values were taken with a mass spectrometer which used as an ion collector a faraday cup. In the present work a particle multiplier was used, with sensitivity roughly proportional to mass (25). This relation was verified for the present system by analysis of a cyclohexane mass spectra obtained in a flow system (cyclohexene source valve and valve to pump both partly open) at a pressure of  $10^{-6}$  torr. The ratio of current to API intensity should be nearly inversely proportional to mass. More generally

$$\frac{i}{i_{\text{API}}} = Dm^x \quad 22.$$

or

$$\log \frac{i}{i_{\text{API}}} = \log D + x \log m \quad 23.$$

where  $i$  is the observed intensity,  $i_{\text{API}}$  the values given in the API tables,  $m$  the mass of the fragment and  $D$  and  $x$  are constants. Figure 9 compares data obtained with Equation 23; the line drawn has a slope -1 (i.e.  $x = -1$ ) and agrees quite well with the data. Many other variables such as differences in pressure and differences in the mass spectrometers and especially differences in method of resolution can lead to deviations from behavior shown in API tables.

The foregoing considerations make cross calibration of relative sensitivities for the various gases rather difficult. Most of these difficulties, however, can be minimized by choosing the mass peaks to

Figure 5. The cracking patterns of n-pentane and n-hexane as given in the American Petroleum Institute table (2)

Both n-pentane and n-hexane have a 57 amu. peak. The relative sensitivities of the 100% peaks are with respect to the 43 amu. peak of n-butane.



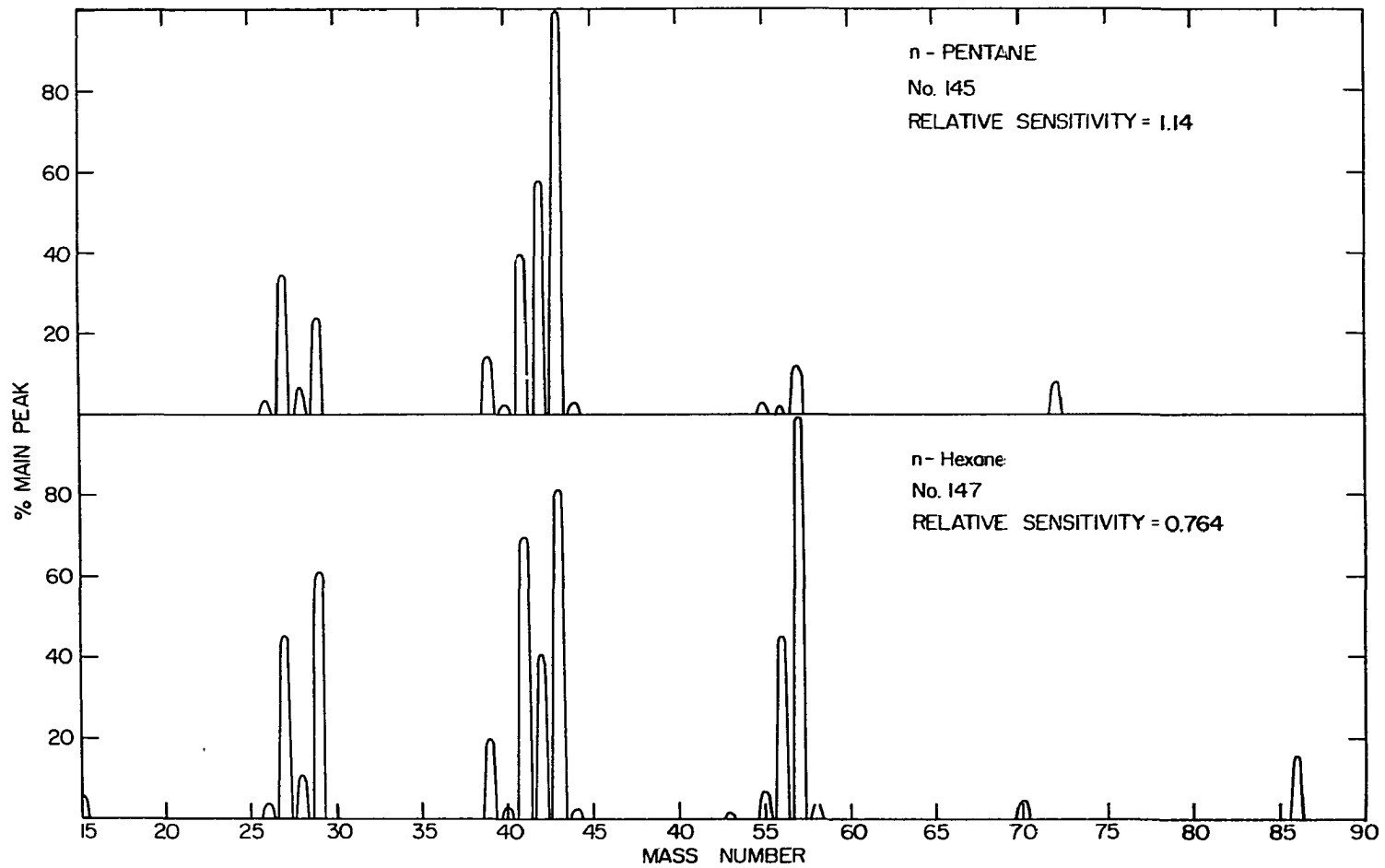


Figure 6. The cracking patterns of cyclohexene and cyclohexane as given in the American Petroleum tables (2)

Cyclohexene has a major peak at 54 amu. whereas cyclohexane has a major peak at 56 amu. with the 55 amu. peak only 33.3% of the 56 peak. The relative sensitivities of the 100% peaks are with respect to the 43 amu. peak of n-butane.

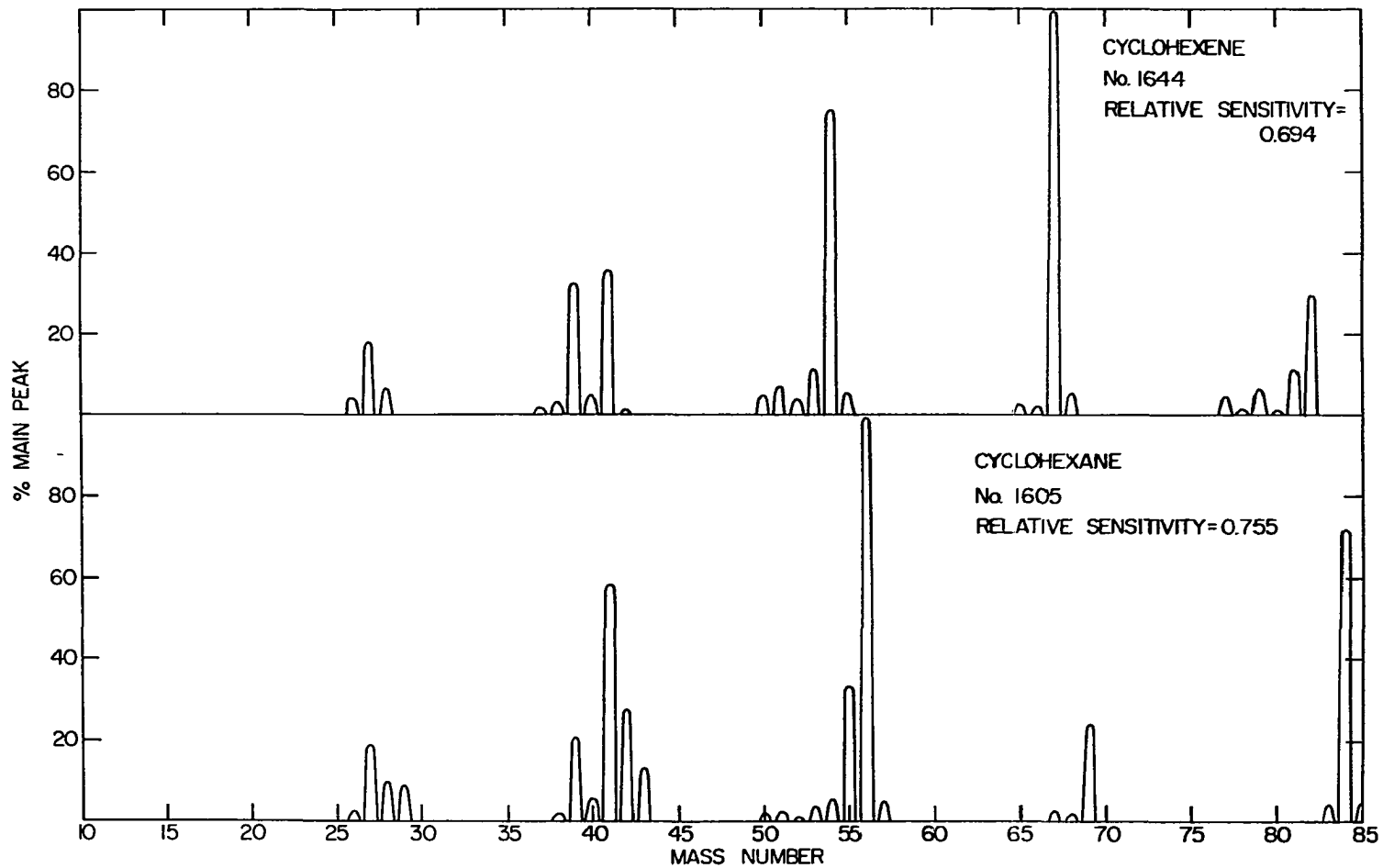


Figure 7. The cracking patterns of benzene and 1,3-cyclohexadiene as given in the American Petroleum Institute tables (2)

The 50 amu. peak of benzene was used to monitor benzene. The 80 amu. peak was used to establish the absence of cyclohexadiene. The relative sensitivities of the 100% peaks are with respect to the 43 amu. peak of n-butane.

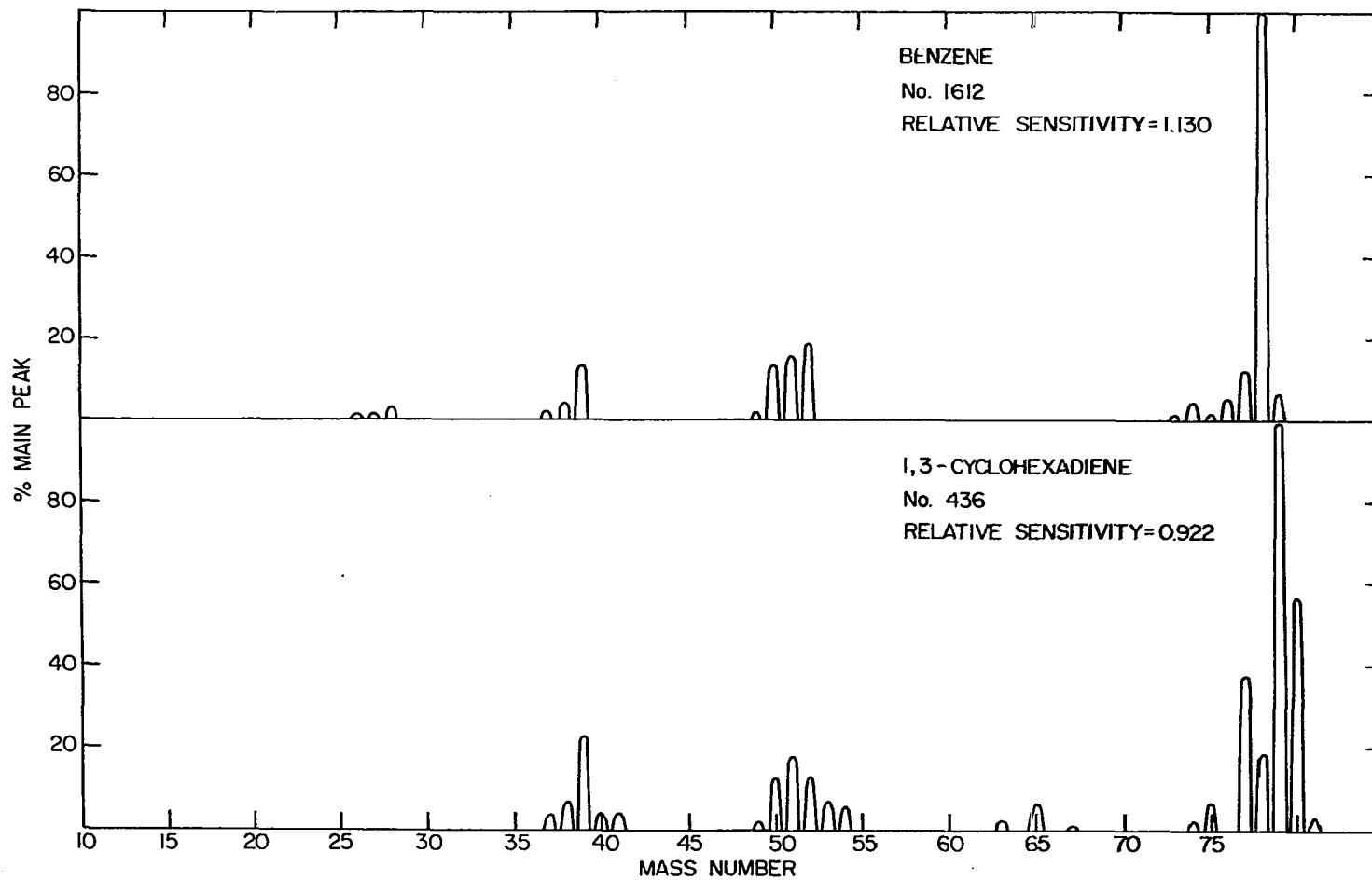


Figure 8. The cracking patterns of 1-hexene and 2-hexene as given in the American Petroleum Institute tables (2)

In 1-hexene the 56 amu. peak is 70% the 57 amu. peak. The relative sensitivities of the 100% peaks are with respect to the 43 amu. peak of n-butane.

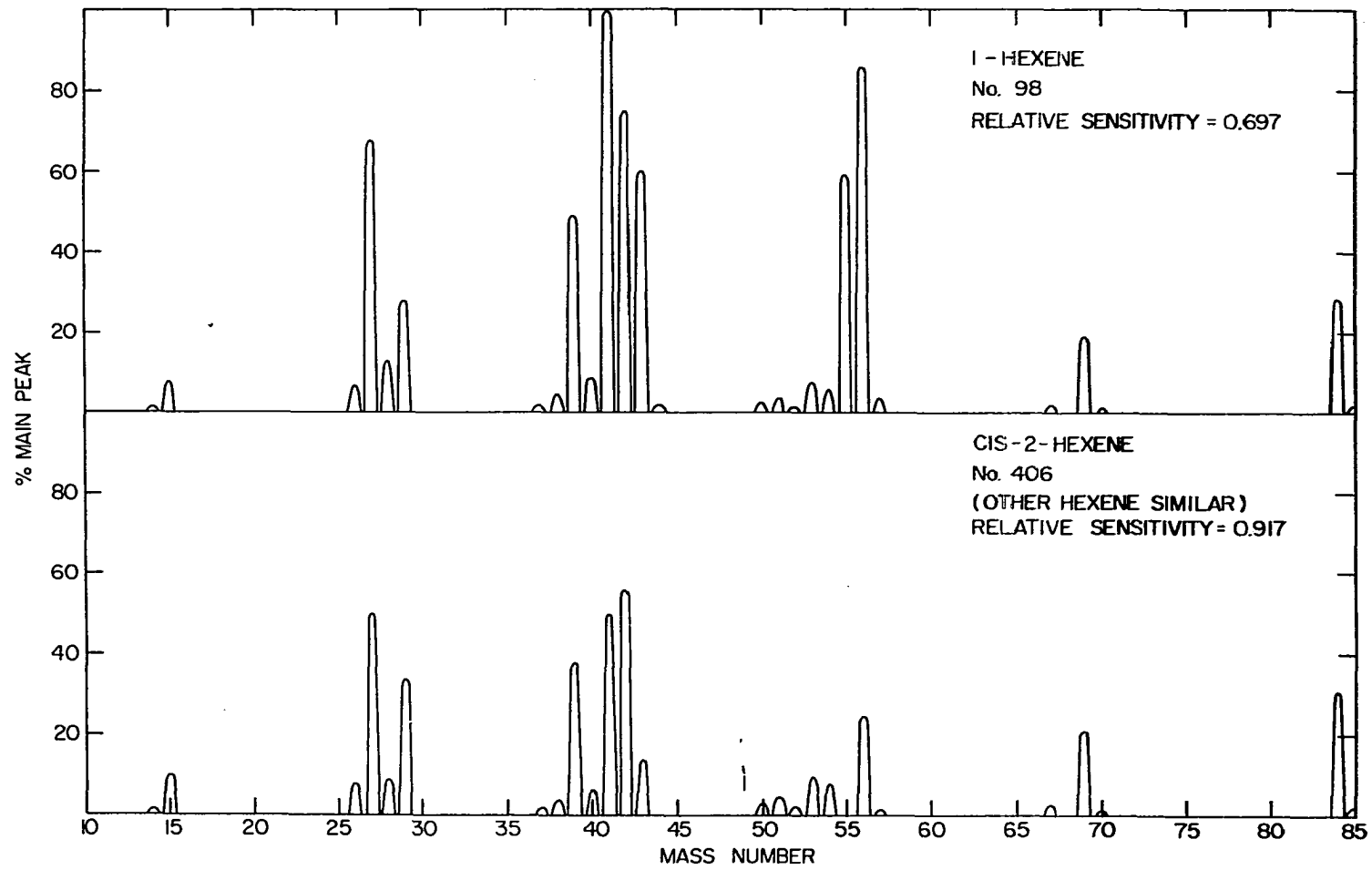
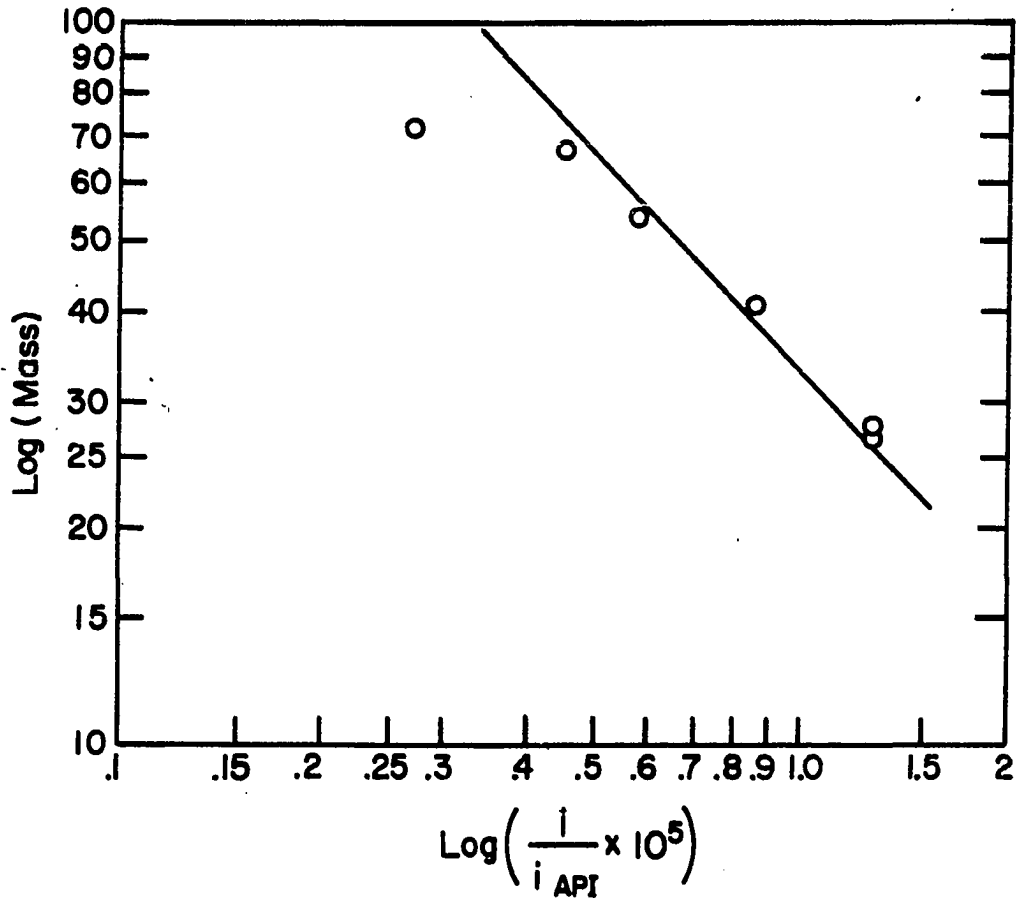


Figure 9. A log-log plot of the atomic mass units for the peaks of cyclohexene vs. the quotient of the observed peak intensities in the quadrupole mass spectrometer by the API listed relative peak intensities (2)

This figure illustrates the dependence of the gain of the particle multiplier on the collected fragment's mass. The line shown with a slope of  $-1$  is the dependence determined by Ploch and Walcher (25).





be followed in a small range. In the present case masses 50, 54, and 56 were picked to follow benzene, cyclohexene and cyclohexane. Scans in other mass ranges were used to determine the presence of other reasonable products, except for hydrogen, none was found in the present work. The mass peak 80 was missing in all the experiments, and therefore no cyclohexadiene was evolved. The mass 55 peak never exceeded 35% of the mass 56 peak; this information plus API tables suffices to prove that no 1-hexene was evolved. This range of peaks (50 to 56) was sufficient to calculate relative pressures of the products.

Absolute pressures in these experiments are unknown since the only pressure indicator used is the ion gauge. The ion gauge will read the pressure within an order of magnitude and is a reproduceable reference for a particular gas since its sensitivity will not change much with time. The mass spectrometer sensitivity, however, does change. This is due to the change in gain of the electron multiplier with gas adsorption on its diode surfaces. For each experiment the mass spectrometer was cross calibrated with the ion gauge so that relative pressures were known from experiment to experiment.

For calibration if  $P_i$  is the pressure reading on the ion gauge and  $i$  is the current from the multiplier of the mass spectrometer for a major mass peak of the species, then  $S_A$ , the sensitivity relative to the ion gauge of species "A", is given by  $S_A = i/P_i$ . The relative sensitivities to various gases can also be calculated from the relative sensitivities compared to n-butane given in the API Tables. It is convenient to define a quantity  $S_{RA}$ , the relative sensitivity of A with respect to n-butane,

as  $S_{RA} = i_{MA}/i_{n\text{-butane}}$ , where  $i_{MA}$  is the absolute sensitivity to the major peak of A and  $i_{n\text{-butane}}$  the absolute sensitivity to mass 43 of n-butane according to the API tables. The pressure of gas B is given in terms of the relative and absolute sensitivities of another gas A that has been calibrated with the ion gauge by

$$P_B = \frac{S_{RA}}{S_{RB}} \frac{i_B}{S_A} \cdot \quad 24.$$

If peaks other than the major peaks are used then the percentages, Z, relative to the major peaks are taken into account by modifying the equation to

$$P_B = \frac{S_{RA} Z_A}{S_{RB} Z_B} \frac{i_B}{S_A} \cdot \quad 25.$$

The supporting electronics for the Ultex 150 mass spectrometer included the 150 control unit, a Keithley 601 electrometer for measurement of the multiplier current and a Beckman high speed Hoffmann recorder Dynograph model R.

## FIELD EMISSION MICROSCOPY-EXPERIMENTAL

Because of the length of time required in a field emission experiment ordinary ultra high vacuums will not suffice and vacuums of  $10^{-13}$  torr or better are needed. These vacuums are easily obtained by immersing a closed field emission microscope in liquid helium. At these temperatures all gases except hydrogen and helium freeze with a residual pressure of less than  $10^{-14}$  torr. Helium is no problem either since its partial pressure in an evacuated field emission tube is less than  $10^{-13}$  torr and at 4°K the diffusion of helium through pyrex is extremely slow. Hydrogen is the only gas which may be present and with suitable means can be controlled.

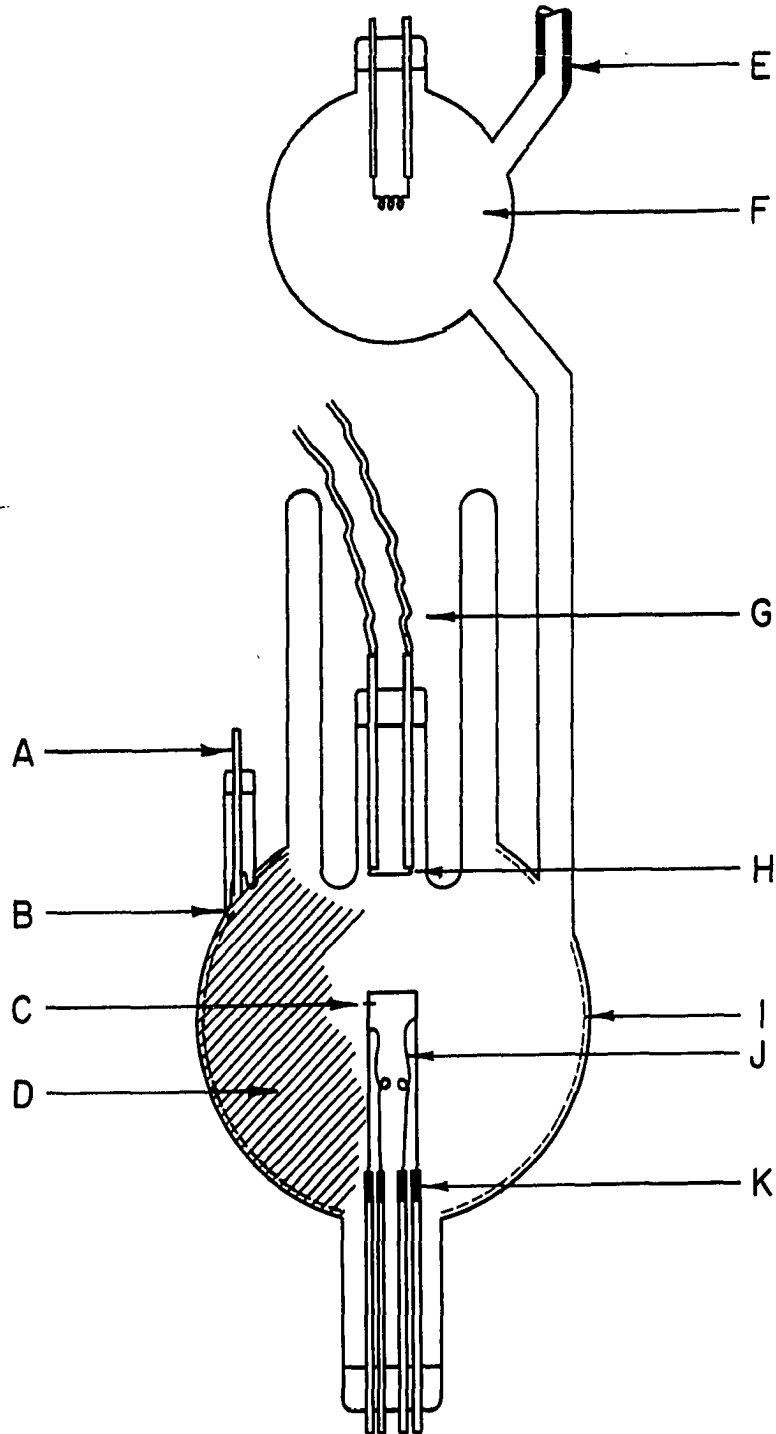
## The Field Emission Microscope

A schematic for the field emission tube is given in Figure 10. The basic parts of this tube are the tip filament assembly, the platinum foil on a reentrant dewar for condensing gases, and the high voltage phosphorescent screen for detection of emitted electrons.

The field emitter tip is mounted on a tungsten filament. This filament is spot welded to a press seal via Nichrome inserts. The inserts help reduce thermal conductivity from the wire to the tungsten leads of the press seal; this facilitates temperature control at the tip. Sensing leads on either side of the tip provide a means of measuring the voltage drop across a standard section of the filament. Knowing the resistance of this section at 295°K and the current through the filament, the temperature is obtainable from Equations 20 and 21. Using

Figure 10. The field emission microscope tube with the components listed below

- A high voltage lead in
- B tungsten hair spring to make electrical contact to screen's conductive coating
- C the field emission tip
- D phosphorescent screen
- E thick wall tubing for sealing off vacuum system
- F getter bulb
- G electrical leads to platinum foil
- H platinum foil for storage of condensable gases
- I conductive coating (tin oxide film)
- J tungsten sensing leads
- K nichrome heat barriers



the sensed voltage and the current one can electronically control the temperature by comparing the resistance of this section to an external resistor.

To make the field emitter tip, a 5 mil tungsten wire is electrically etched in dilute KOH solution to a very fine tungsten fiber. This fiber is spot welded nearly in the center of the filament between the sensing leads. It is then etched further until only a small tip remains. Usually, inspection of this tip under 500 power white light, air microscope shows the tip to be too small for resolution. The tip must point toward the screen after the press seal is resealed to the tube.

When the press seal holding the filament tip assembly is sealed to the tube an unobstructed path exists between the field emission tip and the platinum foil; this is essential because of the trapping ability of any surface at 4°K.

The platinum foil is used as a storage place for condensable gases. This foil is spot welded to a two lead press seal which is part of a reentrant dewar. Most hydrocarbons can be stored on such a foil provided the reentrant dewar is cooled with liquid nitrogen. Reentrant walls extending beyond the foil help reduce radiative heating to the foil. When the gas is needed for dosing the tip, the foil is heated slightly by electrical resistance heating.

In operation a magnified image of the field emission tip can be seen on a phosphorescent screen. This screen is biased to a positive potential of 2 to 6 kilovolts with respect to ground. Electrical contact to the screen is accomplished by coating the inside of the tube with tin oxide. A small tungsten spring spot welded on a press seal

contacts this coating by spring pressure.

To eliminate hydrogen a getter bulb is connected to the field emission tube. By vaporizing the titanium wire a metallic coating is built up on the inside of the bulb. Hydrogen adsorbs on this metallic film and is subsequently buried when another layer of metal is deposited. Since the vapor pressure of hydrogen is appreciable at 4°K it is essential to have this getter pump, especially in the case of serial runs without reloading the tube.

#### Gas Loading of the Field Emission Tube

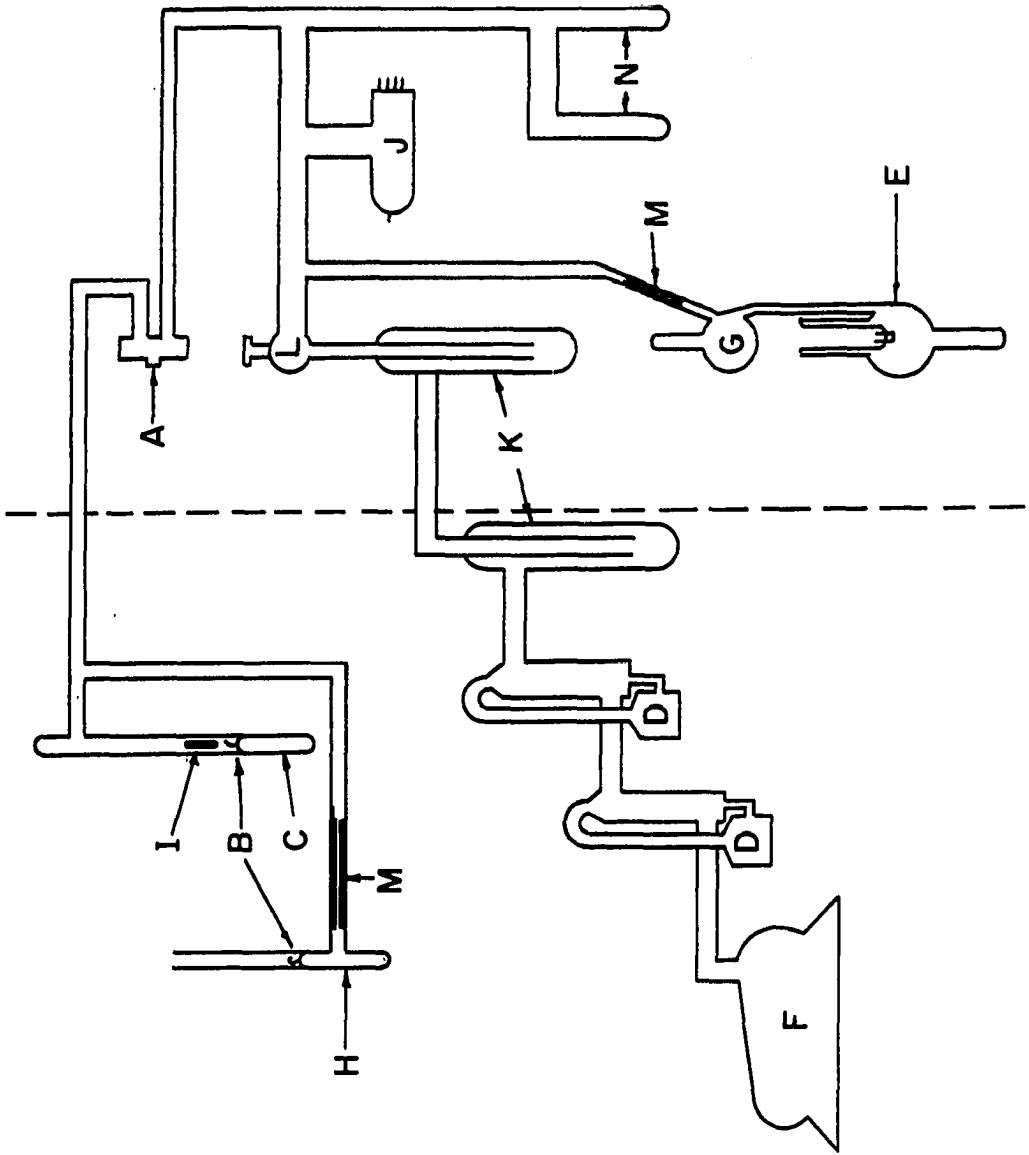
The field emission tube is initially pumped out on an ultra high vacuum gas handling system. Figure 11 indicates the main features of the system used, with diffusion pumps providing evacuation. The tube was sealed to the gas handling system, and system plus tube baked with the pumps on for 8 hours at 400°C by means of a portable oven. Filament and foil were degassed by resistance heating. Following this treatment the pressure in the system (at room temperature) was usually  $2 \times 10^{-9}$  torr. This pressure is certainly low enough for a gas handling system (10).

Gas was admitted to the system by a Granville-Phillips variable leak valve. Before admission to the system the gas was stored in a gas ampule on the non-baked portion of the system. This ampule was opened by breaking a break-off seal with a glass encased iron slug. The ampules of purified benzene and cyclohexene had been previously prepared. An extra ampule was provided to condense out and save unused purified benzene or cyclohexene.



Figure 11. Gas handling high vacuum system with the components listed below

- A Granville-Phillips variable leak valve
- L Granville-Phillips type "L" valve
- J ion gauge
- N distillation thimbles
- M thick wall tubing for sealing from the vacuum system
- E field emission tube
- K liquid nitrogen cooled traps
- D diffusion pumps
- F fore pump
- H gas ampule for saving unused gases
- C gas ampule with sample gas
- B break off seals
- I iron slug encased in pyrex



By closing a type "L" Granville-Phillips valve between the pumps and the system a closed system was obtained. This valve prevented excessive loss of the gas used to load the tube.

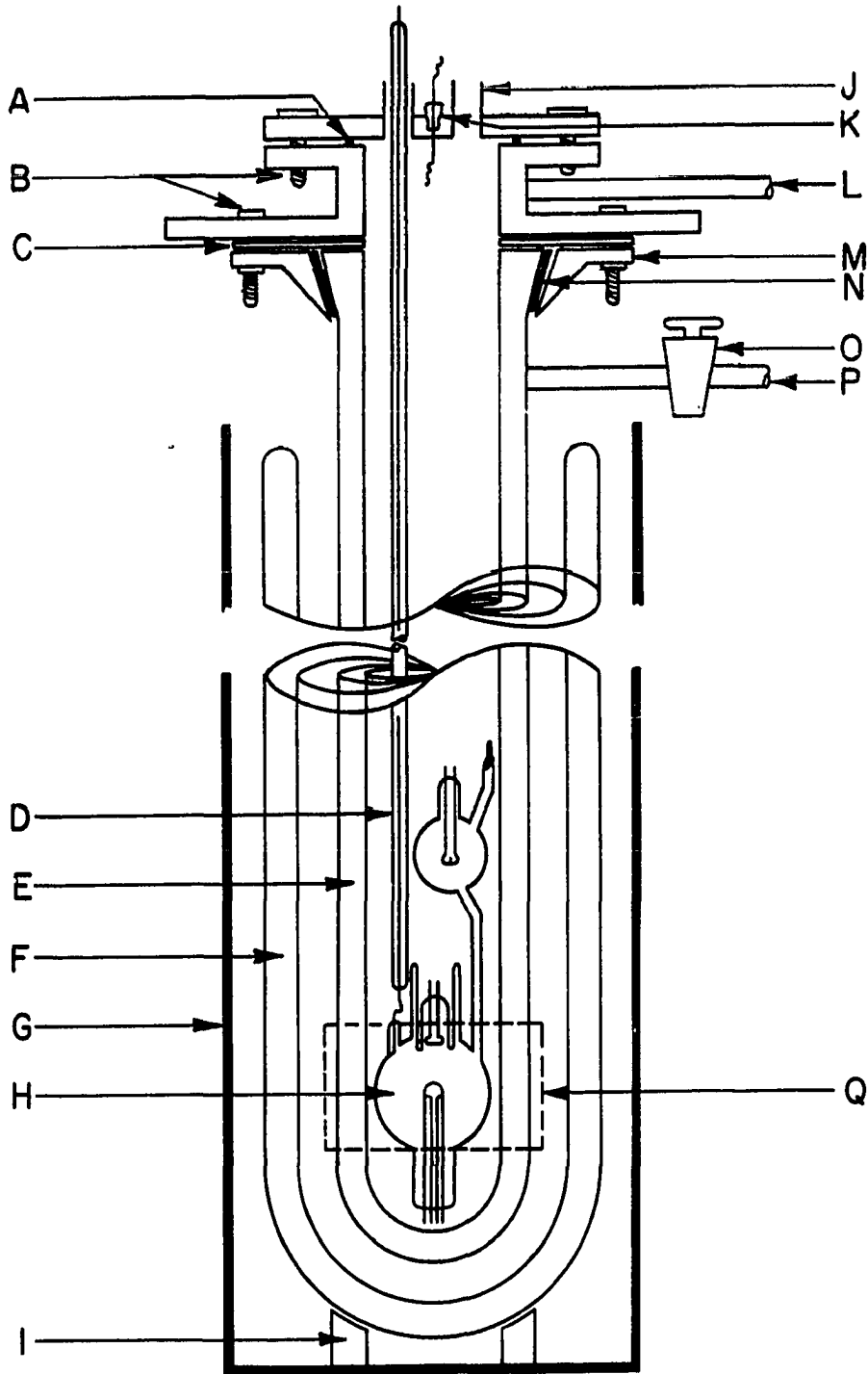
To load the tube the reentrant dewar was filled with liquid nitrogen to cool the platinum foil. With the "L" valve closed the gas was admitted to the system through the variable leak and condensed on the foil. Enough gas condensed on the foil to form a visible deposit. After pumping on the tube with the "L" valve open and the variable leak valve shut, the tube was sealed off and removed from the system. A section of thick wall tubing between the system and the tube helped in this process. The thick wall tubing collapsed evenly upon heating with a glass-blowing torch, making sealing and separation simple. At no time from the admission of the gas to the tube until the placement of the tube in the liquid nitrogen cooled cryostat was the temperature of the foil allowed to exceed 77°K.

#### The Cryostat

A diagram of the cryostat used is given in Figure 12. The main parts of the cryostat were two silvered dewars. The outer dewar for liquid nitrogen coolant had a permanently evacuated jacket. The inner dewar vacuum jacket was provided with a pump out port. This was for flushing with dry nitrogen gas and pumping to eliminate any helium gas (which diffuses through pyrex at such a rate as to destroy the insulating properties of the jacket after several days). Slits permitted observation of liquid nitrogen and liquid helium levels inside the dewars. A 60 x 100 mm. window to the inside of the cryostat permitted the field

Figure 12. The cryostat with the components listed below

- A rubber "O" ring
- B tightening bolts
- C rubber gasket
- D evacuated glass high voltage probe
- E liquid helium pyrex dewar
- F liquid nitrogen pyrex dewar
- G steel safety casing
- H field emission tube
- I cork ring
- J liquid helium transfer inlet
- K BNC electrical feed throughs
- L pump out port
- M pipe flange fitting
- N rubber gasket
- O stop cock
- P pump out port to liquid helium dewar jacket



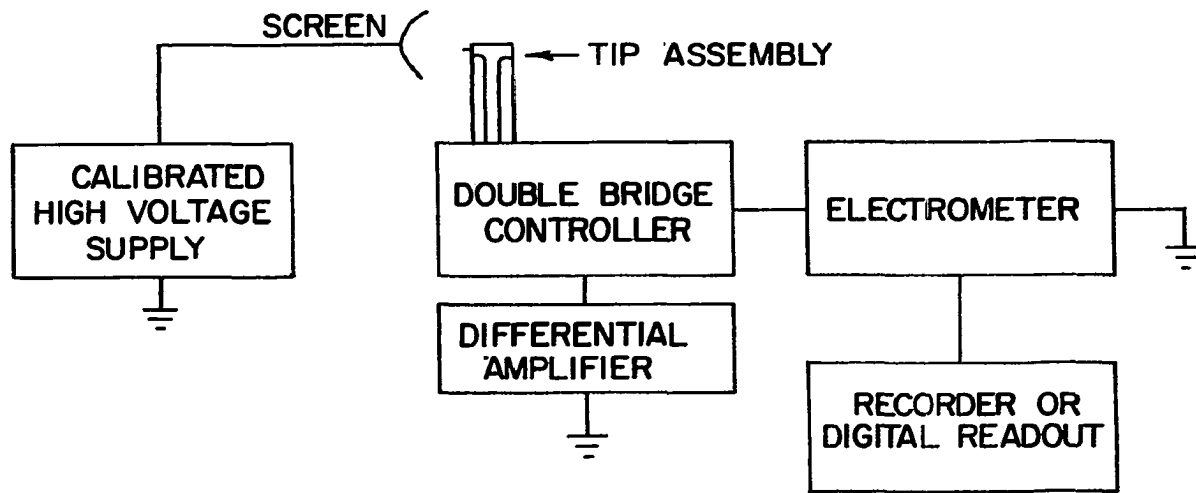
emission pattern to be observed and photographed. A metal casing with appropriate slit and window surrounded these dewars. An air tight collar closed off the inner space to the inner dewar. The removable top of this collar contained electrical feed throughs, a special high voltage probe and a tubular opening for the liquid helium transfer tube. A pump out port was also provided on this collar for flushing out and pumping the inner space.

To prepare for an experiment the outer dewar was filled with liquid nitrogen and the collar top was replaced with a plexiglass plate to keep moisture out of the inner space. The field emission tube was connected to the high voltage probe, which is attached to the collar top, and all electrical connections were made. The plexiglass plate was then removed and the tube lowered into the inner space. With the collar top bolted in place the vacuum jacket of the inner dewar was flushed with nitrogen gas and then pumped to less than a micron pressure. A lower pressure of nitrogen was not necessary since it condenses on the dewar wall at  $4^{\circ}\text{K}$ . To eliminate the possibility of a fogged window due to condensed nitrogen the inner space was cyclically flushed with helium gas and pumped. With helium gas in the inner space, helium was then transferred.

#### Electronics for Field Emission

A block diagram of the electronics used is given in Figure 13. The high voltage source used was a Fluke model 410B. A Keithley 601 or 610B or a Cary vibrating reed model 31 electrometer was used for current measurements. All electrometers used were accurate to within 2% generally and 1% relatively on a single current range; accuracy was

Figure 13. Block diagram of electronics used in field emission

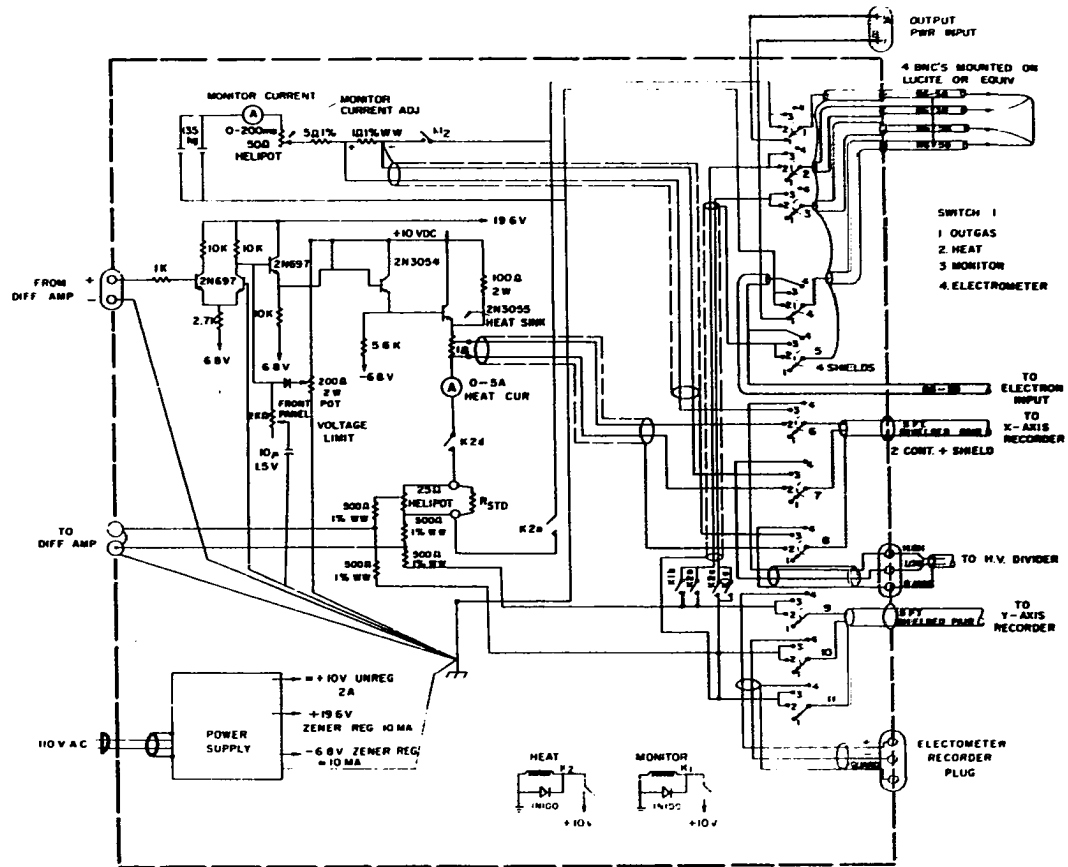




limited by specifications of the feedback resistors. A simple power supply was used for heating the platinum foil gas supply. The special Kelvin double bridge tip temperature controller was built and designed by the Ames Laboratory Instrumentation Group. A circuit diagram of this controller is given in Figure 14. The differential amplifier used in conjunction with this bridge was a Sanborn model 860-4300.

The principle of operation of the tip temperature controller is as follows. A resistance corresponding to resistance between the sensing leads at the desired tip temperature is dialed in on a ten turn potentiometer. With the power current going through both this resistor and the filament any difference in resistance can be sensed as a difference in two potential drops, one between the sensing leads, the other across the potentiometer. With the aid of a differential amplifier this difference is used to control the power source. With proper damping and gain, the resistance of the section between the sensing leads can be controlled to within 1%.

Figure 14. Kelvin double bridge tip temperature controller



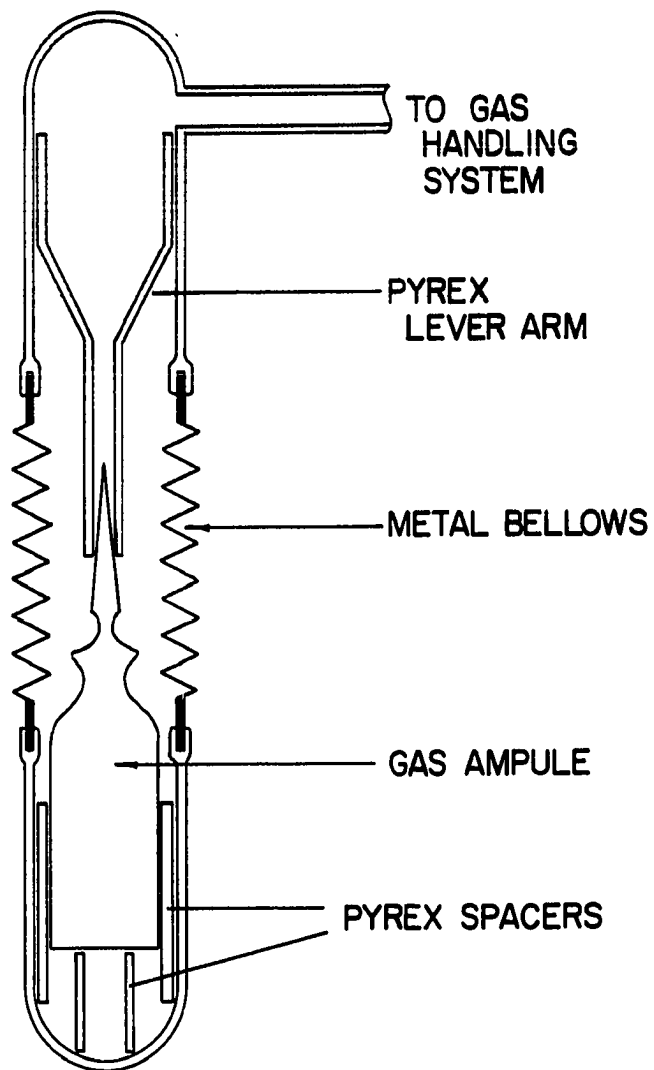
## GAS PREPARATION

The benzene and cyclohexene were supplied by James Hinton, Valparaiso, Florida. Manufacturer's analysis specified maximum total impurities of 0.02% for cyclohexene and 0.001% for benzene. These chemicals were always handled in vacuums of  $1 \times 10^{-8}$  torr ambient or less. The chemicals originally were contained in ampules with break off necks. These necks were broken under high vacuum using metal bellows (Figure 15) to transmit torque. Before admission to the vacuum system the ampules were cleaned externally with acetone and dried.

After breaking the neck of the ampule the gas to be transferred was vacuum distilled several times. The gas was then transferred to gas ampules provided with break off seals. The gas was condensed on the inside of the ampule by cooling the ampule to liquid nitrogen temperature. These ampules were then sealed by collapsing a thick wall tube under vacuum.

Figure 15. Vacuum tight container for opening gas ampules

The metal bellows which are sealed well enough for ultra high vacuums are flexible even with the tube evacuated. To admit a new ampule the top of this tube was glass blown open and the ampule replaced; the tube was then resealed and leak tested.



## FIELD EMISSION RESULTS

## Migration Studies

Migration studies using the field emission microscope can be helpful in determining the number of bonds a species initially makes to the surface. Multiple bonding of benzene to metals has been suggested by Agronomov and Mishechenko (1) and Selwood (29), and preferential adsorption on planes of proper geometry is the fundamental assumption of the multiplet theory of catalysis (5,33). It has also been shown that preferential adsorption will lead to an irregular migration boundary (14).

The migration studies were carried out by dosing the field emission tip in the absence of the electrical field. It is necessary to leave the field off for these shadowing experiments since the benzene is highly polarizable and an electric field will make the benzene travel in a curved trajectory. This deflection with the field on will result in the entire tip being dosed. With the field off a shadowed deposit can be obtained. The tip is heated until the boundary moves.

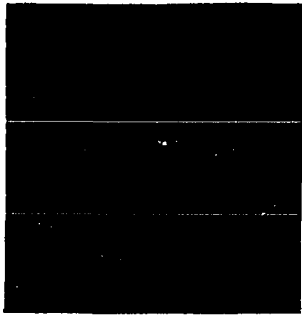
Figure 16 shows the migration at about 85°K. Initially the upper portion of the tip is covered with a multilayer, a monolayer band crosses the tip equatorially and the bottom half is bare. The monolayer lowers the work function whereas the multilayer acts as a dielectric layer and inhibits emission. This gives the field emission pattern the appearance of a narrow band.

Upon further heating the boundaries of both layers move away from the central region. Both layers move uniformly and are not slowed or stopped by a particular plane.

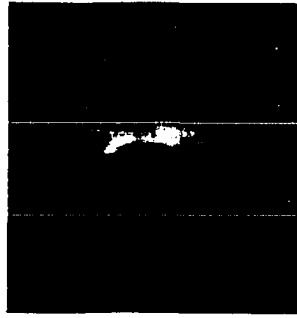
Figure 16. Migration of benzene on a tungsten field emission tip

Dosing of this tip was from the top in these pictures. After shadowing at 4°K only a narrow low work function band emits above which is an insulating dielectric multilayer and below the higher work function clean tungsten. Upon successive heatings first the boundary between the chemisorbed layer and the clean tungsten and then the boundary between the chemisorbed layer and the multilayer move away from the equator of the tip. Both migration fronts are linear. The bottom portion of the pictures at 90°K and 95°K shows a pattern which is referred to as a pseudo-clean pattern.

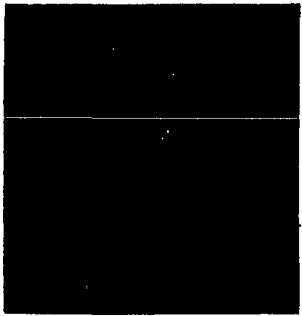




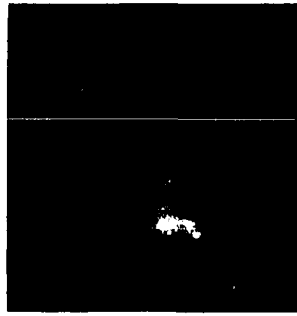
Shadowed Benzene  
Dose at 4°K.



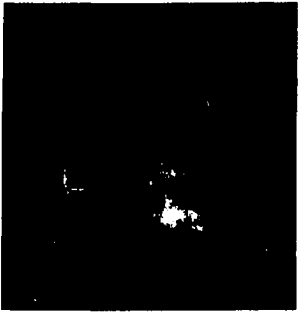
Migration at 80°K  
for 10 sec.



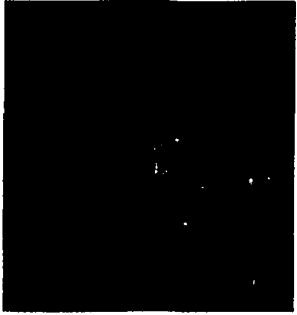
Migration at 80°K  
for 60 sec.



Migration at 90°K  
for 20 sec.



Migration at 90°K  
for 60 sec.



Migration at 95°K  
for 10 sec.

If the multiplet idea (5) were applicable for benzene adsorbed on tungsten a preferential adsorption should occur on certain planes, which is not consistent with the migration behavior. This should also apply to other types of multiple bonding, such as acetylenic and ethylenic type (14) bonding. Singular bonding, such as  $\pi$ -complexing or single sigma bonding, is the only alternative left to explain the experimental results.

The exclusion of the multiplet idea for benzene is tenable in light of Taylor's (32) thermodynamic arguments to explain catalytic activity. This is also in agreement with recent hydrogen exchange work for benzene adsorbed on nickel (15). The absence of any patterns resembling ethylene or acetylene adsorbed on tungsten up to 800°K also lends weight to a singularly bonded species; this will be seen in the next section.

The increase in field emission current following dosing at a given voltage indicates benzene must be chemisorbed, otherwise the dielectric layer would lower the current. If a non-chemisorbed polar species were produced it would line up in the high electric field with the negative portion away from the surface; this would be true even at very low temperatures due to the high electric field as can be seen by the Langevin relation

$$\bar{\mu} = \mu_0 \left( \coth \frac{\mu_0 F}{k T} - \frac{k T}{\mu_0 F} \right) \quad 26.$$

where  $\bar{\mu}$  is the average effective dipole moment. Therefore, chemical bonding to the surface has been proven since the work function decreased and field emission current at a particular voltage increased with adsorption.

## Dependence of Field Emission on Reaction Temperature

Information regarding the reaction path can be deduced by following the dosed tip work function dependence on temperature. The change in the work function can be taken as a measure of the extent of a reaction. If no "window" effect occurs one can assign a  $\Delta\phi$  for a monolayer for each species, and assume linearity with coverage for each adsorbate according to Equation 5, and assume further that changes in work function contributed by each species are additive (8). Then

$$\Delta\phi = \sum_j \theta_j \Delta\phi_j \quad 27.$$

where each species is assigned a particular  $j$ . From this, if one reaction is assumed to occur, the extent of the reaction,  $a$ , occurring on the surface can be written as

$$a = \frac{\Delta\phi_i - \Delta\phi}{\Delta\phi_i - \Delta\phi_f} \quad 28.$$

where  $i$  and  $f$  designate initial and final values. This assumes that each product is either completely adsorbed or completely desorbed, at least to the extent that no difference can be detected experimentally.

During dosage with the field on, the field emission current increases to a maximum and then drops to below the current for the clean tungsten. This is to be expected since initially a chemisorbed layer is forming which changes the work function linearly with coverage. In this case the work function decreases with adsorption of benzene or cyclohexene. This is followed by second layer formation and a dielectric barrier. This second layer is often accompanied by the formation of "molecular

images" which were first observed by Mueller and Melmed (24). Presence of "molecular images" produces Fowler-Nordheim plots with breaks or curves. In the present case the second layer and "molecular images" are of no interest and dosage to only a simple monolayer was studied.

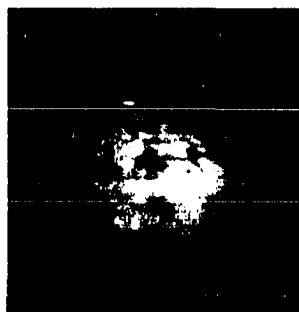
The simplest method of dosing at  $4^{\circ}\text{K}$  is to heat up the platinum foil with constant voltage heating. By gradually increasing the voltage passed through the foil and monitoring the field emission current a point is finally reached where the field emission current increases. When the current then reached a maximum heating of the foil was stopped. The decrease in the work function observed for dosing in this manner with benzene was about 1.0 eV and for cyclohexene usually 0.8 eV. If the tip was dosed at  $150^{\circ}\text{K}$  with benzene a second layer did not form. For a tip dosed heavily at  $4^{\circ}\text{K}$  the second layer usually desorbed readily around  $175^{\circ}\text{K}$ .

To measure the extent of the reaction at various temperatures, the tip was dosed and heated for 20 seconds to successively higher temperatures. After each heating the tip was allowed to cool back to  $4^{\circ}\text{K}$  and series of voltage and current readings were taken for a Fowler-Nordheim plot. Additional heating at a given temperature did not significantly change the work function. This behavior has been previously observed by Arthur (4).

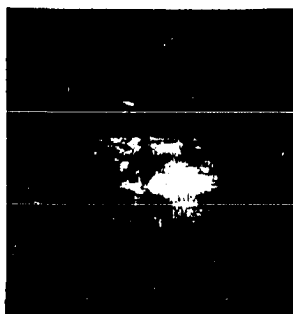
Benzene-dosed tungsten produced a pattern, similar to that for clean tungsten, characterized by large non-emitting roughly circular areas corresponding to principle crystal faces set in a nearly uniformly emitting background. For simplicity this type of pattern will hereafter be referred to as "pseudo-clean". Figure 17 shows such a pattern with a few molecular images appearing as bright spots. No evidence of a pattern

Figure 17. Field emission micrograph of a benzene dosed tungsten tip

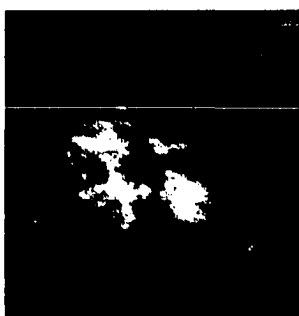
The patterns seen in these pictures are pseudo-clean with a few molecular images showing as bright emission areas. Very little change in the pattern can be detected below 800°K.



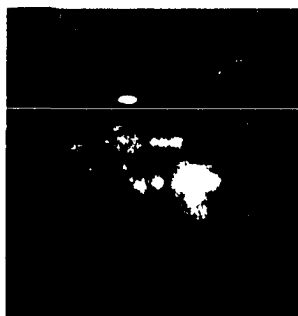
Benzene on W  
Heated to 200°



Heated to 300°K



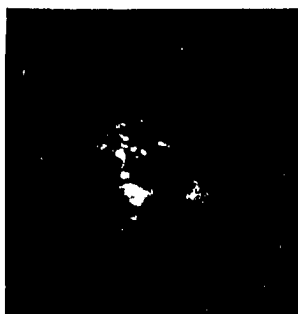
Heated to 500°K



Heated to 550°K



Heated to 700°K



Heated to 850°K

characteristic of hydrogen appeared on a fully covered surface.

In the plot of work function vs. temperature Figure 18 shows that there appears to be a uniform decomposition. The behavior of the decomposition seems to be independent of the starting dose temperature. Figure 19 shows three plots of work function vs. temperature for tips that were dosed to about the same extent. The curves agree well and the small differences could easily be due to differences in dosage.

Figures 20 thru 23 show a series of field emission patterns of a tip that had been dosed very lightly on one side (bottom side) and heavily on the other (top side). Very little change appears until around 437°K. Up to this point the upper portion of the tip had a lower work function than the lower portion and consequently emitted more intensely. This shows the pseudo-clean pattern as seen in previous patterns. Beyond 437°K the bottom portion is seen better and at 580°K predominates due to the high work function of the upper portion. From this temperature up to 912°K the bottom part of the pattern is similar to the atomic nitrogen pattern observed by Ehrlich (11). This suggests a chemisorbed species similar to chemisorbed atomic nitrogen. The radical C-H is isoelectronic with atomic nitrogen and is a likely possibility. C-H radical has been proposed to account for poisoning of tungsten by ethylene and acetylene (14). Atomic carbon or both atomic carbon and C-H radical are alternate possibilities. Beyond 912°K a typical carbon on tungsten pattern (14,22) is observed and above 1000°K a pattern that might be typical of surface  $W_2C$  (18,22) appears. Figure 24 presents the single-point work function determinations for this series with regions where changes are occurring indicated.

Figure 18. Work function dependence on reaction temperature for clean tungsten dosed with a benzene monolayer and for tungsten with the degradation products of  $800^{\circ}\text{K}$  originally on the surface and then dosed with benzene

After the initial doses and work function determinations the tip was successively heated to higher temperatures (abscissa), cooled to  $4^{\circ}\text{K}$  and the work function (ordinate) determined. The work function was determined from the slope of the Fowler-Nordheim plot with the clean tungsten work function assumed to be 4.5 eV. It was assumed that no change occurred in the slope of the clean tungsten Fowler-Nordheim plot since the same tip was used throughout both experiments.



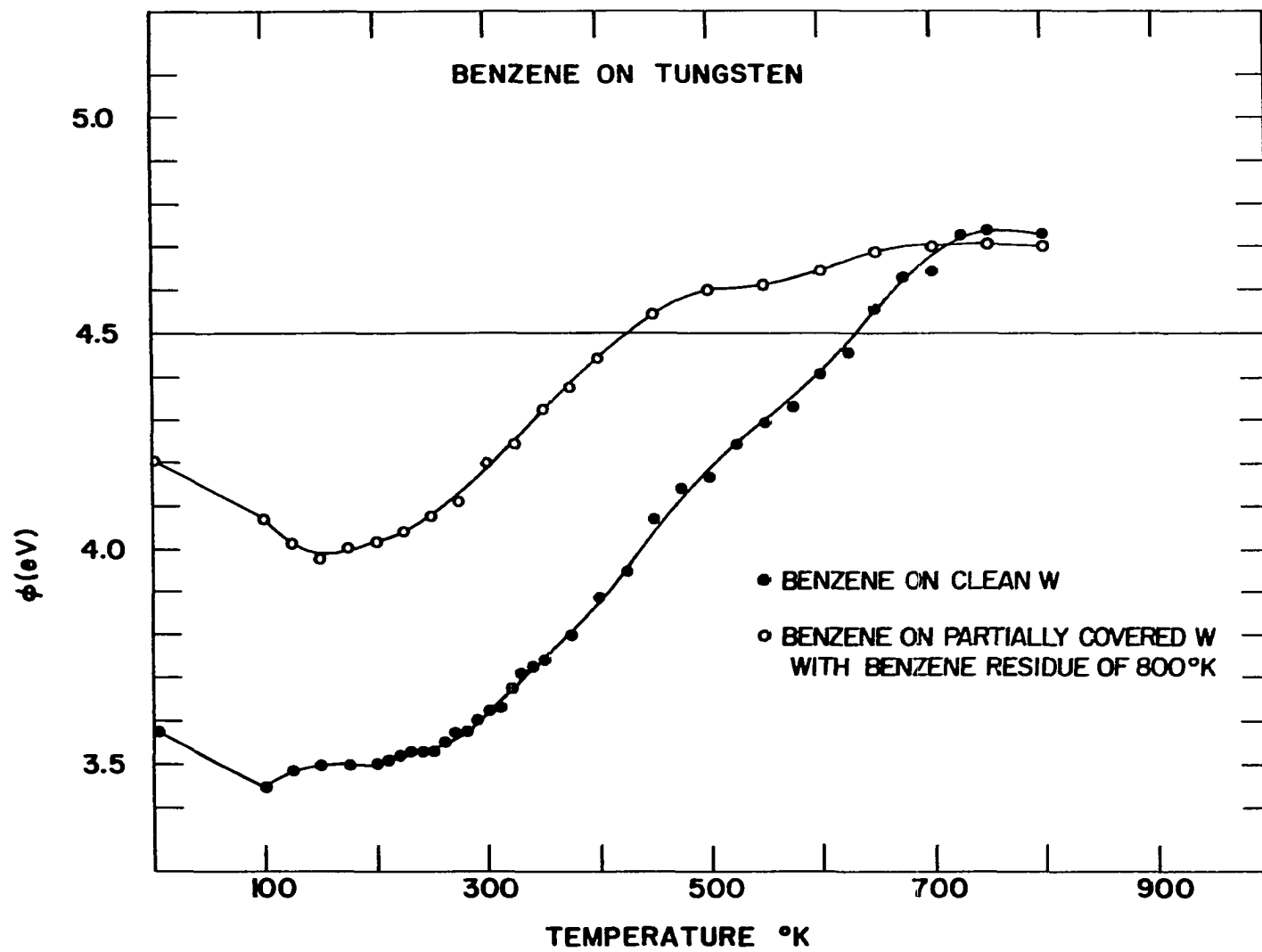


Figure 19. Work function dependence on reaction temperature for tungsten dosed with benzene with the tungsten at three different dosing temperatures

After the initial dose (with the tip at 4°K, 150°K or 300°K) and work function determination the tip was successively heated to higher temperatures (abscissa), cooled to 4°K and the work function (ordinate) determined. The work function was determined by the Fowler-Nordheim method with the clean tungsten work function assumed to be 4.5 eV. In these experiments the benzene flux and dosing time were sufficient to develop more than a monolayer.

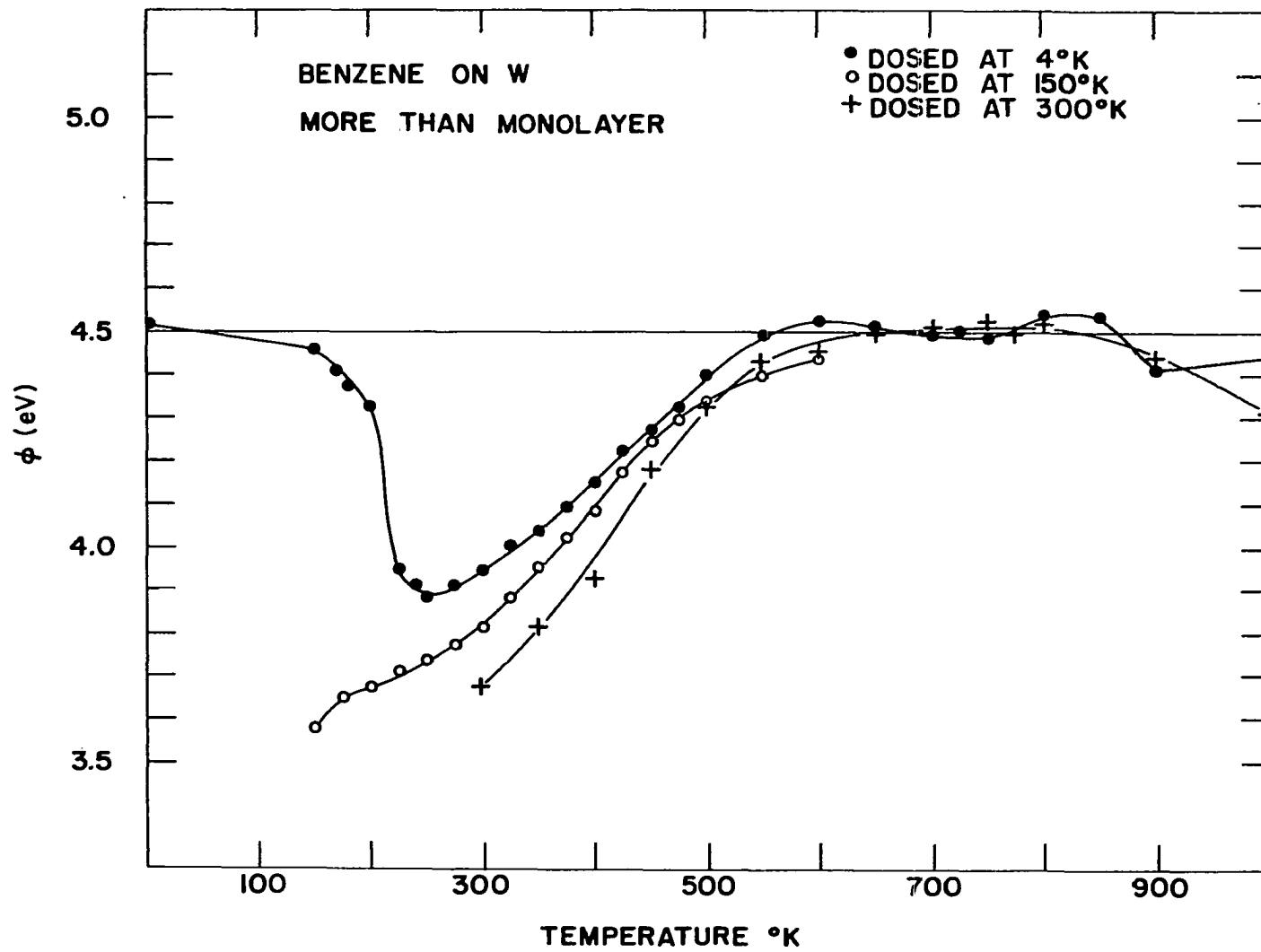
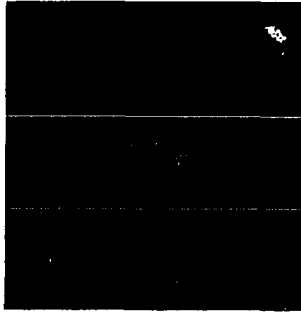
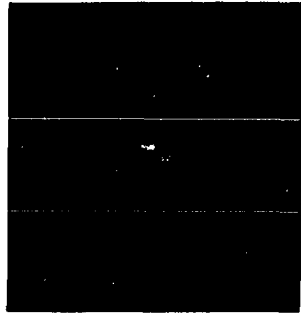


Figure 20. Field emission micrograph of a tungsten tip with a monolayer of benzene on the upper half and less than monolayer of benzene on the lower half

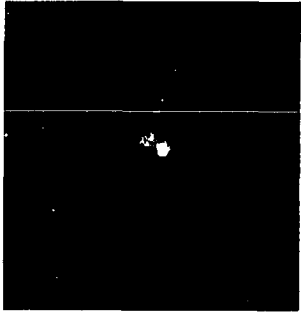
Since chemisorbed benzene lowers the work function only the upper half is observed initially. The tip was heated for 30 sec. to each of the indicated temperatures and allowed to cool to 4°K for photographing. A very slight change is observed at the reaction temperature of 307°K.



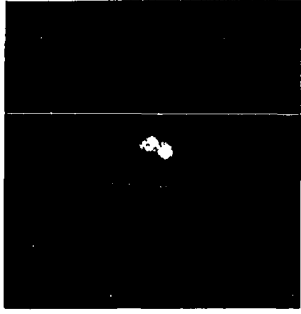
Clean Tungsten  
 $\phi = 4.50 \text{ eV}$



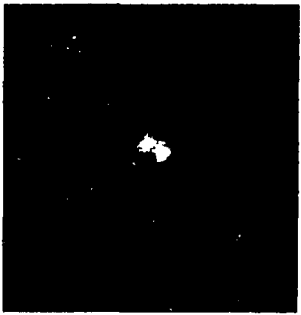
Benzene Dosed at 4°K  
 $\phi = 4.18 \text{ eV}$



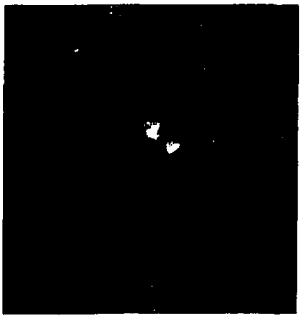
Heated to 98°K  
 $\phi = 4.15 \text{ eV}$



Heated to 105°K  
 $\phi = 4.13 \text{ eV}$



Heated to 148°K  
 $\phi = 4.15 \text{ eV}$



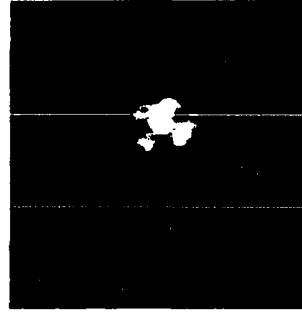
Heated to 307°K  
 $\phi = 4.37 \text{ eV}$

Figure 21. A continuation of the series of photographs of Figure 20

A gradual change occurs from reaction temperatures of 350°K to 510°K due to the increasing work function of the heavily dosed upper portion. Increased work function of this portion requires an increase in applied voltage to obtain an image and consequently increasing the emission from the lightly dosed lower portion.



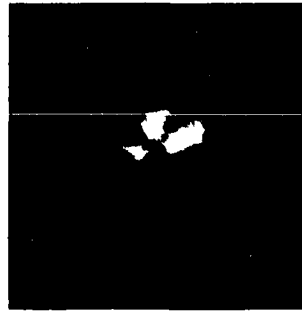
Heat to 350°K  
 $\phi = 4.49$  eV



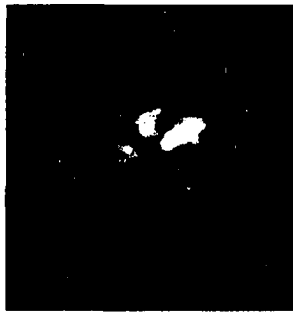
Heated to 365°K  
 $\phi = 4.53$  eV



Heated to 402°K  
 $\phi = 4.62$  eV



Heated to 437°K  
 $\phi = 4.71$  eV



Heated to 472°K  
 $\phi = 4.80$  eV

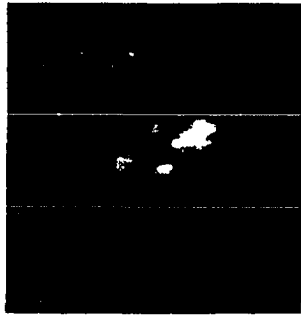


Heated to 510°K  
 $\phi = 4.85$  eV

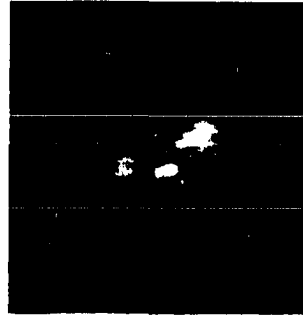
Figure 22. A continuation of the series of photographs of Figure 21.

With increasing reaction temperature the work function increases and the upper portion becomes considerably less emitting than the lightly dosed lower portion. The latter starts emitting a pattern similar to tungsten with atomically adsorbed nitrogen (11).

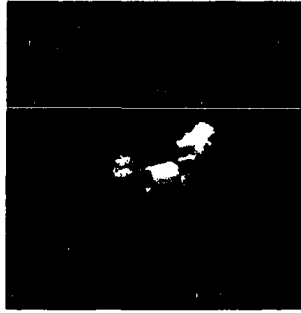




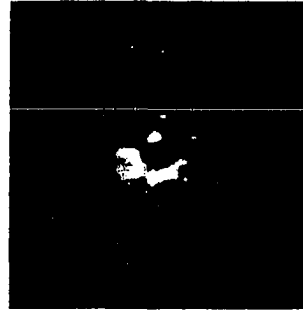
Heated to 545°K  
 $\phi = 4.89$  eV



Heated to 580°K  
 $\phi = 4.91$  eV



Heated to 615°K  
 $\phi = 4.91$  eV



Heated to 645°K  
 $\phi = 4.91$  eV



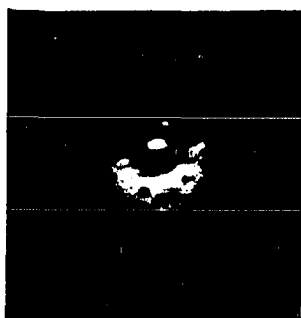
Heated to 675°K  
 $\phi = 4.91$  eV



Heated to 792°K  
 $\phi = 4.88$  eV

Figure 23. A continuation of the series of photographs of Figure 22.

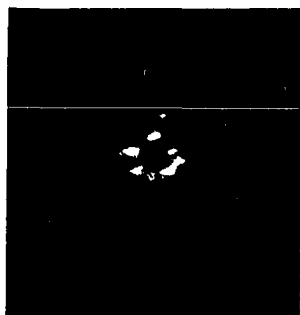
Degradation products start to migrate at reaction temperature of  $912^{\circ}\text{K}$  to produce a pattern typical of carbon on tungsten at  $970^{\circ}\text{K}$  (14). This changes with increased reaction temperature to a pattern believed typical of surface  $\text{W}_2\text{C}$  (18,22).



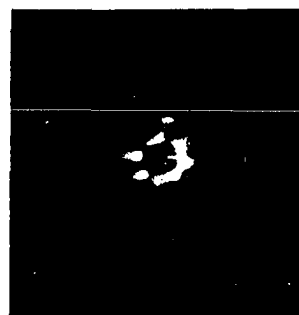
Heated to 852°K  
 $\phi = 4.86$  eV



Heated to 912°K  
 $\phi = 4.83$  eV



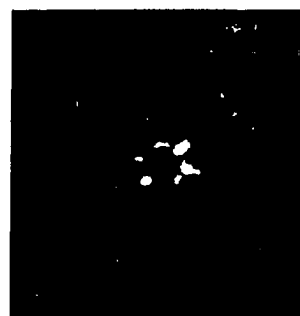
Heated to 940°K  
 $\phi = 4.78$  eV



Heated to 970°K  
 $\phi = 4.75$  eV



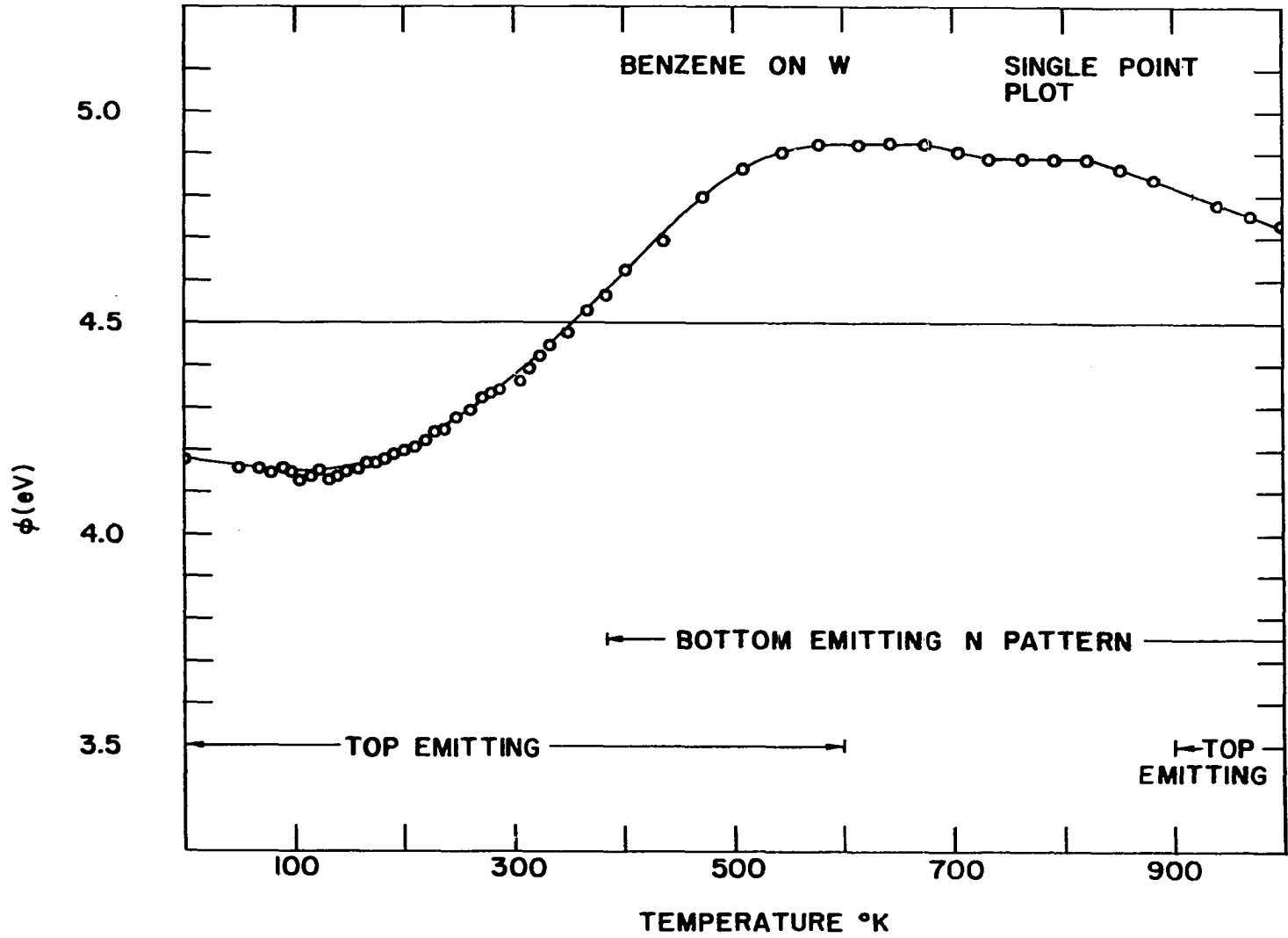
Heated to 1032°K  
 $\phi = 4.66$  eV



Heated to 1230°K  
 $\phi = 4.62$  eV

Figure 24. Work function dependence on reaction temperature for tungsten dosed with benzene as shown in Figures 20 through 23

This is the single point work function determinations which accompany the field emission micrographs shown in Figures 20 through 23. Regions are labelled to show emitting portion of tip (which shows bright in micrographs). Notice that the bottom half of the tip can only be seen if the total measured work function is greater than the work function of clean tungsten.



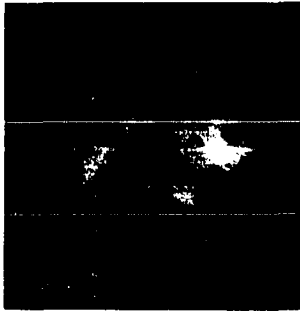
The entire series of field emission experiments of benzene on tungsten suggests a simple uniform decomposition. The benzene might possibly decompose first to acetylenic type species or to C-H radicals before breaking down to adsorbed carbon and hydrogen. This series also shows that benzene or the residue left in its decomposition if once chemisorbed is not mobile.

Figure 25 presents the field emission micrograph sequence for tungsten dosed with cyclohexene and successively heated. Below 300°K the pseudo-clean pattern prevails and at 300°K and above a pattern identical to that obtained with acetylene adsorbed on tungsten develops. This is in contrast to benzene which retains the pseudo-clean pattern until surface carbon begins to appear at 800°K. Equation 5 would imply that, lacking any crystal plane preferential adsorption, the cyclohexene would create a pseudo-clean pattern. Quite the contrary occurs and anisotropy of the work function, implying anisotropy of adsorption, implies acetylene like adsorption. If two point attachment of cyclohexene is assumed to explain the peculiar anisotropy, a reasonable explanation for the identity of the cyclohexene and acetylene patterns above 300°K is two site bonding of cyclohexene with the site spacings the same as for acetylene. In the cyclohexene case below 300°K there may be other species present on the surface, such as chemisorbed benzene, which would produce a pseudo-clean pattern; this is indeed consistent with what is found by flash filament experiments to be discussed in later sections.

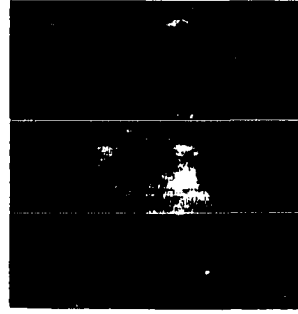
For the assumed two site adsorption for cyclohexene there are two considerations indicating adsorption on adjacent sites spaced  $2.74\text{\AA}$  or  $3.16\text{\AA}$  apart; the other prevalent site spacing on tungsten is  $4.47\text{\AA}$ .

Figure 25. Field emission micrographs of tungsten dosed with cyclohexene

The cyclohexene chemisorbed on tungsten produces a pseudo-clean pattern at 4°K. Heating to higher temperatures for 30 sec. produced little change in the pattern until a reaction temperature of 300°K was reached. It is assumed at this temperature adsorbed benzene (produced in the disproportionation reaction and responsible for the pseudo-clean patterns) is desorbed. Above 300°K reaction temperatures patterns identical to those produced with chemisorbed acetylene are observed.



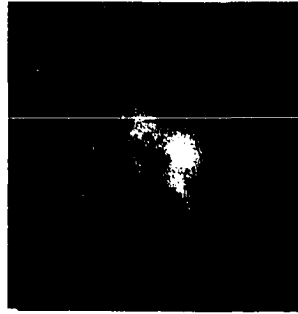
Clean Tungsten  
 $\phi = 4.50 \text{ eV}$



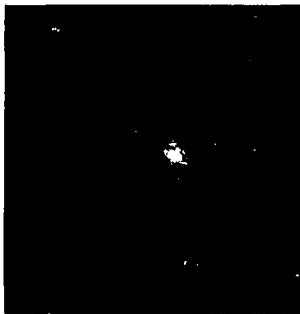
Cyclohexene dose at  
 $4^\circ\text{K}$   $\phi = 4.08 \text{ eV}$



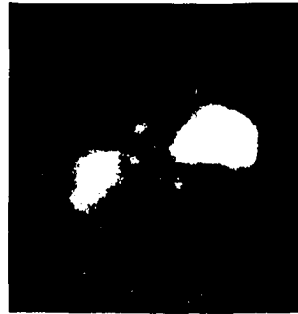
Heated  $175^\circ\text{K}$   
 $\phi = 3.75 \text{ eV}$



Heated to  $300^\circ\text{K}$   
 $\phi = 4.08 \text{ eV}$



Heated to  $375^\circ\text{K}$   
 $\phi = 4.35 \text{ eV}$



Heated to  $500^\circ\text{K}$   
 $\phi = 4.62 \text{ eV}$



First, patterns are markedly similar to those for acetylene, as previously stated; migration studies of acetylene on tungsten (14) indicate preference for planes with a large number of  $2.74\text{\AA}$  and  $3.16\text{\AA}$  spacings and indeed adsorption of acetylene on sites separated by  $4.47\text{\AA}$  would require severe strain. Secondly, trans addition of cyclohexene to the surface which is required for adsorption on  $4.47\text{\AA}$  spacings would necessitate ring strain whereas cis addition would not. The cis addition requires the small  $2.74\text{\AA}$  and  $3.16\text{\AA}$  spacings for two point attachment. Even if bonds formed in trans addition were stronger than for cis addition it seems unlikely that the difference in energy would pay the cost of ring strain<sup>2</sup>. This cis addition is in contrast to the ethylene chemisorption where trans addition seems predominant (14).

Cis addition of cyclohexene to tungsten would force adsorption in a boat form and, on the surface, this has two possible configurations. In one form the points of the boat are pointed away from the surface and in the other form they are pointed toward the surface. The difference in the two forms can be seen in Figure 26 along with the cis and trans configurations of adsorbed ethylene.

The plot of work function against temperature for cyclohexene on tungsten shown in Figure 27 is similar to that for benzene on tungsten suggesting decomposition via benzene intermediate or decomposition via the same intermediates as benzene decomposition. One outstanding difference was the marked work function instability in the intermediate

---

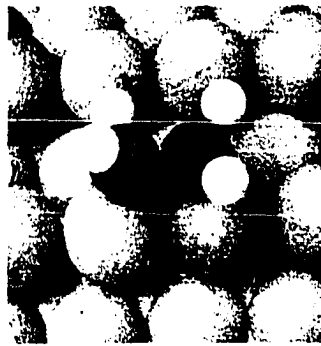
<sup>2</sup>The "strained" ring needed here, with four atoms coplanar, would require about 10 kcal.

Figure 26. Models for possible configurations of ethylene and cyclohexene chemisorbed on a tungsten surface

Ethylene can form two  $\sigma$ -bonds to the surface by trans addition across the 4.47Å tungsten spacing and by cis addition across the 2.74Å and 3.16Å spacings. Cyclohexene can add only cis across the 2.74Å and 3.16Å spacings in the boat form but in two configurations, one in which the points of the boat are away from the surface and one with the points toward the surface.



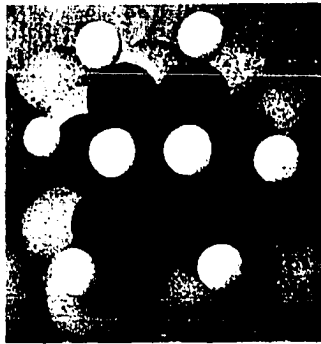
"trans" adsorbed ethylene



"cis" adsorbed ethylene



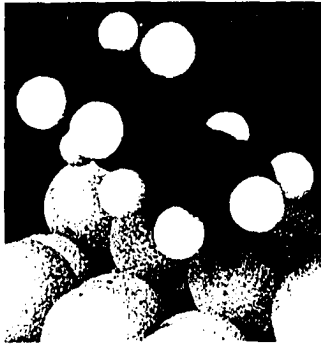
adsorbed cyclohexene  
boat points up  
side view



adsorbed cyclohexene  
boat points up  
top view



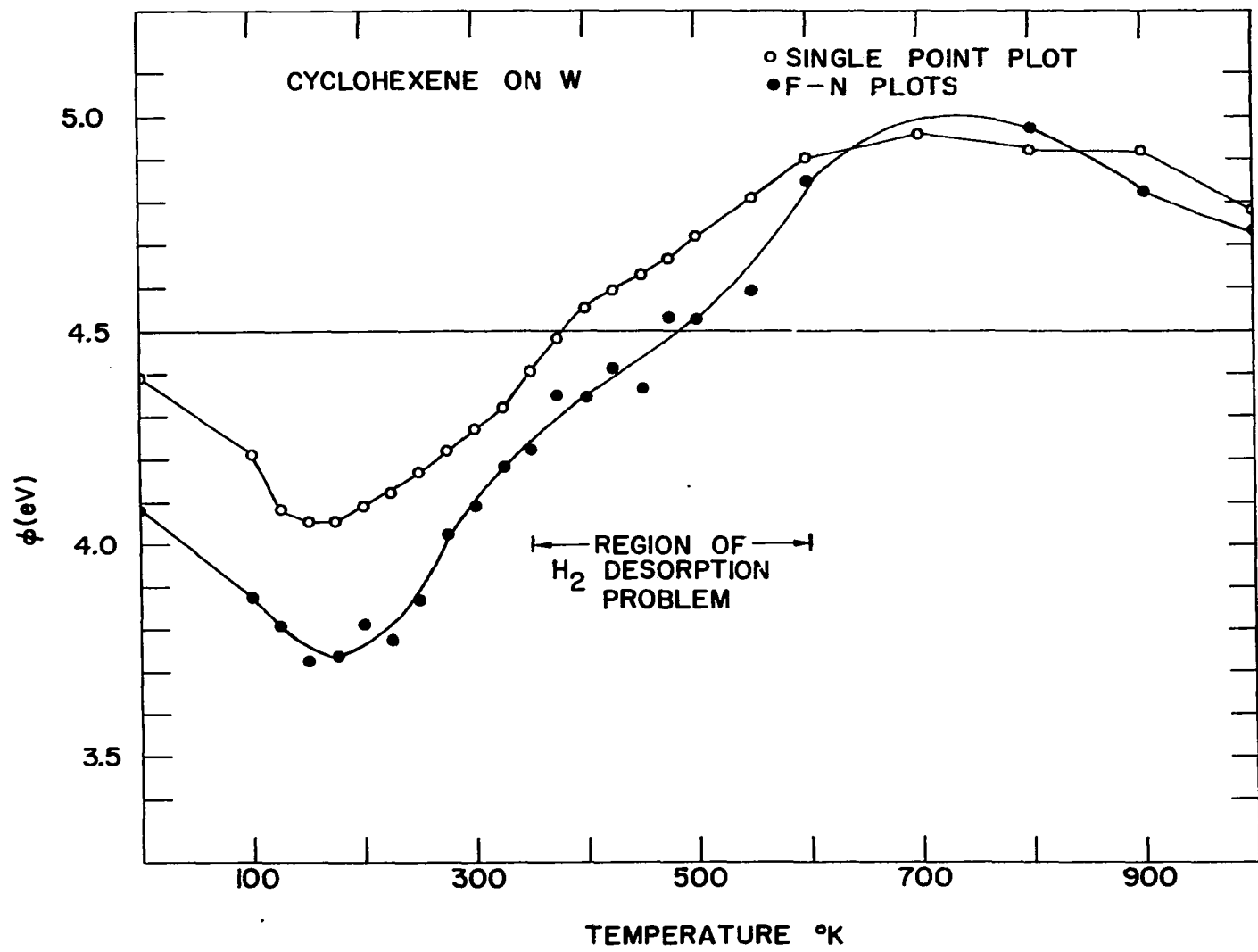
adsorbed cyclohexene  
boat points down  
side view



adsorbed cyclohexene  
boat points down  
angle view

Figure 27. Work function dependence on reaction temperature for tungsten dosed with cyclohexane

After initial dose and work function determination the tip was successively heated to higher temperature (abscissa) for 30 sec., cooled to 4°K and the work function (ordinate) determined. The work function was determined by both the Fowler-Nordheim method and the single point method with the clean work function assumed to be 4.5 eV. In the region between 350°K and 500°K considerable hydrogen desorption created scatter in the Fowler-Nordheim points. Since the single point determinations can be taken rapidly less scatter is observed with this method. The hump in the plot, indicative of surface hydrogen, is therefore resolved by the single point method.



temperature range in the cyclohexene case. The work function tended to lower under the influence of the electrical field. This indicates a field induced reaction, probably the desorption of hydrogen since hydrogen increases the work function (16).

## FLASH FILAMENT RESULTS

## Hydrogenation of Surface Residue

Attempts were made to hydrogenate the residue of benzene decomposition in an effort to obtain some clue as to the composition of the surface intermediates. With the reentrant dewar filled with liquid nitrogen the filament was cleaned by heating to incandescence and allowed to cool for 4 minutes. A pressure of about  $10^{-7}$  torr of benzene was maintained for about 10 seconds allowing about a monolayer to adsorb. The filament was then flashed to  $800^{\circ}\text{K}$  and again allowed to cool. A pressure of  $10^{-6}$  torr of hydrogen was then established with the ground glass valve closed. With the mass spectrometer scanning rapidly from mass 10 to 80 a second flash to  $800^{\circ}\text{K}$  was initiated. In this experiment as well as in the cases where the first flash was to  $500^{\circ}\text{K}$ ,  $400^{\circ}\text{K}$ ,  $375^{\circ}\text{K}$ , and  $300^{\circ}\text{K}$  only methane was evolved.

This result would be expected if the residue were C-H or individual carbon atoms chemisorbed. It does not, however, in any way prove this. The experiment was carried out with the thought that if more complex species did exist on the surface then more complex species might be seen upon hydrogenation.

## High Pumped Flash Filament Experiments

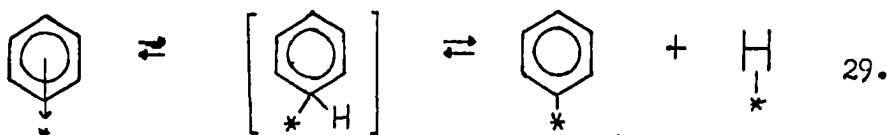
The integral of dosing pressure over time is proportional to the total number of molecules striking the surface during the dose. From Equation 1 it can be shown that a  $10^{-6}$  torr-sec. dose of benzene will cause  $2.5 \times 10^{14}$  per cm. molecules to impact the tungsten surface; this




value is equivalent to about one molecule of benzene per four surface tungsten atoms.

In the present work pressures were measured with a gauge calibrated for nitrogen and doses reported in torr-sec. nitrogen equivalent. Since the sensitivity of this gauge for benzene is at least three times as great as for nitrogen (23) the benzene doses are one third or less the nitrogen equivalent dose.

The filament was dosed at 90°K, then heated with a 0.5 amp heating current with the ground glass valve open; the pressure was recorded for the duration of the flash. Two distinct results were obtained, depending on dosage. For doses of less than  $2.7 \times 10^{-6}$  torr-sec. (nitrogen equivalent) only hydrogen was evolved upon flashing; above this value both benzene and hydrogen would desorb.

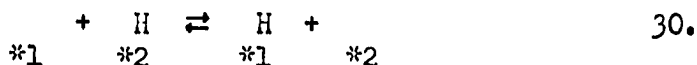
These two facts are most easily rationalized in terms of the dissociative  $\pi$ -complex model proposed by Garnett and Sollich-Baumgartner (15) as represented in Equation 29.



Here  designates a metal  $\pi$ -complexed benzene,  is a phenyl group  $\sigma$ -bonded to metal and  is chemisorbed hydrogen. Retention of resonance energy is in conflict with some current ideas of benzene chemisorption where it is believed the resonance energy is destroyed (31). The postulated intermediate is a phenyl group  $\sigma$ -bonded to both metal and hydrogen with a great deal of its resonance energy retained. As coverage increases the  $\pi$ -complex, requiring only one site per molecule, would be increasingly favored.



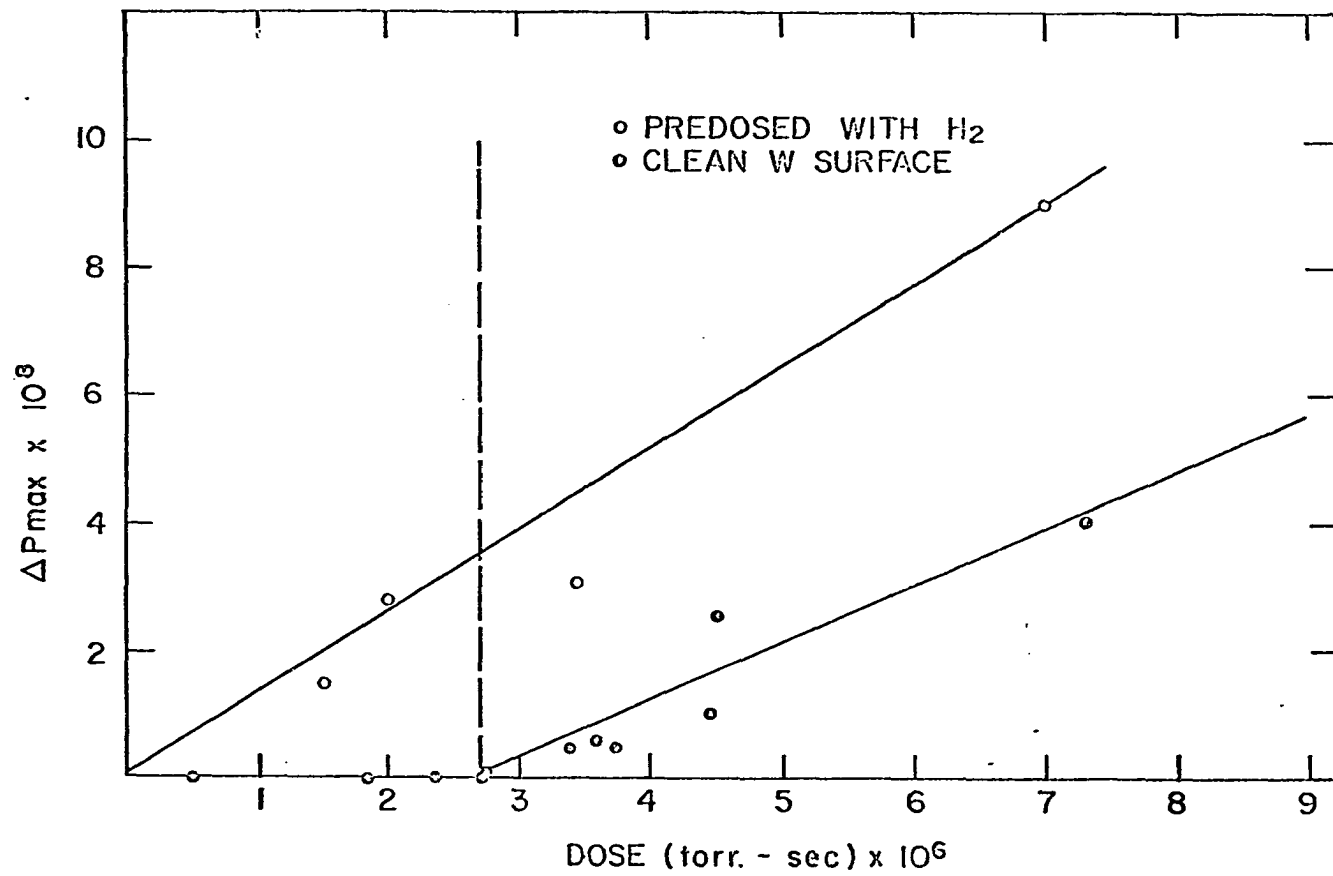
To test this mechanism a series of experiments was carried out with hydrogen preadsorbed on the tungsten filament and benzene subsequently adsorbed. The evolution of benzene was then followed in a high pumped system. Control experiments without preadsorbed hydrogen were also conducted. Figure 28 shows the results of this series. The pressures of benzene shown in this figure are the maxima of observed desorption peaks and are only roughly proportional to the total amount of benzene evolved. The important feature of the figure is that without preadsorbed hydrogen no benzene is evolved below  $2.7 \times 10^{-6}$  torr-sec. dosage whereas with hydrogen preadsorbed this is not the case. When this experiment was carried out using deuterium in place of hydrogen, however, no deuterated benzene was formed although benzene was still evolved below dosages of  $2.7 \times 10^{-6}$  torr-sec. This surprising result suggests two interpretations. First, the hydrogen may be so immobile at the temperature of adsorption that only the hydrogen on a site adjacent to the  $\sigma$ -bonded phenyl group can react to regenerate  $\pi$ -bonded benzene. This would be reasonable if hydrogen migration were slow and definitely involved jumps to adjacent sites, as shown symbolically in Equation 30.



Here the symbols \*1 and \*2 designate distinct and neighboring hydrogen bonding sites. Indeed, Gomer (16) has shown that hydrogen is not appreciably mobile on a scale of the size of a field emission tip below 200°K. Gomer's studies concerned hydrogen migration into regions devoid of chemisorbed molecules. Second, chemisorbed hydrogen may block the

Figure 28. Benzene evolution from a tungsten surface as a function of dosage and hydrogen pre-dosage

The pressure burst of benzene in a high pumped system is shown as a function of dosage. This was done for both initially clean tungsten and tungsten pre-dosed with hydrogen. In the region left of the dashed line benzene evolution does not occur without hydrogen preadsorption.



chemisorption of benzene. This second assumption would imply that if deuterium were adsorbed and then benzene the hydrogen products in the flash would be only deuterium. This is not the case; the hydrogen products are statistically mixed  $H_2$ , HD, and  $D_2$ .

The high pumped flash of Figure 29 has another peculiar feature, that is hydrogen is evolved in large amounts at  $1000^\circ K$  and above. This means that the kinetic analysis will be complicated by the fact that hydrogen is still being evolved in a region where the filament itself will start to pump hydrogen by pyrolytic production of atomic hydrogen. This implies a constantly changing pumping speed and hydrogen production in the temperature range from  $800^\circ K$  to  $1500^\circ K$ . Correction for the pumping speed is therefore very difficult. A new experimental technique will need to be introduced to overcome this situation.

During the course of these experiments no hydrogenated species were detected in the gas phase; only the cracking pattern of pure benzene was observed. Thus, tungsten will not catalyse the hydrogenation of benzene.

Figure 30 shows the total pressure curves for the flash decomposition of cyclohexene from tungsten in the high pumped system. Figure 31 shows a similar curve with the ion current for mass 2 read from the mass spectrometer. This mass 2 reading also includes in it the mass 2 portion of the cracking pattern of cyclohexene, cyclohexane, and benzene. These are shown to be evolved and correspond to the mass 2 peaks observed below  $300^\circ K$ . The rest of the mass 2 current corresponds to hydrogen evolution only. Figure 32 shows the partial pressures of cyclohexene, cyclohexane, and benzene produced in a similar experiment. The peaks monitored for these species were 54, 56, and 50 respectively. No other

Figure 29. Hydrogen desorption from a benzene covered tungsten surface

Hydrogen evolution in a high pumped system is given as a function of the filament temperature. A heating rate of about  $20^{\circ}$  per sec. and a pumping speed of about 20 l. per sec. were used. The curve indicates that hydrogen is evolved to a considerable extent at  $1000^{\circ}\text{K}$ .

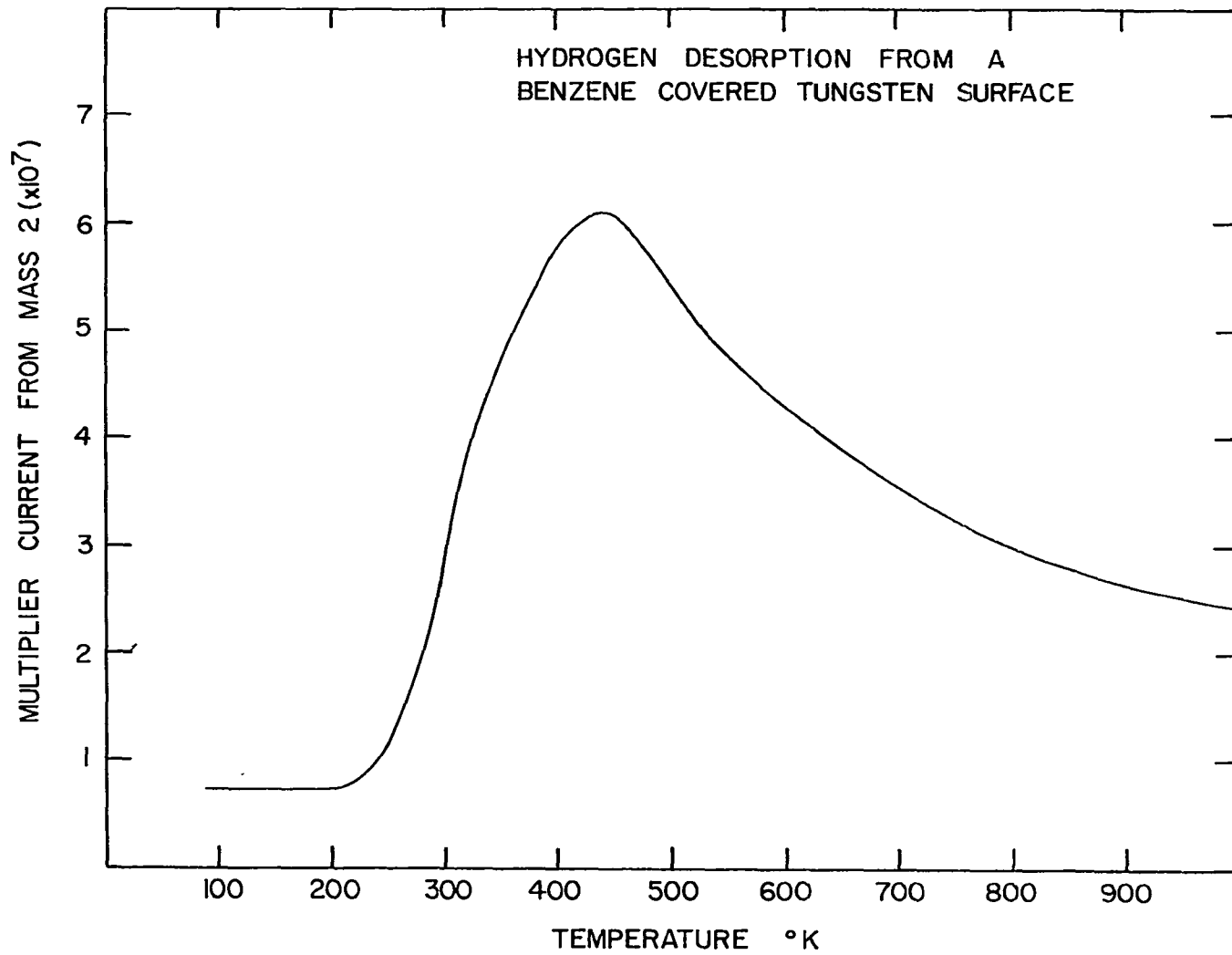


Figure 30. Total gas desorption from heating tungsten filament dosed with cyclohexene in a high pumped system

Four different dosages, 0.56, 0.80, 1.4 and  $3.1 \times 10^{-6}$  torr-sec., of cyclohexene on tungsten are followed by a flash and the total pressure monitored with an ion gauge. The pressure is given as a function of flash time and filament temperature.

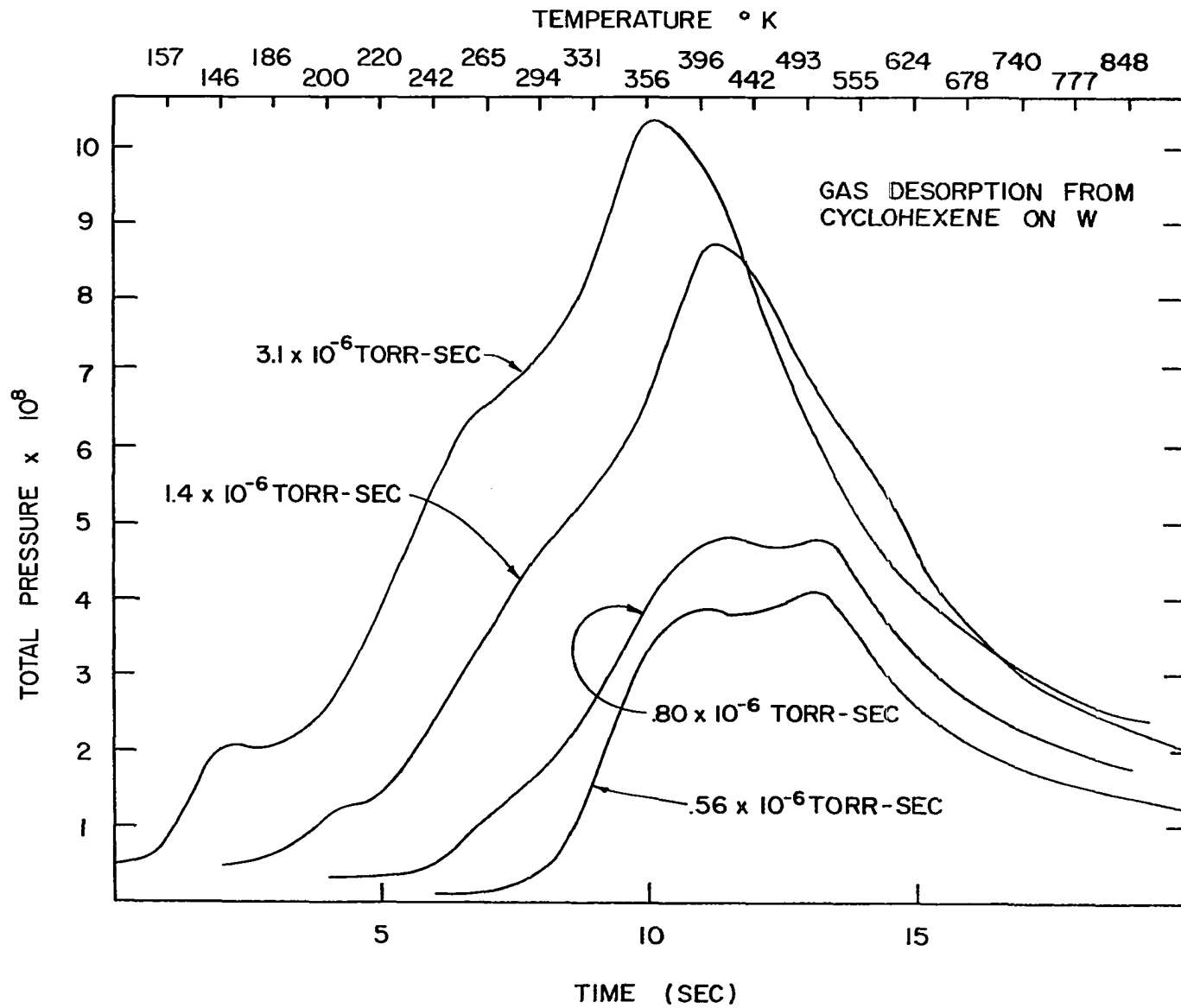




Figure 31. Total pressure and mass 2 ion current in a high pumped system during the heating of a tungsten filament initially covered with cyclohexene

The total pressure and mass 2 ion current are shown as functions of filament temperature which increased at about  $20^{\circ}$  per sec.

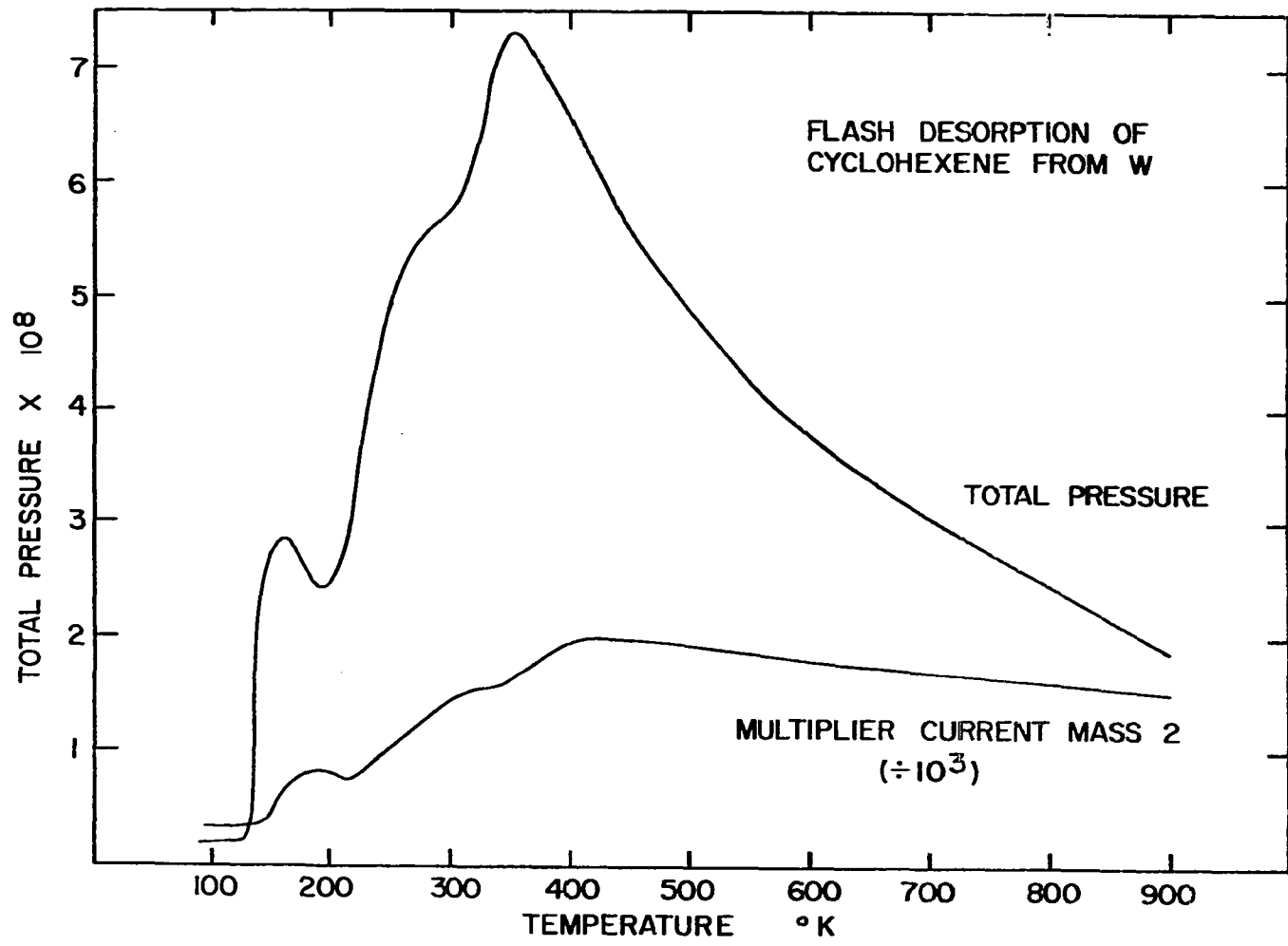
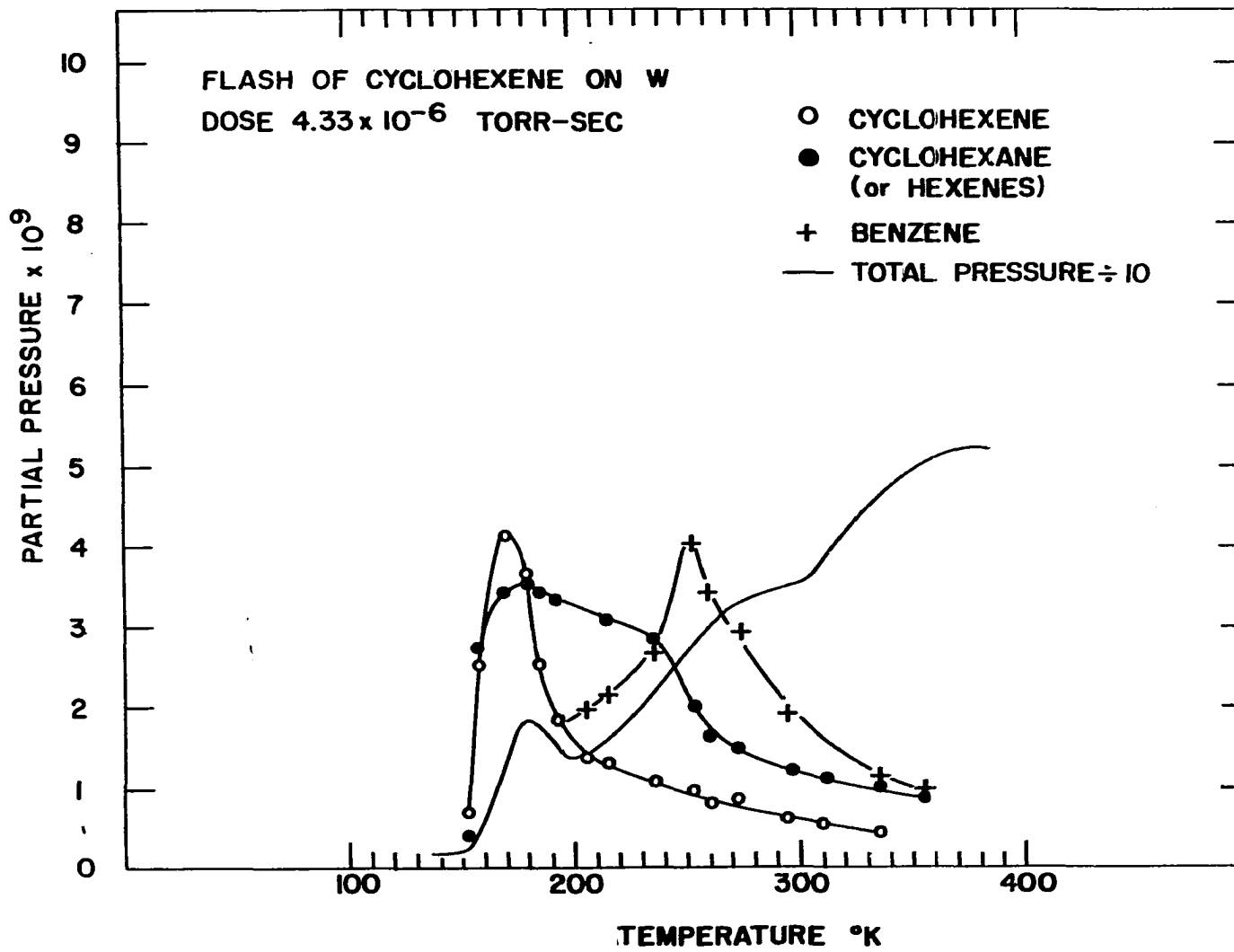
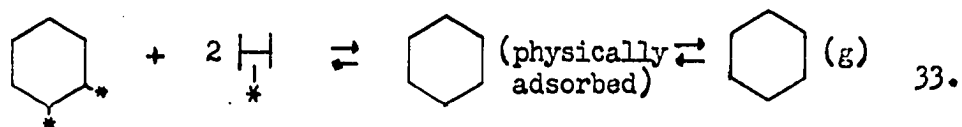
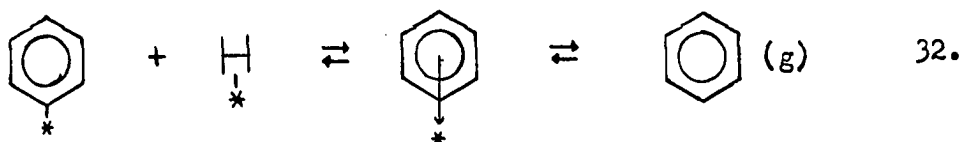
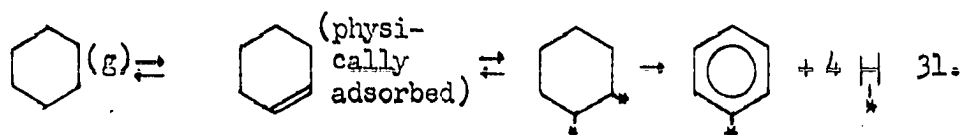


Figure 32. Total pressure and partial pressures of cyclohexene, cyclohexane and benzene during the heating in a high pumped system of a tungsten filament initially covered with cyclohexene

Mass peaks 50, 54 and 56 were used to monitor the partial pressures of benzene, cyclohexene and cyclohexane respectively. These partial pressures are shown as functions of filament temperature which increased about  $20^{\circ}$  per sec.



species were observed. The cyclohexane and benzene were given off in ratio of about 2:1 as would be expected from stoichiometric disproportionation of cyclohexene. Cyclohexane and benzene differ in desorption temperature suggesting that disproportionation occurred and the products were held either in a physically adsorbed layer or as the case of benzene in a weak chemisorbed state as a  $\pi$ -complex. The following sets of reactions are therefore proposed.



Reaction 31 of this series suggests possible rapid hydrogenation of cyclohexene in contrast to behavior reported on other metals and the behavior expected in a Rideal-Eley type mechanism (6) for hydrogenation of alkenes as proposed by N. C. Gardner (14). There is also no provision for poisoning the surface if it is assumed that the  $\pi$ -complexed benzene is easily desorbed. According to Figure 32  $\pi$ -complexed benzene will rapidly leave the surface at temperatures of 250°K to 300°K or higher. This is in contrast to the ethylene case where it is believed that at room temperature the ethylene will leave a considerable number of C-H radicals on the tungsten surface which poison the hydrogenation.

## Room Temperature Hydrogenation and Disproportionation

As a control experiment a tungsten filament at room temperature was exposed to ambient CO pressure for several hours. Hydrogen was admitted to the reaction cell with the ground glass valve shut. This was followed by admission of cyclohexene. During and after admission of cyclohexene the gas phase was monitored with the mass spectrometer using 0.1 second scans. Absolutely no benzene or cyclohexane was observed.

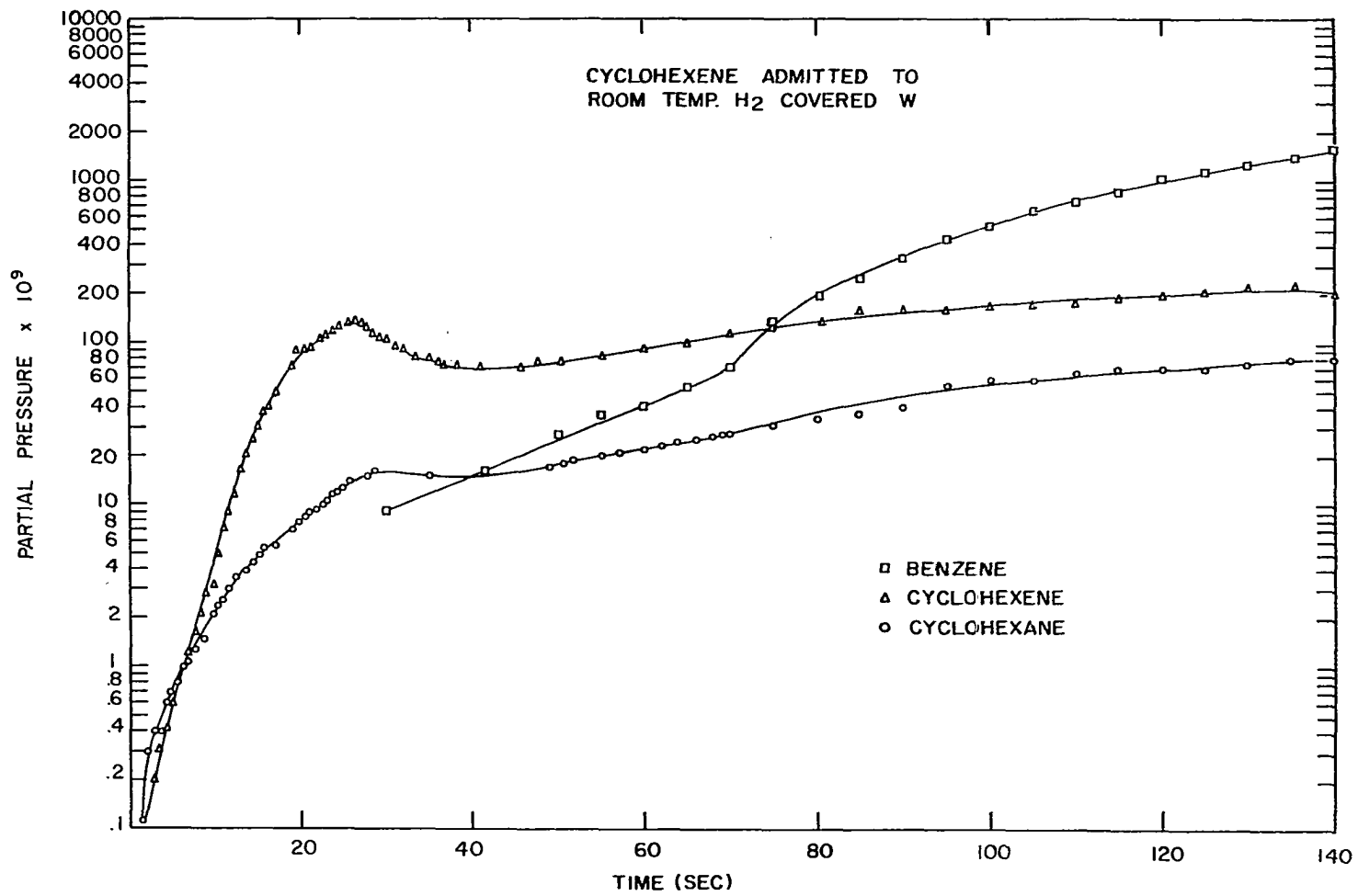
For another control the filament was contaminated by adsorbing cyclohexene and flashing to 1000°K producing a carbon covered surface. Again, admission of cyclohexene did not result in benzene or cyclohexane production.

With a clean tungsten surface, however, a very rapid hydrogenation of cyclohexene was observed. This was followed by a slow but continuous disproportionation. These results are shown in Figure 33. The benzene was difficult to observe below  $1 \times 10^{-8}$  torr partial pressure. This is because the 50 mass peak for benzene is only a 15% peak; cyclohexene also has a small 50 peak in its cracking pattern and this must be subtracted before the benzene pressure can be calculated. To obtain pressures a cross calibration with the ion gauge was made immediately after the experiment with the glass valve open and  $10^{-7}$  torr cyclohexene pressure. This flow system made it possible for nearly all the gas to be cyclohexene.

Since the hydrogenation starts immediately upon admission of cyclohexene to the reaction cell at a pressure of  $10^{-9}$  torr and less, any mechanism which requires abstraction of hydrogen from chemisorbed cyclohexene must be ruled out. Further, in absence of preadsorbed hydrogen the self-hydrogenation is accompanied by benzene production. This

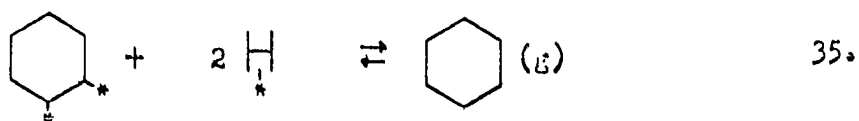
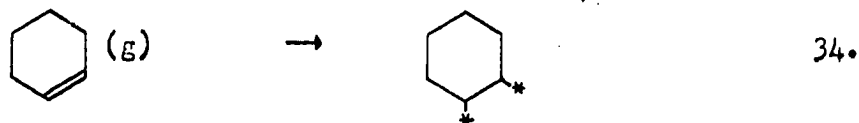
Figure 33. The hydrogenation and disproportionation of cyclohexene on hydrogen covered tungsten at room temperature

Masses 50, 54 and 56 (benzene, cyclohexene and cyclohexane respectively) were monitored when cyclohexene was exposed at room temperature to a tungsten wire that had been cleaned and predosed with hydrogen. An initial fast hydrogenation is followed by a continuous disproportionation.





strongly indicates reaction of adsorbed cyclohexene with chemisorbed hydrogen. Field emission patterns indicate that cyclohexene is chemisorbed. Therefore, evidence favors the reactions



The double attachment model is proposed to account for the lack of pseudo-clean field emission patterns above 300°K for cyclohexene on tungsten.

#### Decomposition of Benzene and Cyclohexene

Figures 34 and 35 show the pressure behavior during a slow flash in the system with the ground glass valve shut. These two figures are for benzene decomposition and cyclohexene decomposition respectively. With the valve shut a nearly closed system is obtained. There is enough of a leak through the valve to the D. I. pump to allow relative pressure readings. The flashes were accomplished using a current density of about  $3.1 \times 10^3$  amps per  $\text{cm}^2$  (0.5 amp through 5 mil wire) through the filament. At this rate large pumping corrections are needed to compensate for the leak through the ground glass valve.

The shoulder on the cyclohexene desorption peak makes the kinetic analysis very difficult. This shoulder, as seen before, is due to evolution of cyclohexene, cyclohexane, and benzene. The benzene decomposition curve, however, presents no complication of this type and it could be assumed that cyclohexene decomposition proceeds via a benzene intermediate.

Figure 34. Total pressure rise during the heating of a tungsten wire dosed with benzene

The heating current passed through the 5 mil tungsten wire was 0.5 amp. and the pressure rise in the reaction cell is proportional to the D. I. pump current on the pumped side of the ground glass valve. A fairly large correction is needed to compensate for pumping.

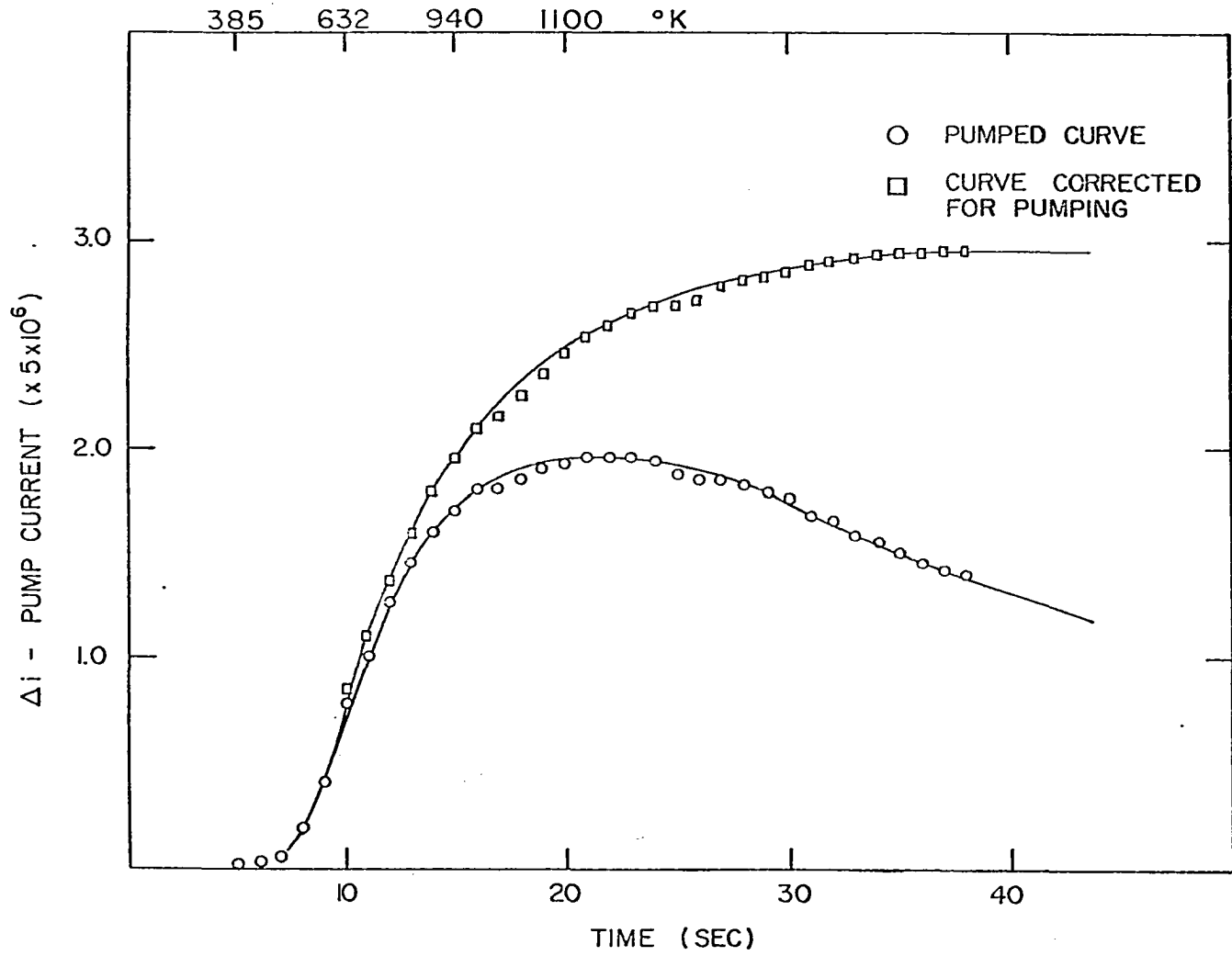
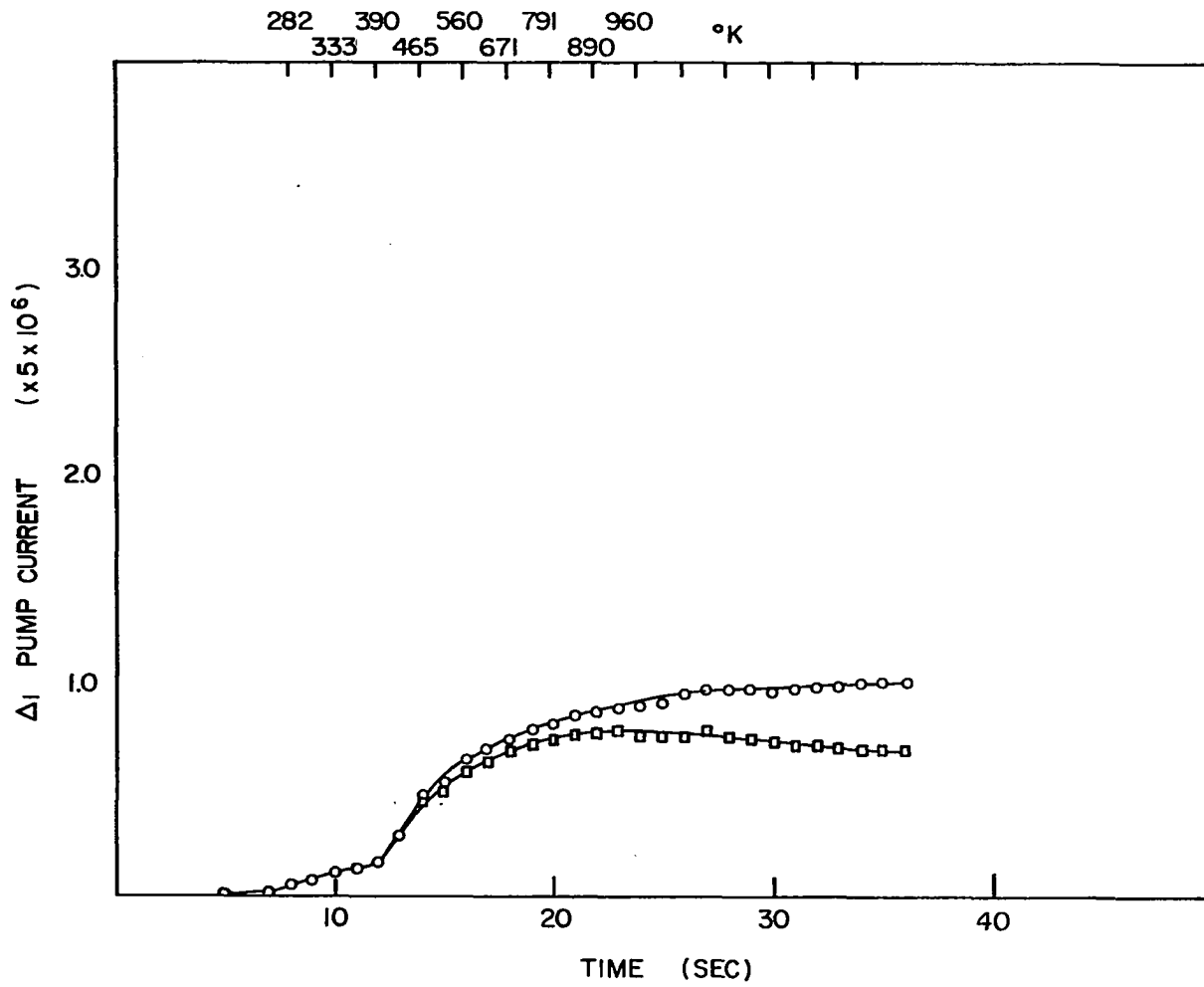


Figure 35. Total pressure rise during the heating of a tungsten wire dosed with cyclohexene

The heating current passed through the 5 mil tungsten wire was 0.5 amp. and the pressure rise in the reaction cell is proportional to the D. I. pump current on the pumped side of the ground glass valve. The small hump in the pressure rise at 300°K renders the kinetic analysis difficult.



Interpretation of the decomposition curve Figure 34 is complicated by filament pumping of hydrogen above  $1100^{\circ}\text{K}$ , as explained previously. The pumping speed corrections were made after 35 sec. at which time the filament was pumping considerably. The hydrogen that is desorbing above  $1100^{\circ}\text{K}$  is important for kinetic analysis; the total hydrogen desorbed is a vital piece of information in this analysis.

To overcome these difficulties the experiment was carried out in the following fashion. The filament was flashed with 1.85 amps from  $90^{\circ}\text{K}$  to about  $800^{\circ}\text{K}$ . At this point an A. C. current of constant voltage was applied taking the temperature to  $2000^{\circ}\text{K}$  in less than 0.1 sec. Since the flash to  $800^{\circ}\text{K}$  occurs in 2 seconds the pumping correction from the glass valve leak is negligible (less than 1%). Above  $1500^{\circ}\text{K}$  the pumping speed is essentially constant. Therefore, the observed pumping speed in the A. C. region can be assumed to start immediately after application of the A. C. voltage.

Figure 36 shows a typical desorption trace with the accompanying heating rate curve. The desorption curve corrected for pumping in the A. C. heating region is given as a broken line. This curve is normalized; that is all pressures are given relative to the final corrected pressure as 1. The pressure was measured with an ion gauge on the pumped side of the ground glass valve.

Figure 37 shows first and second order kinetic plots for this experiment. It is clear that the second order plot is linear and the first order plot is not. Figure 38 gives second order plots for various coverages of benzene. There appears to be a slight trend toward a more negative slope with decreased coverage. Figure 39 gives a comparison

Figure 36. An example of the pressure burst and temperature rise during a fast flash

1.85 amps was passed through a 5 mil tungsten wire that was dosed with benzene. The pressure rise was measured on the pumped side of the ground glass valve with an ion gauge. No pumping correction is necessary due to the low pumping and high heating rate until the filament is rapidly heated with A. C.; this correction is shown as a dashed line.

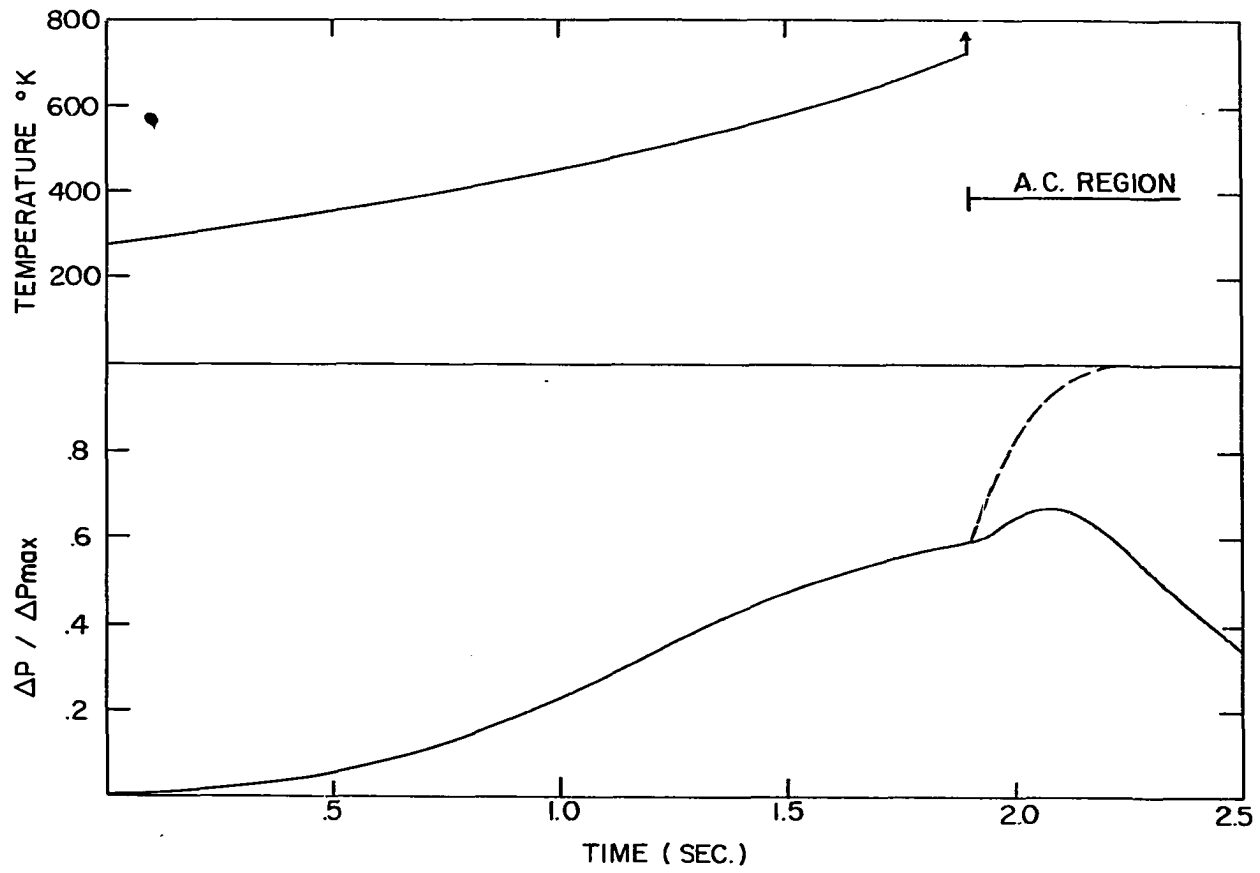




Figure 37. First and second order kinetic analysis of benzene decomposition on tungsten

The  $\log \log_e n_0/n$  vs.  $1/T$  and  $\log \frac{n_0 - n}{n}$  vs.  $1/T$  are

plotted to determine the kinetic order and activation energy for the degradation of benzene on a tungsten surface. Since hydrogen is being monitored  $n$  refers to the amount of hydrogen remaining on the surface (either as surface hydrogen or bonded to benzene) and  $n_0$  is the final amount of hydrogen desorbed (and also the amount initially present on the surface).

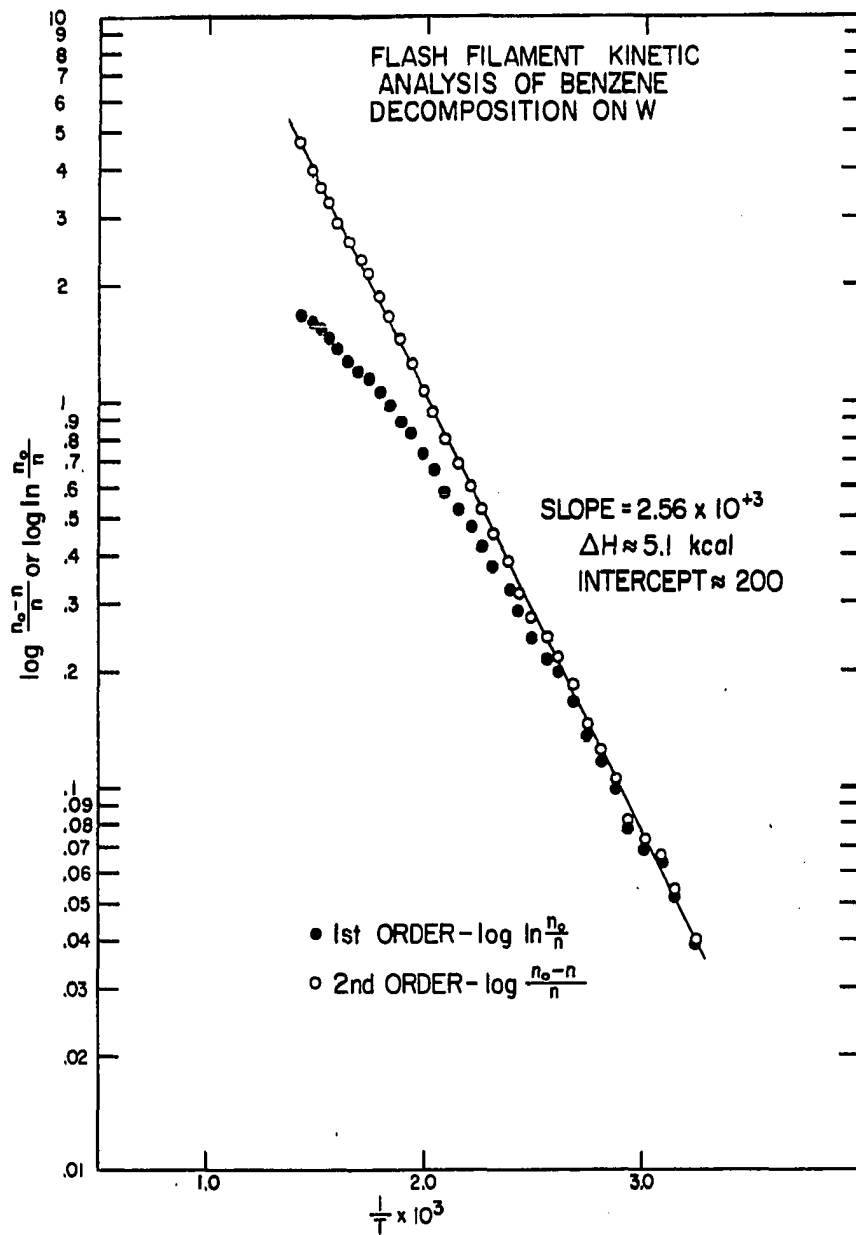


Figure 38. Second order kinetic plots of benzene degradation on tungsten for five different initial dosages as indicated

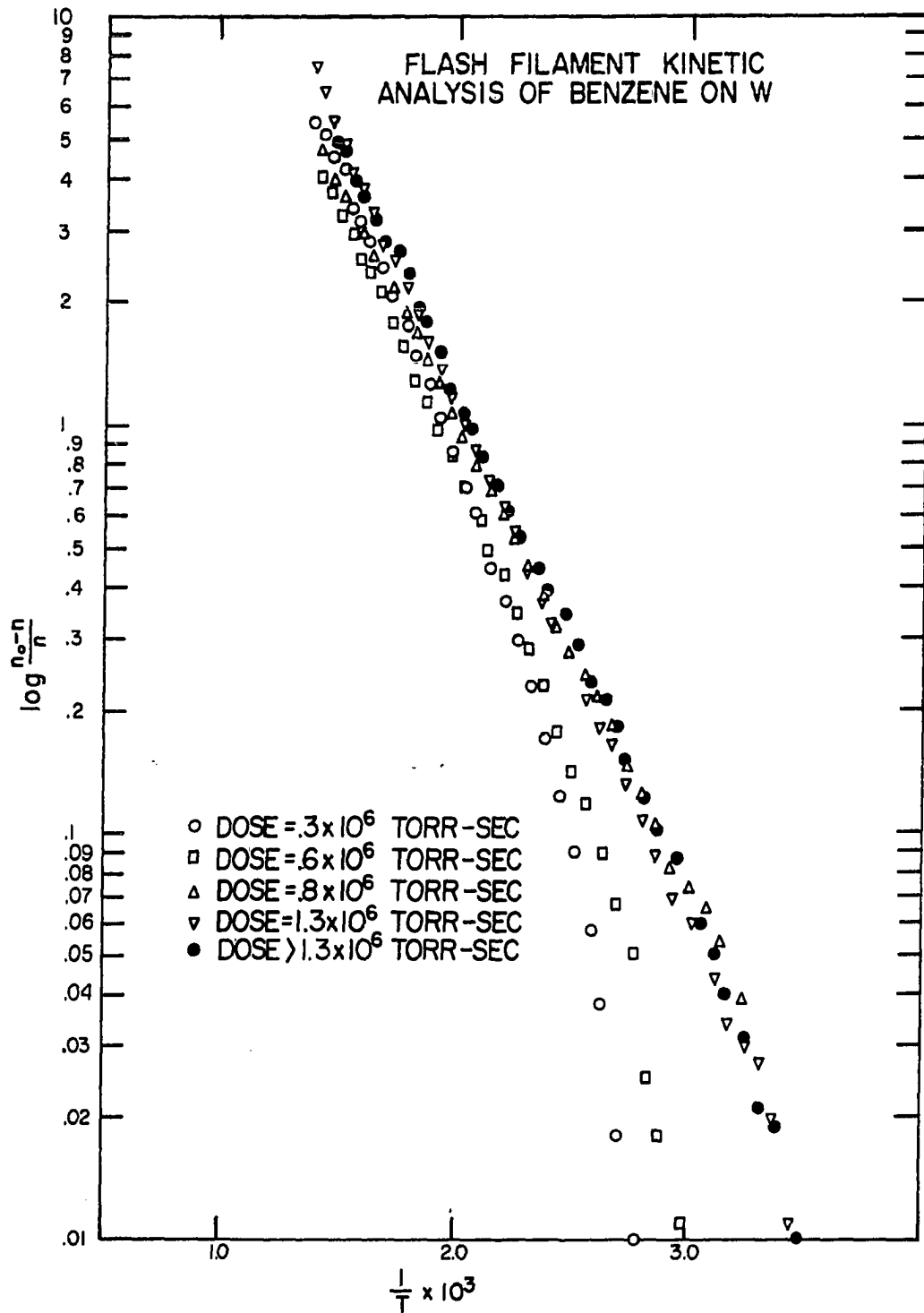
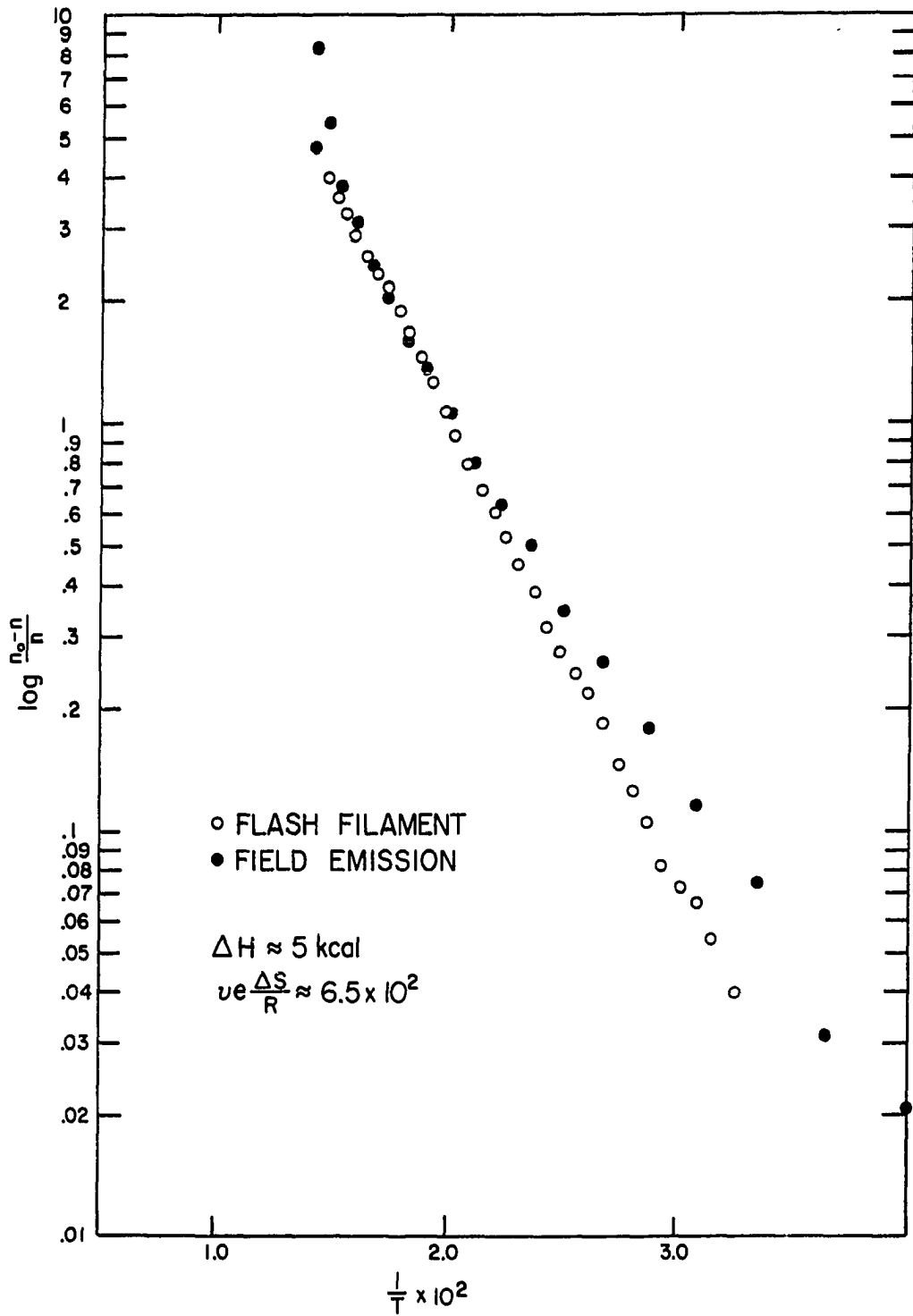


Figure 39. A comparison of second order kinetic plots found by flash filament and field emission techniques

With field emission results the extent of reaction  $a$  is taken as proportional to  $n_0 - n$ .



of the flash filament with the field emission results using Equation 28.

The activation energy of 5 kcal. and frequency factor of about  $10^2$  obtained from data presented in Figures 36 and 37 seem rather improbable and the former is in marked disagreement with the value of around 27 kcal. expected from the high pumped flash (Figure 29) using Redhead's rule (Equation 18). To think of the decomposition reaction, however, as a simple second order reaction is unrealistic. If the hydrogen is produced by a second order combination of atomically adsorbed hydrogen, it is surely preceded by some reaction, or reactions, involving production of the hydrogen from the chemisorbed hydrocarbon.

One possibility is a reaction sequence represented by the following



where K is an equilibrium constant and k is a second order rate constant. Assuming monolayer initial coverage and expressing the chemical species in terms of monolayers then

$$1 = [\text{AH}] + [\text{A}] \quad 38.$$

and

$$1 = [\text{AH}] + [\text{H}] + 2[\text{H}_2] \quad 39.$$

where the brackets designate amounts in terms of monolayers. Since

$$K = \frac{[\text{A}][\text{H}]}{[\text{AH}]} \quad 40.$$

and

$$\frac{2 d[H_2]}{dt} = k [H]^2 \quad 41.$$

then the equation

$$\frac{d[AH]}{dt} \left( 1 + \frac{(K+1)}{[AH]^2} - \frac{2}{[AH]} \right) = -kK^2 \quad 42.$$

can be derived. If  $K \gg 1$  then this equation can be approximated by

$$\frac{-d[AH]}{dt} \frac{1}{[AH]^2} = kK \quad 43.$$

which is the second order rate expression with the rate constant modified by multiplication with the equilibrium constant. Since  $K$  can be expressed as

$$K = \exp(\Delta S/R - \Delta H_e/RT) \quad 44.$$

where  $\Delta S$  is the entropy change and  $\Delta H_e$  is the enthalpy change in the equilibrium reaction as written, then the observed  $\Delta H$  in Figures 37 and 38 is the sum of  $\Delta H_e$  for the equilibrium and  $\Delta H^\ddagger$  from the rate constant.  $\Delta H^\ddagger$  for reaction 37 should be at least 10 kcal; this is the activation energy for desorption of hydrogen from a surface highly covered with hydrogen, and it is greater at lower coverages. This means  $\Delta H_e$  would be about -5 kcal. For the assumption, then, that  $K \gg 1$  between 250°K and 800°K for the duration of the observed desorption  $\Delta S$  need only be slightly positive. If the frequency factor is taken to be  $10^{-2}$  as



expected<sup>3</sup> if the migration of the atomic hydrogen were completely unhindered then this would give  $\Delta S \approx 6$  e.u. It would not be too surprising if the frequency factor were lower since there should be considerable hindrance to free motion on the surface. This would give a higher value for  $\Delta S$ . A value of  $K \gg 1$ , as assumed in obtaining Equation 43, is therefore not physically unreasonable.

This treatment of the problem is probably still an oversimplification. The species designated A that has not yet been identified could be the phenyl group or C from the proposed C-H radical. The second alternative would imply easy breakdown of benzene chemisorbed to C-H. The first case would require that the phenyl group once formed will break down rapidly to yield all six hydrogens.

A stepwise reaction path involving all species from  $C_6H_6$  down to  $C_6$  could also be proposed. The seven rate constants furnish more parameters than can profitably be employed with the present data; similar comments would apply to any mechanism involving a large number of steps.

---

<sup>3</sup>Although often referred to as the frequency factor for the second order rate expression, this factor also contains a term to take into account the density of adsorbed molecules (or adatoms) on the surface (i.e.,  $10^{15}$  molecules  $cm^{-2}$ ). The dimensions of  $v$  are  $cm^2$  molecules<sup>-1</sup> sec<sup>-1</sup>.

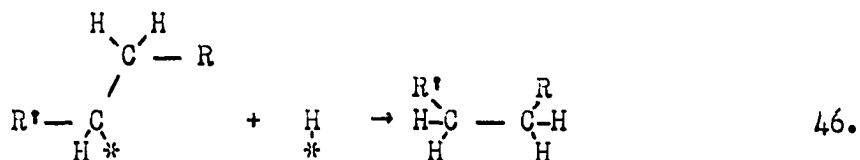
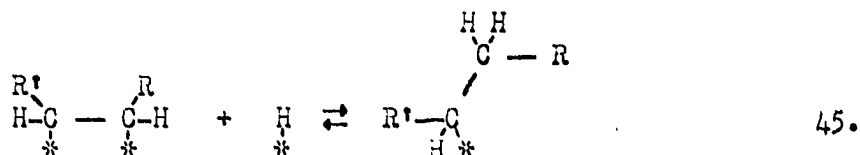
## DISCUSSION

It is apparent from this investigation that tungsten is catalytically active for both hydrogenation and disproportionation. It does not, however, appear to be active for the hydrogenation of benzene. It is easily poisoned by CO, and probably by other gases, but is not poisoned by the products from cyclohexene or benzene at least at room temperature. This freedom from the self-poisoning reaction is probably due to the stability of the benzene ring.

Field emission observation indicates that benzene chemisorbs with a single bond to the tungsten surface. This bond is probably of a  $\pi$ -type. Cyclohexene on the other hand exhibits bonding behavior similar to acetylene suggesting two bonds to the tungsten surface. In such a case, as mentioned earlier, cyclohexene would most likely be chemisorbed in the boat forms as illustrated in Figure 26.

In the boat form on a fully covered surface it is hard to imagine how hydrogenation of cyclohexene could occur by a reaction in which cyclohexene impinges on a chemisorbed cyclohexene and extracts two hydrogen atoms. It would seem that only those hydrogens bonded to the alkene carbons which are bonded to the tungsten would be active enough to be extracted in such a fashion. These hydrogens would be sterically difficult to reach. There is, furthermore, the experimental evidence of hydrogenation at a rapid rate when the surface coverage of cyclohexene could not possibly be great enough for this type of mechanism to operate. It is also interesting that hydrogenation occurs rapidly in spite of acetylenic site adsorption, in contrast to ethylenic type adsorption. Acetylene,

however, hydrogenates very poorly; this indicates that it is not how adsorption occurs on the surface but what it is that is adsorbed. This apparent independence of adsorption geometry could lend support to the half hydrogenated state that has been proposed by many authors. This mechanism proposes the steps

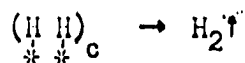
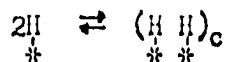


In this case the original geometric arrangement of the carbon atoms on the surface has little effect on the progress of the reaction. Regardless of the mechanism proposed it must include chemisorbed hydrogen as its hydrogen source.

The absolute absence of the intermediate cyclohexadiene in the disproportionation indicates that this species in the chemisorbed state is strongly bonded and unstable toward production of chemisorbed benzene. It would be interesting to see if a similar thing could be said about cyclohexene if cyclohexadiene were adsorbed. From the temperature range over which it desorbs it seems likely that only physically adsorbed cyclohexene can be removed from the surface.

The decomposition reaction responsible for poisoning of hydrogenation reactions well above room temperature, appears to occur by a sequence of two or more reactions. This type of mechanism may be rather

general. For example a two step desorption for hydrogen could be proposed in the following way



in which the symbol  $\left( \underset{*}{\text{H}} \underset{*}{\text{H}} \right)_c$  denotes two hydrogen atoms chemisorbed on adjacent sites. This complex would behave much like a caged complex in solution reactions. The reaction sequence could account for the variation in desorption rate with coverage without necessity for assuming an activation energy for desorption which varied with coverage. Similar mechanisms could be proposed as an alternative to  $\alpha'$  of Equation 17 for simple hydrocarbons as well (4).

The  $\pi$ -complex model differs importantly from that proposed by Smith and Meriwether (31,6). According to their model, benzene loses its resonance energy on chemisorption, and this happens before any addition of hydrogen can occur. If this latter were not the case the activation energy for hydrogenation would be at least equal to the resonance energy of 35 kcal. The experimentally determined activation energy was 7.4 kcal. so that Smith and Meriwether claim benzene must be adsorbed in such a manner that its resonance is destroyed. The  $\pi$ -complex model does not require destruction of resonance and the activated species could easily be similar to 1,3- or 1,4-cyclohexadiene which respectively have heats of formation only 5.6 kcal. and 7.4 kcal. greater than that for benzene.

## SUMMARY

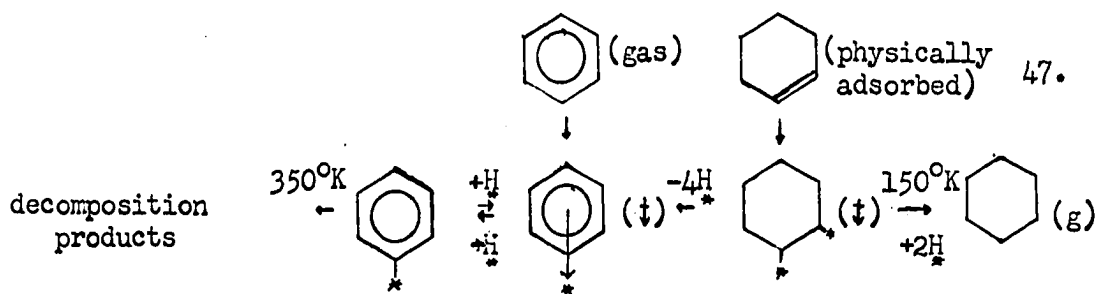
The following conclusions have been drawn from field emission and flash filament studies for the adsorption and reactions of benzene and cyclohexene on tungsten surface:

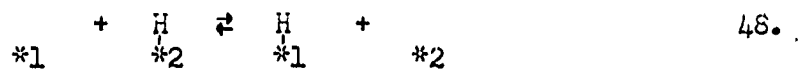
- 1) Disproportionation and hydrogenation of cyclohexene can occur on a tungsten surface.
- 2) Benzene does not hydrogenate at low pressures and temperatures ranging from 90°K to 800°K. Since the rate of chemisorption of benzene would be limited by the rate of desorption of products it seems unlikely that at higher pressures that this situation could be changed.
- 3) Benzene chemisorbs in the first layer initially with a weak single bond, presumably a  $\pi$ -complex type bond and is not the type of bond expected in the multiplet theory. This weak bond is locally strong enough to prevent migration of the chemisorbed benzene. Below 150°K a second physically adsorbed layer can be deposited on top of the chemisorbed layer. This physically adsorbed layer is mobile on top of the chemisorbed layer above 85°K.
- 4) Cyclohexene chemisorbs associatively with two sigma bonds to the tungsten surface and probably in the boat form.
- 5) Chemisorbed phenyl groups and chemisorbed hydrogen appear to exist in an equilibrium with  $\pi$ -bonded benzene.
- 6) Hydrogen does not appear to migrate readily with adsorbed benzene present even up to room temperature. This suggests that

a hydrogen adatom requires an adjacent vacant site for mobility.

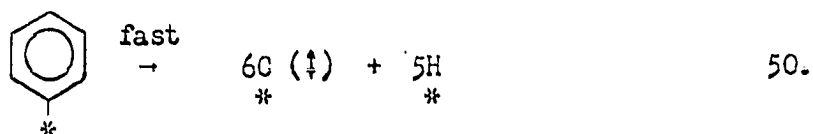
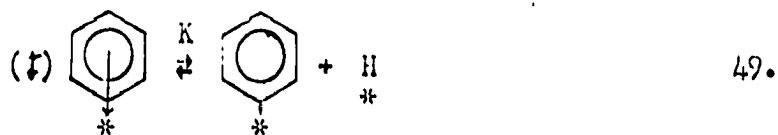
- 7) Cyclohexene can be hydrogenated continuously on tungsten at room temperature; in contrast to ethylene and acetylene, self poisoning does not occur at room temperature. The degradations of cyclohexene (to hydrogen and benzene) and of ethylene (to hydrogen and acetylene or carbon fragments) on tungsten are both irreversible. In the former case degradation products are desorbable in the presence of surface hydrogen and so the reaction does not self-poison, whereas in the latter case the acetylene (or carbon fragments) is not desorbable and eventually blocks the surface.
- 8) No cyclohexadiene is desorbed during flash or isothermal disproportionation of cyclohexene whether or not the surface is predosed with hydrogen. The cyclohexadiene intermediate in the disproportionation of cyclohexene is either too strongly chemisorbed or short lived and possibly both.
- 9) The final decomposition product is probably chemisorbed atomic carbon which above  $1000^{\circ}\text{K}$  converts to  $\text{W}_2\text{C}$ .  $\text{W}_2\text{C}$  is decomposed when tungsten is heated to incandescence to generate a clean tungsten surface.

These conclusions can be summarized in the following formulas.





The symbol ( $\uparrow$ ) designates positive dipole away from the surface whereas ( $\downarrow$ ) designates negative dipole away. Furthermore if the reactions



have some basis in fact then the sum of the activation energy for the kinetic step and the enthalpy for the equilibrium reaction is 5 kcal. With the assumption of a reasonable frequency factor, i.e.  $\nu \approx 10^{-2}$ , then the entropy change for the equilibrium step is equal to or greater than 6 e.u.

## LIST OF SYMBOLS

(in order of appearance)

$\text{\AA}$	Symbol designating Angstroms, $1\text{\AA} = 10^{-8}$ cm.
J	Molecular flux
P	Pressure, usually expressed in torr
k	Boltzmann's constant
T	Absolute temperature
F	Electric field
V	Electrical potential
r	Field emission tip radius
$\beta$	The geometry factor
I	Field emission current
$\mu$	Fermi energy
$\phi$	Work function
A	Emitting area
b	Exponential constant in Fowler-Nordheim equation
C	Intercept in the Fowler-Nordheim plot
$\Delta$	Designates change
$N_s$	Number of surface sites
$\theta$	Surface coverage
$\mu_0$	Perminate dipole moment
S	Slope of the Fowler-Nordheim plot
d	Thickness of adsorbed layer
$\alpha$	Surface polarizability
n	Amount of reactant on surface



t	Time
v	Frequency factor
q	Kinetic order of the reaction
$\Delta H^\ddagger$	Activation energy
R	Gas constant
g	Intercept of $1/T$ vs. $t$ plot
h	Slope of $1/T$ vs. $t$ plot
$V_S$	Volume of system
$T_S$	Temperature of system
$S_S$	Pumping speed
$Q(n)$	Kinetic expression
$\alpha'$	Slope of plot of $H$ dependence on $\theta$
$\Omega$	Electrical resistance
i	Mass peak intensity
$i_{API}$	Relative mass peak intensity recorded in API table
D	Proportionality constant
x	Exponential dependence of mass peak intensity
Z	Relative sensitivities of various gases in a mass spectrometer as recorded in API table
a	Extent of the reaction
K	Equilibrium constant
k	Kinetic rate constant
$\Delta S$	Change in entropy in an equilibrium
$\Delta H_e$	Change in enthalpy in an equilibrium

## LITERATURE CITED

1. Agronomov, A. E. and A. P. Kishehenho. Mechanism of hydrogenation of the C-C double bond on a cobalt catalyst. Vestnik Moskovskogo Universiteta Seriiâ 2, Khimii 19:74. 1964.
2. American Petroleum Institute. Mass spectral data: Research project 44. Washington, D.C., National Bureau of Standards. 1949-1959.
3. Anderson, J. R. and C. Kemball. Catalytic exchange and deuteration of benzene over evaporated metallic films in a static system. Advances in Catalysis 9:51. 1957.
4. Arthur, J. R., Jr. A study of surface reactions by field emission microscopy. Unpublished Ph.D. thesis. Ames, Iowa, Library, Iowa State University of Science and Technology. 1961.
5. Balandin, A. A. The nature of active centers and kinetics of catalytic dehydrogenation. Advances in Catalysis 10:96. 1958.
6. Bond, G. C. Catalysis by metals. New York, N.Y., Academic Press, Inc. 1962.
7. Corson, D. R. and P. Lorrain. Introduction to electromagnetic fields and waves. San Francisco, Calif., W. H. Freeman and Company. 1962.
8. Crowell, A. D. and A. L. Norberg, Jr. Work function changes produced by chemisorption on surfaces with different types of adsorption sites. Journal of Chemical Physics 37:714. 1962.
9. Culver, R. V. and F. C. Tompkins. Surface potentials and adsorption process on metals. Advances in Catalysis 11:67. 1959.
10. Ehrlich, G. The interaction of nitrogen with tungsten surface. Journal of Physical Chemistry 60:1388. 1956.
11. Ehrlich, G. Modern methods in surface kinetics: field emission microscopy. General Electric Research Laboratory. Schenectady, N.Y., Report No. 63-RL-(3376M). 1963.
12. Ehrlich, G. Modern methods in surface kinetics: macroscopic measurements. General Electric Research Laboratory. Schenectady, N.Y., Report No. 63-RL-(3375M). 1963.
13. Fowler, R. H. and L. Nordheim. Electron emission in intense electric fields. Royal Society of London Proceedings A119:173. 1928.

14. Gardner, N. C. A study of the surface reactions of hydrocarbons on tungsten by field emission microscopy. Unpublished Ph.D. thesis. Ames, Iowa, Library, Iowa State University of Science and Technology. 1966.
15. Garnett, J. L. and W. A. Sollich-Baumgartner. Catalytic deuterium exchange reactions with organics. XIV. Distinction between associative and dissociative  $\pi$ -complex substitution mechanism. *Journal of Physical Chemistry* 68:3177. 1964.
16. Gomer, R., R. Wortman and R. Lundy. Mobility and adsorption of hydrogen on tungsten. *Journal of Chemical Physics* 26:1147. 1957.
17. Good, R. H. and E. W. Mueller. Field emission. *Handbuch der Physik* 21:176. 1956.
18. Harris, G. W. Sticking probability of hydrocarbons on tungsten (abstract). *Dissertation Abstracts* 26:3187. 1965.
19. Hayward, D. O. and B. E. W. Trapnell. *Chemisorption*. Washington, D.C., Butterworths. 1964.
20. Hickmott, T. W. Interaction of hydrogen with tungsten. *Journal of Chemical Physics* 32:810. 1960.
21. Janz, G. J. Thermodynamics of the hydrogenation of benzene. *Journal of Chemical Physics* 22:751. 1954.
22. Klein, R. Surface migration of carbon on tungsten. *Journal of Chemical Physics* 22:1406. 1954.
23. Mimeault, V. J. Flash desorption and isotopic mixing of simple diatomic gases on tungsten, iridium and rhodium. Unpublished Ph.D. thesis. Ames, Iowa, Library, Iowa State University of Science and Technology. 1966.
24. Mueller, E. W. and A. J. Helmed. Study of molecular patterns in the field emission microscope. *Journal of Chemical Physics* 29:1037. 1958.
25. Ploch, W. and W. Walcher. Correction in mass-spectrometric abundance measurements in consequence of the mass dependence of the electron-release by means of isotopic ions. *Review of Scientific Instruments* 22:1028. 1951.
26. Redhead, P. A. Thermal desorption of gases. *Vacuum* 12:203. 1962.
27. Rye, R. R. Calibration of resistance with temperature for tungsten. Iowa State University of Science and Technology Ames Laboratory Monthly Report 5/16-6/15. 1966.

28. Santeler, D. J., D. W. Jones, D. H. Klockeboer and F. Pagano. Vacuum technology and space simulation: prepared under contract NASw-680 by Aero Vac Corporation. Washington, D.C., Scientific and Technical Information Division, National Aeronautics and Space Administration. 1967.
29. Selwood, P. W. The mechanism of chemisorption: benzene and cyclohexane on nickel (silica), and the catalytic hydrogenation of benzene. *American Chemical Society Journal* 79:4637. 1957.
30. Smith, H. A. The catalytic hydrogenation of aromatic compounds. *Catalysis* 5:175. 1957.
31. Smith, H. A. and H. T. Meriwether. The catalytic hydrogenation of the benzene nucleus. V. The hydrogenation of benzene, the cyclohexadienes and cyclohexene. *American Chemical Society Journal* 71:413. 1949.
32. Taylor, H. S. The Balandin multiplet hypothesis of dehydrogenation of cycloparafins. *American Chemical Society Journal* 60:627. 1938.
33. Trapnell, B. M. W. Balandin's contribution to heterogeneous catalysis. *Catalysis* 3:1. 1951.
34. Wojciechowski, K. F. Statistical theory of adsorption on solid surfaces with different adsorption sites. *Acta Physica Polonica* 27:893. 1965.
35. Young, R. D. and H. E. Clark. Effect of surface patch fields on field-emission work-function determinations. *Physical Review Letters* 17:351. 1966.

## ACKNOWLEDGEMENTS

It is with pleasure the author acknowledges Dr. R. S. Hansen whose guidance and help has made this work possible.

The author would also like to thank Robert R. Rye for the use of the flash filament equipment constructed by him.